Title

Co-infection interactions and emergent plant viruses: biology of polerovirus, umbravirus, and tlaRNA disease complexes

Author

Erickson, Anna

Publication Date

2023

Peer reviewed|Thesis/dissertation

Co-infection interactions and emergent plant viruses: biology of polerovirus, umbravirus, and tlaRNA disease complexes

By

ANNA C. ERICKSON
DISSERTATION

Submitted in partial satisfaction of the requirements for the degree of

DOCTOR OF PHILOSOPHY

in

Plant Pathology

in the

OFFICE OF GRADUATE STUDIES

of the

UNIVERSITY OF CALIFORNIA

DAVIS

Approved:

Bryce W. Falk, Chair

Savithramma Dinesh-Kumar

Diane Ullman

Committee in Charge

2023

Acknowledgements

First I would like to express my gratitude to my thesis advisor Professor Emeritus Bryce W. Falk for not only accepting me as a graduate student in his lab, but for all of the support, mentorship, and patience he has extended to me over the years. Not only is Bryce an amazing and inspiring scientist, he is a great P.I. and person overall. It has always been clear he truly cares for his students' and employees' wellbeing, and he always encourages us to do what is best for ourselves and our professional development.

I would also like to thank my thesis committee members, Dr. Savithramma Dinesh-Kumar and Dr. Diane Ullman, for the guidance they gave me regarding my thesis work. I would also like to thank my qualifying exam committee members, Dr. Savithramma Dinesh-Kumar, Dr. George Bruening, Dr. Richard Bostock, Dr. Joanne Emerson, and Dr. Clare Casteel for their valuable guidance as well.

I will also be forever grateful to all of the Falk lab members that have cycled through the lab during my time here. I am truly lucky to have met and worked alongside so many brilliant and inspiring scientists and people. I'd like to extend special thanks to Dr. Jun Jiang and Dr. Yen-Wen Kuo, who fielded the most of my questions and were an invaluable source of support and help in developing my skills as a plant virologist, and without them I surely could not have accomplished what I have. I feel truly fortunate for the time I've spent in the Falk lab, and all the wonderful and memorable opportunities it has afforded me.

I also thank all of the wonderful and loving friends I've made along the way, whose companionship helped make this experience not only tolerable but enjoyable as well. Beyond what I've learned and the degree I am walking away with, my favorite part of this experience has been all of the wonderful people I've met and supportive friendships I've made.

Lastly, but most importantly, I would like to thank my parents, Laurie Nettleton-Erickson and Kurt Erickson. They were endlessly supportive and encouraging of my creative and academic pursuits, and of me as a person in general. Without their love and support, I can't say I'm sure I would have had the confidence and belief in myself to pursue this degree. While they were unfortunately not able to see me begin or finish this journey, I have no doubt they would be proud of what I've accomplished and how much I've grown as a person. Thank you mom and dad, I love and miss you, and will continue to live my life in a way that would make you proud.

Co-infection interactions and emergent plant viruses: biology of polerovirus, umbravirus, and tlaRNA disease complexes

Abstract

In this thesis work I broadly present research that investigates the biology of coinfection interactions that occur in mixed infections of poleroviruses, umbraviruses, and tombusvirus-like associated RNAs (tlaRNAs), which in nature form particularly unique asymmetrically obligate virus disease complexes. I also present work detailing the identification of emergent poleroviruses, umbraviruses, and tlaRNAs specifically associated with the Carrot motley dwarf (CMD) disease complex, as well as work on the identification and biological characterization of an emergent polerovirus—not currently known to be associated with such viral disease complexes as are described in this work—that was originally identified in Korea in a barley (*Hordeum vulgare*) plant sample exhibiting symptoms of yellow dwarf disease.

Virus disease complexes composed of a polerovirus, umbravirus, and/or tlaRNAs are widely known to cause greatly enhanced symptom development in various economically important plant hosts and are sometimes associated with increased virus accumulation of one or more of the coinfecting viruses. There are several coinfection interactions known to occur in such disease complexes, such as the ability of poleroviruses to support systemic movement of tlaRNAs—which on their own are completely immobile—within a plant host, and to also support aphid transmission of both tlaRNAs and umbraviruses—neither of which is independently aphid transmissible—by way of transcapsidation of the genomic RNAs of these viruses in polerovirus capsid proteins. Additionally, while poleroviruses are known to be phloem limited and cannot move between cells not associated with the phloem, it has been found that coinfection with an

umbravirus can help a coinfecting polerovirus escape this phloem limitation and be able to move amongst mesophyll cells and as a result, in some instances, also become mechanically transmissible, a function of which poleroviruses are not independently capable. What is less known is how umbraviruses and tlaRNAs interact with one another in these disease complexes.

In Chapter 2 of this work, I used aphid inoculation of the polerovirus Turnip yellows virus (TuYV) along with agroinoculation of infectious clones of the CMD associated umbravirus Carrot mottle virus (CMoV), CMD tlaRNAs gamma and sigma, and the TuYV tlaRNA ST9 to combine these viruses in different ways in the model host plant *Nicotiana benthamiana*, in order to observe the biological consequences of different coinfection pairings with a focus on symptom development, systemic movement of the tlaRNAs, virus accumulation, and altered modes of transmission, i.e. aphid or mechanical. In terms of symptom development, I found that all coinfections that included CMoV, except for coinfections of CMoV with tlaRNA gamma, resulted in greatly enhanced symptom development, while all other coinfections were asymptomatic, suggesting that in this experimental system CMoV acted as the driver of symptom development. In terms of virus accumulation, while several different coinfection combinations resulted in variable increases of each of the coinfecting viruses—as determined by RT-qPCR—the most dramatic accumulation increases were observed for TuYV and CMoV in co-infections that also included tlaRNA ST9, showing this tlaRNA strongly upregulates the accumulation of TuYV and CMoV by some as yet unknown mechanism.

The most notable findings of this work, however, were the interactions that occurred between CMoV and the tlaRNAs. It was found that not only could CMoV support systemic movement of all of the tlaRNAs used in this study, although with variable efficiencies—tlaRNAs sigma and ST9 moved systemically in coinfections with CMoV 100% of the time, whereas

gamma only moved 40% of the—time, but CMoV could also impart mechanical transmissibility to tlaRNAs sigma and ST9, but not tlaRNA gamma, indicating different tlaRNAs differ in their capacity for various coinfection interactions. Given the near complete lack of studies investigating interactions between umbraviruses and tlaRNAs, these results were particularly exciting. It was also intriguing to find that in triple infections of TuYV and CMoV with either tlaRNA sigma or ST9, the efficiency with which TuYV could be co-mechanically transmitted with CMoV greatly increased (54% and 77%, respectively) relative to the rate at which TuYV was co-mechanically transmitted from plants co-infected with only CMoV (11%), suggesting coinfection with tlaRNAs sigma or ST9 facilitates interaction between CMoV and TuYV in some way. All together the results of this study highlight the variability of coinfection interactions that can occur between poleroviruses, umbraviruses, and tlaRNAs and demonstrate that some of these interactions can be rather non-specific—despite TuYV and tlaRNA ST9 having not been found in natural co-infections with the CMD associated umbravirus CMoV, these viruses nonetheless were able to interact with one another.

In Chapter 3 of this work, I further highlight the plasticity of these disease complexes by identifying emergent poleroviruses, umbraviruses, and tlaRNAs in parsley, carrot, and cilantro samples exhibiting typical symptoms of CMD; in many samples combinations of these viruses not previously known to occur were observed. The viruses historically associated with CMD include the polerovirus Carrot red leaf virus (CRLV), the umbraviruses CMoV and carrot mottle mimic virus (CMoMV), and a multitude of tlaRNAs including a8, a25, alpha, beta, gamma, and sigma. In addition to identifying these recognized CMD associated viruses, we found three emergent poleroviruses (two recently reported poleroviruses and one that appears to be a novel recombinant polerovirus), two emergent umbraviruses that were recently reported as novel

species, however according to our data we believe these to actually be highly divergent strains of CMoV, as well a newly described tlaRNA. Most of these emergent viruses have not previously been reported to occur in the United States, nor have they been formerly recognized to be associated with CMD. The finding of these viruses in varying combinations with each other and the previously known CMD associated viruses highlights the modularity of these disease complexes, which has important epidemiological implications.

Lastly, in Chapter 4 I describe the identification of an emergent polerovirus—barley virus G (BVG)—that had not previously been reported in the U.S.. Since its initial discovery, BVG has been found in multiple other countries and species of monocot plants, however all reports on this virus were limited to detection by RT-PCR and sequencing based assays. To begin to understand the biology of this virus, I constructed an infectious BVG clone, which I used to establish an infection in *N. benthamiana* by agroinoculation. From the BVG agroinoculated *N. benthamiana* plants I was able to partially purify infectious BVG virions which I fed to three different species of aphids, which allowed me to identify two competent insect vectors—one efficient (the corn aphid, *Rhopalosiphom* maidis) and one inefficient (the bird cherry-oat aphid, *R. padi*)—of this virus. I subsequently used the newly identified efficient aphid vector to perform a small host range study to determine the effects of BVG on symptom development in plant species in which it has been previously described, as well as a couple additional species in which it has not. Altogether the work presented here expands on what we already know about interactions between poleroviruses, umbraviruses, and tlaRNAs in virus disease complexes comprised of these viruses and the intriguing specificities and non-specificities of these interactions. It also highlights the utility of RT-PCR based diagnostic assays in combination with high throughput sequencing technology for the identification of emergent viruses.

Table of Contents

Chapter 1

Introduction

Biology of mixed plant virus infections

While much of our understanding of plant viruses comes from studies on single virus infections, it is recognized that mixed viral infections not only occur, but are common, especially in the plant kingdom (Rochow 1972; Alcaide et al. 2020; Syller 2012; Vance 1991; Murant et al. 1985; Creamer and Falk 1990; Salvaudon, De Moraes, and Mescher 2013; Wang et al. 2009; Tatineni, Alexander, and Qu 2022; Wamaitha et al. 2018: Bergua et al. 2016). The outcomes of such mixed infections—both in terms of effects on the coinfecting viruses and effects on the host—are highly variable depending on the co-infecting viruses involved, how closely related the co-infecting viruses are to one another, the order in which each co-infecting virus is inoculated into the host, the host in which the co-infection occurs, host age at the time of infection, and environmental conditions. The effects of mixed virus infections can be viewed with respect to effects on symptom development in the host and with respect to effects on the co-infecting viruses (Alcaide et al., 2020; Syller 2012). In terms of symptom development, mixed infections that result in enhanced symptom development are referred to as synergistic infections, while those that attenuate or prevent symptom development are considered antagonistic or protective (Folimonova 2020). Virus-virus interactions in mixed infections are broadly referred to as being neutral (neither virus is affected), antagonistic (one or both viruses is negatively affected), or synergistic (one or both viruses is positively affected), and in some cases inverse effects (one virus is positively affected while the other is negatively affected) can also be observed (Alcaide et al,. 2020). Such interactions can alter viral accumulation) , transmission mode (i.e. insect vectored transmission or mechanical transmission) and transmission efficiency, as well as how and where each virus can move within the plant host.

A particularly interesting variation of viral synergism, and the primary focus of the work presented herein, is known as helper-dependence, or transcomplementation, which describes a phenomenon in which one virus (the helper) encodes proteins with functions that the co-infecting (dependent) virus lacks, thereby imparting these functions to the dependent virus (Syller 2012). Oftentimes this interaction is obligatory for one or more of the co-infecting viruses. Mixed infections comprised of a polerovirus (family *Solemoviridae*), an umbravirus (family *Tombusviridae*), and/or a tombusvirus-like associated RNA (tlaRNA; unclassified) represent a particularly interesting system in which synergistic, asymmetrically obligate transcomplementation interactions occur between these co-infecting viruses (Abraham et al. 2014; Watson et al., 1998; Yoshida 2020; Watson et al., 1964; Watson and Falk 1994; Mo et al. 2007; Hull and Adams 1968; Taliansky et al., 2000; Naidu et al., 1999; Falk and Duffus 1984; Falk et al., 1999; Campbell et al., 2020; Storey and Ryland 1957). All three of these viruses have single stranded, positive sense RNA genomes, and are capable of autonomous replication within a host plant, however they differ in their abilities to move within the plant host and to be transmitted to new hosts.

Poleroviruses, umbraviruses, and tombusvirus-like associated RNAs (tlaRNAs)

Polerovirus genomes are about 5-6 kb of ssRNA and encode six open reading frames (ORFs) (Delfosse et al., 2021). ORF0 encodes a protein that has been shown in some (but not all) poleroviruses to function as a suppressor of the host RNA interference (RNAi) defense response, and functions by targeting Argonaut 1 (Ago1) proteins—a key component of the RNA induced silencing complex (RISC) which drives the RNAi response—for degradation (Delfosse et al., 2021; LaTourrette et al., 2021). ORF1 encodes a multifunctional, replication associated polyprotein that harbors two transmembrane domains, a serine protease motif, the viral genome

binding protein (VPg), and a C-terminal nucleic acid interaction domain. ORF 2 encodes the viral RNA dependent RNA polymerase (RdRp), which is expressed as a fusion protein with P1 via a -1 frameshift mechanism. ORF3a encodes a small molecular weight protein that facilitates systemic movement, along with the major movement protein encoded by ORF4; while these proteins help support systemic movement within phloem cells they do not support cell-to-cell movement between mesophyll cells, thereby restricting polerovirus localization to the phloem tissues. The capsid protein, encoded by ORF3, is also required for systemic movement as well as aphid transmission. Readthrough of ORF3 to ORF5 via an amber stop codon produces the P3/P5 fusion protein, which is cleaved and incorporated into the virion capsid, and is required for polerovirus acquisition by aphid vectors and likely plays a role in the insect vector specificity of these viruses (Brault et al., 2005). Poleroviruses are phloem-limited in their plant hosts and are aphid-transmitted in a circulative-nonpropagative manner and can persist autonomously in nature without the need of a helper virus (LaTourrette et al., 2021). However they have been found to benefit from co-infections with umbraviruses and/tlaRNAs, in some instances gaining functions such as the ability to move cell-to-cell in non-phloem tissues and to be mechanically transmitted, or to show increased viral accumulation in mixed vs. single infections (Ryabov et al. 2001; Alcaide et al. 2020; Chen et al., 2022; Zhou et al., 2017; Hoffman et al., 2001; Watson et al. 1998; Sanger et al. 1994).

Umbraviruses have ssRNA genomes of ~4 kb and encode only four ORFs (Taliansky and Robinson 2003; Syller 2003; Ryabov and Taliansky 2020). Similar to poleroviruses, the ORFs one and two of umbraviruses encode, respectively, a replication associated protein and a viral RdRp that is expressed as a P1/P2 fusion protein. ORFs three and four encode long distance and cell-to-cell movement proteins, respectively, which enable these viruses to move systemically

within phloem cells as well as within and between mesophyll cells (cell-to-cell movement). The ORF3 encoded protein has also been shown to form protective ribonucleoprotein (RNP) complexes with umbravirus and heterologous virus genomic RNAs and can protect viral RNAs against the host nonsense mediated decay (NMD) (Ryabov, et al. 2007; Macfarlane, et al. 2007; Taliansky et al. 2003; Ryabov et al., 2001; May et al. 2020).While umbraviruses can independently replicate and spread throughout their plant hosts, they do not encode their own capsid proteins and therefore cannot be transmitted to new host plants by insect vectors, and while they can be mechanically transmitted to new hosts, this is not a prominent means of transmission in the field, though no epidemiological studies have been done to verify this. As such umbraviruses are thought to obligately coincide with a co-infecting polerovirus, which enables them to become aphid transmissible via transcapsidation of the umbravirus genomic RNA by poleroviral capsids, however, there are several recent reports in which newly identified umbraviruses have been detected in infected plants in the absence of a co-infecting polerovirus (Lim et al. 2019; Zheng et al., 2022). In some polerovirus-umbravirus coinfections, it has been found that the polerovirus can escape phloem limitation and gain cell-to-cell movement and sometimes even become mechanically transmissible, however this does not hold true for all polerovirus-umbravirus combinations (Zhou et al. 2017; Jiang et al. 2021; Ryabov et al. 2001; Nurkiyanova et al. 2001).

TlaRNAs have ssRNA genomes of ~2.8 kb and only encode two ORFs—ORF1a and ORF 1b—which encode a viral RdRp which is expressed as a 1a/1b fusion protein via readthrough of an amber stop codon. Beyond being able to replicate themselves, tlaRNAs are incapable of any type of movement within a host plant nor can they be efficiently transmitted to new hosts (Campbell et al. 2020). Some studies have found that some tlaRNAs can be

mechanically transmitted at low levels, however given their lack of any type of movement protein they are incapable of moving beyond the inoculation zone (Passmore et al. 1993). Therefore these viruses are almost entirely dependent on coinfection with a compatible helper virus that can facilitate their movement within and between host plants (Schönegger et al. 2022; Yoshida 2020; Chen et al., 2022). The first tlaRNA discovered (ST9) was found obligately coinfected with the polerovirus turnip yellows virus (TuYV), which supports systemic movement and aphid transmission of ST9 (Falk and Duffus 1984). Therefore, since similar disease complexes comprised of a polerovirus, tlaRNA or satellite virus, and an umbravirus were discovered, most subsequent studies have largely focused on polerovirus-tlaRNA and polerovirus-umbravirus transcomplementation interactions, and until recently have neglected umbravirus-tlaRNA interactions. A recent study by Chen et al. (2022) investigated for the first time transcomplementation interactions between an umbravirus (tobacco busy top virus; TBTV) and a tlaRNA (tobacco vein distorting virus associated RNA; TVDVaRNA) of the tobacco bushy top disease (TBTD) complex, demonstrating that TBTV could support TVDVaRNA systemic movement in the absence of a coinfecting polerovirus. In Chapter 2 of this work, I corroborate these findings in my own experiments, and expand on them by demonstrating that umbravirus coinfection can also facilitate mechanical transmission of some tlaRNAs.

Polerovirus, umbravirus, and tlaRNA disease complexes relevant to this work

To date, multiple natural disease complexes consisting of a polerovirus, and umbravirus, and/or a tlaRNA—or sometimes a satellite virus—have been identified, most of which result in enhanced symptom development and have been observed to cause significant and economically damaging losses in important agronomic crop plants; prominent examples include the groundnut rosette disease (GRD) complex (Storey and Ryland 1957; Reddy et al. 1985; Evans 1954; Naidu

et al., 1999), the carrot motley dwarf (CMD) complex (Yoshida 2020; Watson and Falk 1994; Gibbs et al, 1996; Watson and Serjeant, 1964), the tobacco bushy top disease (TBTD) complex (Abraham et al. 2014; Xiao et al., 2010; Mo et al. 2007; Mo et al., 2011; Chen et al., 2022), and the TuYV and ST9aRNA complex (Falk et al., 1989; Rasochová et al. 1997; Falk et al., 1999), among others.

Of relevance to the work presented in this thesis are the carrot motley dwarf (CMD) and the TuYV and ST9aRNA disease complexes. CMD affects plants in the family *Apiaceae* (*Umbelliferae*) such as carrots (*Daucus carota*), parsley (*Petroselinum crispum*), chervil (*Anthriscus cerefolium*), and cilantro (*Coriandrum sativum*), and occasional outbreaks of this disease have been recorded throughout the world wherever these plant crops are grown (Yoshida 2020; Watson and Falk, 1994; Murant et al., 1969; Morton et al., 2003; Tang et al., 2009; Watson and Serjeant 1964; Gibbs and Waterhouse 1996). CMD has historically been known to be associated with coinfections of the polerovirus carrot red leaf virus (CRLV), one of two umbraviruses—carrot mottle virus (CMoV) and carrot mottle mimic virus (CMoMV)—and/or one or more of a variety of tlaRNAs—CRLVaRNAs a8, a25, alpha, beta, gamma, and sigma, among others (Watson et al. 1998; Yoshida 2020; Gibbs et al. 1996; Murant et al. 1985). In a recent publication, the TuYV ST9aRNA and a newly described tlaRNA—arracacha latent virus E associated RNA (ALVEaRNA) isolated from arracacha (*Arracacia xanthorrhiza*) plants were also found in symptomatic carrot plants (Schönegger et al. 2022). In this system, CRLV is known to impart aphid transmissibility to the tlaRNAs and CMoV, as well as support systemic movement of the CRLVaRNAS (Elnagar and Murant 1978).

TuYV and ST9 were first isolated from shepherd's purse plants (*Capsella bursa-pastoris*) plants and it was found that the presence of ST9 resulted in dramatically enhanced leaf yellowing

and stunting symptoms (Falk and Duffus 1984). In addition to TuYV supporting the systemic movement and aphid transmission of ST9, as previously mentioned, the presence of ST9 was associated with a significant increase in the accumulation of TuYV RNA and capsid proteins, although a commensurate increase in ST9 aRNA was not observed (Falk and Duffus, 1984; Passmore et al. 1993; Sanger et al. 1994).

Preview into the works presented herein

In Chapter 2 of this work I use aphid inoculation of TuYV and agroinoculation of infectious clones of the CMD associated umbravirus CMoV, the CRLVaRNAs gamma and sigma, and the ST9aRNA, to establish different virus infection combinations in the model plant host *Nicotiana benthamiana,* and explore the effects these have on symptom development, virus accumulation, systemic movement of tlaRNAs, and on the ability of each of these viruses to be aphid and/or mechanically transmitted. It should be noted that I used TuYV, in place of CRLV, as the polerovirus partner for two primary reasons, the first being that we did not have on hand the specific aphid vector—*Cavariella aegopodii*—of CRLV and therefore would not be able to perform the aphid inoculation experiments, and the second being that *N. benthamiana* is known to be a non-host of CRLV, which would limit the control we had on establishing specific combinations of each of these viruses.

In Chapter 3 of this thesis, I detail the use of RNA sequencing (RNAseq) technology to identify potentially emergent poleroviruses, umbraviruses, and tlaRNAs in carrot, parsley, and cilantro plant samples exhibiting typical symptoms of CMD that were submitted to our lab for diagnosis. As a result, we found two recently identified poleroviruses which have not been previously known to occur in the United states, nor have they been formally associated with CMD disease. We also identified a putatively novel polerovirus that appears to either be a

recombinant of a known polerovirus and an unknown polerovirus that shares sub-species level homology with another recently described polerovirus—Trachyspermum ammi polerovirus (TaPV) that, again, has neither been described in the U.S. or in association with CMD. Additionally, we found two recently described umbraviruses not previously found in the U.S., that were proposed to be novel umbraviruses; however, our analyses suggest that these viruses are more likely highly divergent strains of CMoV rather than distinct novel species. We also identified the ALVEaRNA in some of the carrot samples, as well as some of the parsley samples, in which it has not been previously described. This work expands the number of polerovirus and tlaRNA species found to be associated with CMD, and serves as a first report of these viruses in the U.S.. It also raises questions as to what factors may be contributing to this expansion of emergent viruses associated with this particular disease complex, and shows the variety of interactors and their plasticity for interacting partners.

The work in Chapter 4 takes a detour from the theme of mixed virus infections in chapters 2 and 3, but is in keeping with the pursuit of emergent poleroviruses. In this chapter I detail the identification of yet another polerovirus that had not been previously known to occur in the U.S., the monocot infecting polerovirus barley virus G (BVG). BVG was first identified in Korea in 2016, and in the short time since has been found in multiple other countries and monocot hosts (Erickson et al. 2023). All prior reports of BVG only described its identification by RT-PCR and sequencing based assays, but none had begun to characterize the biology of this virus. Driven to know more about the biological workings of this virus, I constructed an infectious cDNA clone of BVG. With this clone I was able to partially purify infectious virions from agroinfected *N. benthamiana* plants, and feed these virions to several different aphid species, thereby allowing me to identify two aphid vectors—one of which was quite efficient—

of this virus. Furthermore, having a compatible aphid vector on hand, I was able to conduct a small monocot host range study with BVG, to identify additional hosts which it had not been known to infect, and to determine if it was responsible for the disease symptoms observed in monocot species in which it had previously been identified. Additionally, while we do not formally present this data, we conducted preliminary experiments in which we co-inoculated BVG and the tlaRNAs used in Chapter 2, and found that the monocot infecting BVG was able to support systemic movement of the ST9aRNA in dicots, which was very intriguing because to date no tlaRNAs have been found associated with a monocot infecting polerovirus in nature. Taken together, the results of these varying research efforts not only expand on what we already knew about the interactions and consequences of polerovirus, umbravirus, and tlaRNA coinfections, but highlights the complexity, diversity, and modularity of virus interactions in these fascinatingly unique viral disease complexes.

References

Abraham, Adane D., Wulf Menzel, Berhanu Bekele, and Stephan Winter. 2014. "A Novel Combination of a New Umbravirus, a New Satellite RNA and Potato Leafroll Virus Causes Tobacco Bushy Top Disease in Ethiopia." *Archives of Virology* 159 (12): 3395–99. https://doi.org/10.1007/s00705-014-2202-4.

Alcaide, Cristina, M. Pilar Rabadán, Manuel G. Moreno-Pérez, and Pedro Gómez. 2020. "Implications of Mixed Viral Infections on Plant Disease Ecology and Evolution." *Advances in Virus Research* 106 (0065–3527): 145–69. https://doi.org/10.1016/bs.aivir.2020.02.001.

Campbell, A. J., Anna Erickson, Evan Pellerin, Nidá Salem, Xiaohan Mo, Bryce W. Falk, and Inmaculada Ferriol. 2020. "Phylogenetic Classification of a Group of Self-Replicating

RNAs That Are Common in Co-Infections with Poleroviruses." *Virus Research* 276 (January). https://doi.org/10.1016/J.VIRUSRES.2019.197831.

Chen, Xiaojiao, Hengming Luo, Jingyi Zhang, Yan Ma, Kehua Li, Feng Xiong, and and Fan Li Yahui Yang, Jiazhen Yang, Pingxiu Lan, Taiyun Wei, Yi Xu, Hairu Chen. 2022. "Synergism Among the Four Tobacco Bushy Top Disease Casual Agents in Symptom Induction and Aphid Transmission." *Frontiers in Microbiology* 13. https://doi.org/10.3389/fmicb.2022.846857.

Creamer, R., and B. W. Falk. 1990. "Direct Detection of Transcapsidated Barley Yellow Dwarf Luteoviruses in Doubly Infected Plants." *Journal of General Virology* 71 (1): 211–17. https://doi.org/10.1099/0022-1317-71-1-211.

Cui-Ji Zhou, Xiao-Yan Zhang, Song-Yu Liu, Ying Wang, Da-Wei Li, Jia-Lin Yu & Cheng-Gui Han. 2017. "Synergistic Infection of BrYV and PEMV 2 Increases the Accumulations of Both BrYV and BrYV-Derived SiRNAs in Nicotiana Benthamiana." *Scientific Reports* 7 (45132): 1–13. https://doi.org/10.1038/srep45132.

Delfosse, Verónica C., Maria P. Barrios Barón, and Ana J. Distéfano. 2021. "What We Know about Poleroviruses: Advances in Understanding the Functions of Polerovirus Proteins." *Plant Pathology* 70 (5): 1047–61. https://doi.org/10.1111/PPA.13368.

Elnagar, S., and A. F. Murant. 1978. "Relations of Carrot Red Leaf and Carrot Mottle Viruses with Their Aphid Vector, Cavariella Aegopodii." *Annals of Applied Biology* 89 (2): 237–44. https://doi.org/10.1111/j.1744-7348.1978.tb07695.x.

Erickson, Anna, Jun Jiang, Yen-wen Kuo, and Bryce W Falk. 2023. "Construction and Use of an Infectious CDNA Clone to Identify Aphid Vectors and Susceptible Monocot Hosts of the Polerovirus Barley Virus G." *Virology* 579: 178–85.

https://doi.org/10.1016/j.virol.2023.01.011.

Evans, A. C. 1954. “Groundnut rosette disease in Tanganyika.” *Annals of Applied Biology* 41 (1): 189–206. https://doi.org/10.1111/j.1744-7348.1954.tb00926.x.

Falk, B.W., J.E. Duffus, and T.J. Morris. 1979. “Transmission, Host Range, and Serological Properties of the Viruses That Cause Lettuce Speckles Disease.” *Phytopathology* 69: 612–17.

Falk, B. W.; Duffus, J. E. 1984. “Identification of Small Single- and Double-Stranded RNAs Associated with Severe Symptoms in Beet Western Yellows Virus-Infected Capsella Bursa-Pastoris.” *Phytopathology* 74 (10): 1224–29. https://doi.org/10.1094/phyto-74-1224.

Falk, B. W., L.-S. Chin, and J. E. Duffus. 1989. “Complementary DNA Cloning and Hybridization Analysis of Beet Western Yellows Luteovirus RNAs.” *Journal of General Virology* 70 (6): 1301–9. https://doi.org/10.1099/0022-1317-70-6-1301.

Falk, B. W., T. Tian, and H. H. Yeh. 1999. “Luteovirus-Associated Viruses and Subviral RNAs.” *Current Topics in Microbiology and Immunology* 239: 159–75. https://doi.org/10.1007/978-3-662-09796-0_9/COVER.

Falk, B.W., T.J. Morris, and J.E. Duffus. 1979. “Unstable Infectivity and Sedimentable Ds-RNA Associated with Lettuce Speckles Mottle Virus.” *Virology* 96 (1): 239–48. https://doi.org/10.1016/0042-6822(79)90187-9.

Folimonova, Svetlana Y. 2020. “Citrus Tristeza Virus: A Large RNA Virus with Complex Biology Turned into a Valuable Tool for Crop Protection.” *PLoS Pathogens* 16 (4): 1–6. https://doi.org/10.1371/journal.ppat.1008416.

Gibbs, M. J., J. I. Cooper, and P. M. Waterhouse. 1996. “The Genome Organization and Affinities of an Australian Isolate of Carrot Mottle Umbravirus.” *Virology* 224 (1): 310–13.

https://doi.org/10.1006/VIRO.1996.0533.

Gibbs, M. J., A. Ziegler, D. J. Robinson, P. M. Waterhouse, and J. I. Cooper. 1996. “Carrot Mottle Mimic Virus (CMoMV): A Second Umbravirus Associated with Carrot Motley Dwarf Disease Recognised by Nucleic Acid Hybridisation.” *Molecular Plant Pathology On-Line*.

Hull, R., and A. N. Adams. 1968. “Groundnut Rosette and Its Assistor Virus.” *Annals of Applied Biology* 62 (1): 139–45. https://doi.org/10.1111/j.1744-7348.1968.tb03857.x.

Hoffman, K., M. Verbeek, A. Romano, A.M. Dullemans, J.F.J.M. van den Heuvel, F. van der Wilk. 2001. “Mechanical Transmission of Poleroviruses.” *Journal of Virological Methods* 91 (2): 197–201. https://doi.org/10.1016/S0166-0934(00)00256-1.

Kim, Sang Hyon, Stuart Macfarlane, Natalia O Kalinina, Daria V Rakitina, Eugene V Ryabov, Trudi Gillespie, Sophie Haupt, John W. S. Brown, and Michael Taliansky. 2007. “Interaction of a Plant Virus-Encoded Protein with the Major Nucleolar Protein Fibrillarin Is Required for Systemic Virus Infection.” *PNAS* 104 (26): 11115–20. https://doi.org/10.1073/pnas.0704632104.

Kim, Sang Hyon, Eugene V. Ryabov, Natalia O. Kalinina, Daria V. Rakitina, Trudi Gillespie, Stuart MacFarlane, Sophie Haupt, John W.S. Brown, and Michael Taliansky. 2007. “Cajal Bodies and the Nucleolus Are Required for a Plant Virus Systemic Infection.” *EMBO Journal* 26 (8): 2169–79. https://doi.org/10.1038/sj.emboj.7601674.

LaTourrette, Katherine, Natalie M Holste, and Hernan Garcia-Ruiz. 2021. “Polerovirus Genomic Variation.” *Virus Evolution* 7 (2): 1–18. https://doi.org/10.1093/VE/VEAB102.

Lianshun Zheng, Shuai Fu, Yi Xie, Yang Han, Xueping Zhou, and Jianxiang Wu. 2022. “Discovery and Characterization of a Novel Umbravirus from Paederia Scandens Plants

Showing Leaf Chlorosis and Yellowing Symptoms." *Viruses* 14 (1821). https://doi.org/https://doi.org/10.3390/v14081821.

Lim, Seungmo, Su Heon, Lee Jae, and Sun Moon. 2019. "Complete Genome Sequence of a Tentative New Umbravirus Isolated from Patrinia Scabiosaefolia." *Archives of Virology* 164 (9): 2375–78. https://doi.org/10.1007/s00705-019-04312-y.

May, Jared P, Philip Z Johnson, Muhammad Ilyas, Feng Gao, and E Simon. 2020. "The Multifunctional Long-Distance Movement Protein of Pea Enation Mosaic Virus 2 Protects Viral and Host Transcripts from Nonsense-Mediated Decay." *MBio* 11 (2): 1–16.

Mo, X.-H., X.-Y. Qin, Z.-X. Tan, T.-F. Li, J.-Y. Wu, and H.-R. Chen. 2007. "First Report of Tobacco Bushy Top Disease in China." *Https://Doi.Org/10.1094/PDIS.2002.86.1.74B* 86 (1): 74–74. https://doi.org/10.1094/PDIS.2002.86.1.74B.

Mo, X. H., Z. B. Chen, and J. P. Chen. 2011. "Molecular Identification and Phylogenetic Analysis of a Viral RNA Associated with the Chinese Tobacco Bushy Top Disease Complex." *Annals of Applied Biology* 158 (2): 188–93. https://doi.org/10.1111/J.1744-7348.2010.00452.X.

Mo, Xiao Han, Zheng Bin Chen, and Jian Ping Chen. 2010. "Complete Nucleotide Sequence and Genome Organization of a Chinese Isolate of Tobacco Vein Distorting Virus." *Virus Genes* 41 (3): 425–31. https://doi.org/10.1007/S11262-010-0524-1/FIGURES/4.

Morton, A., N. J. Spence, N. Boonham, and D. J. Barbara. 2003. "Carrot Red Leaf Associated RNA in Carrots in the United Kingdom." *Plant Pathology* 52 (6): 795. https://doi.org/10.1111/j.1365-3059.2003.00904.x.

Murant, A. F., and I. M. Roberts. 1979. "Virus-like Particles in Phloem Tissue of Chervil (Anthriscus Cerefolium) Infected with Carrot Red Leaf Virus." *Annals of Applied Biology*

92 (3): 343–46. https://doi.org/10.1111/J.1744-7348.1979.TB03883.X.

Murant, A F, R A Goold, I M Roberts, and J Cathro. 1969. “Carrot Mottle-a Persistent Aphid-Borne Virus with Unusual Properties and Particles.” *J. Gen. Virol.* 4: 329–41. https://doi.org/10.1099/0022-1317-4-3-329.

Murant, A F, P M Waterhouse, J H Raschki~, and D J Robinson. 1985. “Carrot Red Leaf and Carrot Mottle Viruses: Observations on the Composition of the Particles in Single and Mixed Infections.” *J. Gen. Virol*. Vol. 66. https://doi.org/10.1099/0022-1317-66-7-1575.

Naidu, R.A.; Kimmins, F. M.; Deom, C.M.; Subrahmanyam, P.; Chiyembekeza, A.J.; van der Merwe, P.J.A. 1999. “Groundnut Rosette: A Virus Disease Affecting Groundnut Production in Sub-Saharan Africa.” *Plant Disease* 83 (8): 700–709. https://doi.org/10.1094/PDIS.1999.83.8.700.

Passmore, Boni K., Margaret Sanger, Lih-Shen Chin, Bryce W. Falk, and George Bruening. 1993. “Beet Western Yellows Virus-Associated RNA: An Independently Replicating RNA That Stimulates Virus Accumulation.” *Proceedings of the National Academy of Sciences of the United States of America* 90 (21): 10168–72. https://doi.org/10.1073/PNAS.90.21.10168.

Rasochová, Lada, Boni K. Passmore, Bryce W. Falk, and W. Allen Miller. 1997. “The Satellite RNA of Barley Yellow Dwarf Virus-RPV Is Supported by Beet Western Yellows Virus in Dicotyledonous Protoplasts and Plants.” *Virology* 231 (2): 182–91. https://doi.org/10.1006/VIRO.1997.8532.

Reddy, D. V. R., A. F. Murant, G. H. Duncan, O. A. Ansa, J. W. Demski, and C. W. Kuhn. 1985. “Viruses Associated with Chlorotic Rosette and Green Rosette Diseases of Groundnut in Nigeria*.” *Annals of Applied Biology* 107 (1): 57–64. https://doi.org/10.1111/j.1744-

7348.1985.tb01547.x.

Rochow, W F. 1972. “The Role of Mixed Infections in the Transmission of Plant Viruses by Aphids.” *Annual Review of Phytopathology* 10 (1): 101–24. https://doi.org/10.1146/annurev.py.10.090172.000533.

Ryabov, Eugene V., Gillian Fraser, Mike A. Mayo, Hugh Barker, and Michael Taliansky. 2001. “Umbravirus Gene Expression Helps Potato Leafroll Virus to Invade Mesophyll Tissues and to Be Transmitted Mechanically Between Plants.” *Virology* 286 (2): 363–72. https://doi.org/10.1006/viro.2001.0982.

Ryabov, Eugene V., David J. Robinson, and Michael Taliansky. 2001. “Umbravirus-Encoded Proteins Both Stabilize Heterologous Viral RNA and Mediate Its Systemic Movement in Some Plant Species.” *Virology* 288 (2): 391–400. https://doi.org/10.1006/viro.2001.1078.

Ryabov, Eugene V., David J. Robinson, and Michael E. Taliansky. 1999. “A Plant Virus-Encoded Protein Facilitates Long-Distance Movement of Heterologous Viral RNA.” *Proceedings of the National Academy of Sciences of the United States of America* 96 (4): 1212–17. https://doi.org/10.1073/pnas.96.4.1212.

Ryabov, Eugene V, and Michael E Taliansky. 2020. “Umbraviruses (Calvusvirinae, Tombusviridae).” https://doi.org/10.1016/B978-0-12-809633-8.21255-7.

Salvaudon, Lucie, Consuelo M. De Moraes, and Mark C. Mescher. 2013. “Outcomes of Co-Infection by Two Potyviruses: Implications for the Evolution of Manipulative Strategies.” *Proceedings of the Royal Society B: Biological Sciences* 280 (1756). https://doi.org/10.1098/rspb.2012.2959.

Sanger, Margaret, Boni Passmore, Bryce W. Falk, George Bruening, Biao Ding, and William J. Lucas. 1994. “Symptom Severity of Beet Western Yellows Virus Strain ST9 Is Conferred by

the ST9-Associated RNA and Is Not Associated with Virus Release from the Phloem." *Virology* 200 (1): 48–55. https://doi.org/10.1006/viro.1994.1161.

Schönegger, Deborah, Bisola Mercy Babalola, Armelle Marais, Chantal Faure, and Thierry Candresse. 2022. "Diversity of Polerovirus-Associated RNAs in the Virome of Wild and Cultivated Carrots." *Plant Pathology* 71 (9): 1892–1900. https://doi.org/10.1111/PPA.13623.

Storey, H. H., and A. K. Ryland. 1957. "Viruses causing rosette and other diseases in groundnuts." *Annals of Applied Biology* 45 (2): 318–26. https://doi.org/10.1111/j.1744-7348.1957.tb00473.x.

Syller, Jerzy. 2003. "Molecular and Biological Features of Umbraviruses, the Unusual Plant Viruses Lacking Genetic Information for a Capsid Protein." *Physiological and Molecular Plant Pathology* 63 (1): 35–46. https://doi.org/10.1016/J.PMPP.2003.08.004.

Syller, Jerzy. 2012. "Facilitative and Antagonistic Interactions between Plant Viruses in Mixed Infections." *Molecular Plant Pathology* 13 (2): 204–16. https://doi.org/10.1111/J.1364-3703.2011.00734.X.

Taliansky, Michael E., D. J. Robinson, and A. F. Murant. 2000. "Groundnut Rosette Disease Virus Complex: Biology and Molecular Biology." *Advances in Virus Research*. Vol. 55. https://doi.org/10.1016/S0065-3527(00)55008-8.

Taliansky, Michael E., and David J. Robinson. 2003. "Molecular Biology of Umbraviruses: Phantom Warriors." *Journal of General Virology*. Microbiology Society. https://doi.org/10.1099/vir.0.19219-0.

Taliansky, Michael, Ian M. Roberts, Natalia Kalinina, Eugene V. Ryabov, Shri Krishna Raj, David J. Robinson, and Karl J. Oparka. 2003. "An Umbraviral Protein, Involved in Long-

Distance RNA Movement, Binds Viral RNA and Forms Unique, Protective Ribonucleoprotein Complexes." *Journal of Virology* 77 (5): 3031–40. https://doi.org/10.1128/jvi.77.5.3031-3040.2003.

Tang, J., B. D. Quinn, and G. R. G. Clover. 2009. "First Report of Carrot Red Leaf Virus - Associated RNA Co-Infecting Carrot with Carrot Red Leaf Virus and Carrot Mottle Mimic Virus to Cause Carrot Motley Dwarf Disease in New Zealand." *Australian Plant Disease Notes* 4: 15–16. https://doi.org/10.1071/DN09006.

Tatineni, Satyanarayana, Jeff Alexander, and Feng Qu. 2022. "Differential Synergistic Interactions Among Four Different Wheat-Infecting Viruses" 12 (January): 1–15. https://doi.org/10.3389/fmicb.2021.800318.

Vance, Vicki Bowman. 1991. "Replication of Potato Virus X RNA Is Altered in Coinfections with Potato Virus Y Mixed Infections with Two Taxonomically Unrelated Infectivity Assays Analyses of Viral RNAs" 494: 486–94.

Veronique Brault, Sophie Perigon, Catherine Reinbold, Monique Erdinger, and and Veronique Ziegler-Graff Daniele Scheidecker, Etienne Herrbach, Ken Richards. 2005. "Polerovirus Minor Capsid Protein Determines Vector Specificity." *Journal of Virology* 79 (15): 9685–93. https://doi.org/10.1128/JVI.79.15.9685.

Wamaitha, Mwathi Jane, Deepti Nigam, Solomon Maina, Francesca Stomeo, Anne Wangai, Joyce Njoki Njuguna, Timothy A. Holton, et al. 2018. "Metagenomic Analysis of Viruses Associated with Maize Lethal Necrosis in Kenya." *Virology Journal* 15 (1). https://doi.org/10.1186/s12985-018-0999-2.

Wang, Deya, Chengming Yu, Guolu Wang, Kerong Shi, Fan Li, and Xuefeng Yuan. 2015. "Phylogenetic and Recombination Analysis of Tobacco Bushy Top Virus in China."

Virology Journal 12 (1): 1–12. https://doi.org/10.1186/s12985-015-0340-2.

Watson, M.; Serjeant, E.P. 1964. "The Effect of Motley Dwarf Virus on Yield of Carrots and Its Transmission in the Field by Cavariella Aegopdiae Scop." *Annals of Applied Biology* 53 (1): 77–93. https://doi.org/10.1111/j.1744-7348.1964.tb03782.x.

Watson, M. T., and B. W. Falk. 1994. "Ecological and Epidemiological Factors Affecting Carrot Motley Dwarf Development in Carrots Grown in the Salinas Valley of California." *Plant Disease*. https://doi.org/10.1094/PD-78-0477.

Watson, Marion, E. P. Serjeant, and E. A. Lennon. 1964. "Carrot Motley Dwarf and Parsnip Mottle Viruses." *Annals of Applied Biology* 54 (2): 153–66. https://doi.org/10.1111/j.1744-7348.1964.tb01179.x.

Watson, Michael T., Tongyan Tian, Elizabeth Estabrook, and Bryce W. Falk. 1998. "A Small RNA Resembling the Beet Western Yellows Luteovirus ST9-Associated RNA Is a Component of the California Carrot Motley Dwarf Complex." *Phytopathology*. Vol. 88. https://doi.org/10.1094/PHYTO.1998.88.2.164.

Yoshida, Naoto. 2020. "Biological and Genetic Characterization of Carrot Red Leaf Virus and Its Associated Virus/RNA Isolated from Carrots in Hokkaido Japan." *Plant Pathology* 69 (7): 1379–89. https://doi.org/10.1111/ppa.13202.

Chapter 2

Dissecting dynamic plant virus synergism in mixed infections of poleroviruses, umbraviruses, and tombusvirus-like associated RNAs (tlaRNAs)

Anna Erickson[1] and Bryce W. Falk[1]

[1]Department of Plant Pathology, University of California, Davis, CA, 95616, USA

Abstract

Mixed infections of a plant infecting polerovirus, umbravirus, and/or tombusvirus-like associated RNAs (tlaRNAs) produce unique virus disease complexes that exemplify 'helper-dependence' interactions, a type of viral synergism that occurs when a 'dependent' virus that lacks genes encoding for certain protein products necessary for it to complete its infection cycle can utilize complementary proteins encoded by a co-infecting 'helper' virus. While much research has focused on polerovirus-umbravirus or polerovirus-tlaRNA interactions, only recently have umbravirus-tlaRNA interactions begun to be explored. To expand on the limited understanding of umbravirus-tlaRNA interactions in such disease complexes, we established various co-infection pairings of the polerovirus turnip yellows virus (TuYV), the umbravirus carrot mottle virus (CMoV), and three different tlaRNAs—carrot red leaf virus aRNAs (CRLVaRNAs) gamma and sigma, and the TuYVaRNA ST9— in the model plant *Nicotiana benthamiana*, then investigated the effects of these different co-infections on tlaRNA systemic movement within the host, and on virus accumulation, and aphid and mechanical transmission of each of these viruses. We found that CMoV alone could support systemic movement of each of the tlaRNAs, making this the second report to demonstrate such an interaction between an umbravirus and tlaRNAs. We also report for the first time that CMoV could also impart mechanical transmissibility to the tlaRNAs sigma and ST9, and that co-infections of either of these tlaRNAs with both TuYV and CMoV increased the efficiency with which TuYV could be mechanically co-transmitted with CMoV.

Introduction

Helper-dependence, also known as transcomplementation, is a particularly interesting example of virus synergism between co-infecting viruses. In such infections, the "helper" virus

encodes a gene(s) product that the "dependent" virus lacks but can utilize, and in some instances this interaction is obligatory for the dependent virus to complete its infection cycle as these proteins facilitate within host movement and/or transmission between hosts (Alcaide et al. 2020; Latham and Wilson 2008; Rochow 1972; Syller 2012). In many instances, such co-infections also result in significantly enhanced symptom development in the host and significantly increased accumulation of one or more of the co-infecting viruses (Barker 1989; Li et al. 2017; Zhou et al., 2017; Murant 1990; Murant et al. 1988; Passmore et al. 1993; Sanger et al. 1994). Mixed infections comprised of a polerovirus, an umbravirus, and/or a co-infecting tombusvirus-like associated RNA (tlaRNA) exemplify this type of viral synergism.

Multiple disease complexes comprised of a polerovirus, an umbravirus, and/or a satellite virus or tlaRNA have been identified that are responsible for causing severe disease outbreaks in economically important crops (Falk and Duffus 1984; Passmore et al. 1993; Sanger et al. 1994; Watson and Serjeant 1964). The groundnut rosette disease (GRD) complex, caused by co-infection of the polerovirus groundnut rosette assistor virus (GRAV), the umbravirus groundnut rosette virus (GRV), and either one of two associated satellite RNAs—which appear to be responsible for symptom severity and GRV encapsidation by GRAV produced capsids—is perhaps the most well studied example of such a viral disease complex that has caused devastating losses in crop production (Hull and Adams 1968; Murant 1990; Murant et al. 1988; Naidu et al. 1998; Storey and Ryland 1955; Taliansky et al. 2000; Taliansky et al. 1996). Another notable example is the carrot motley dwarf (CMD) disease complex, comprised of the polerovirus carrot red leaf virus (CRLV), the umbravirus carrot mottle virus (CMoV), and/or one of several CRLV associated RNAs (CRLVaRNA) (Watson et al. 1964; Watson et al. 1998;

Murant et al. 1969). CMD occurs globally, anywhere that carrots are produced, and has caused epidemics resulting in severe crop losses (Watson and Serjeant 1964; Watson and Falk 1994).

Viruses in the genus *Polerovirus* (family *Solemoviridae*) are phloem limited and obligately vectored by aphids, often in a species-specific manner; they encode their own capsid proteins (CP) and are capable of *in planta* systemic movement (Peter et al. 2009; Mayo and Ziegler-Graff 1996; Pagán and Holmes 2010; Brault et al. 1995). Umbraviruses are mechanically transmissible, non-phloem limited viruses in the family *Tombusviridae* that can move cell-to-cell and systemically within their plant hosts but lack genes encoding for their own CP and the capacity to be independently transmitted by an insect vector (Taliansky and Robinson 2003; Taliansky et al. 2003; Nurkiyanova et al. 2001; Kim et al. 2007). TlaRNAs are small (~2.8 kb) putative viruses that only encode a replicase protein, making them incapable of independent movement within their plant hosts or transmission to new hosts, and as such are exclusively found co-infecting with a polerovirus, sometimes in association with an umbravirus (Falk and Duffus 1984; Watson et al. 1998; Passmore et al. 1993; Campbell et al. 2020).

One such virus complex is the polerovirus TuYV with the ST9aRNA in shepherd's purse (*Capsella bursa-pastoris* (*C. b-p*)) plants, which produces significantly enhanced symptom development and TuYV accumulation, and in which the ST9aRNA gains systemic movement and aphid transmissibility through encapsidation by TuYV capsid proteins (Sanger et al. 1994; Falk and Duffus 1984; Passmore et al. 1993). Another pertinent example is the aforementioned carrot motley dwarf (CMD) disease complex, which also shows enhanced symptom development in various apiaceous hosts, and in which CMoV and CRLVaRNAs are known to be dependent on CRLV for aphid transmission (Watson and Falk 1994; Waterhouse and Murant 1983; Watson et al. 1998; Murant et al. 1985; Murant et al. 1969). Genome maps of each of these viruses and the

proteins they encode are depicted in Figure 1. It has also been found that some poleroviruses can, presumably, utilize the cell-to-cell movement proteins (MPs) of a co-infecting umbravirus, allowing the polerovirus to presumably escape phloem limitation and become mechanically transmissible (Zhou et al. 2017; Ryabov et al. 2001a; Hoffman et al. 2001). While there are a good number of studies on polerovirus-tlaRNA and polerovirus-umbravirus interactions, there currently exist few studies on umbravirus-tlaRNA interactions.

To further parse the various virus-virus interactions that occur in these disease complexes, we used aphid inoculation of TuYV in combination with agroinfiltration of infectious clones of CMoV and three tlaRNAs—CRLVaRNAs Gamma and Sigma, and ST9aRNA, heretofore referred to simply as Gamma, Sigma, and ST9—to generate single, double, and triple infections of each of these viruses and examine their effects on symptom development, systemic movement of tlaRNAs, and on aphid and mechanical transmission of each of these viruses. In this study, TuYV was used in place of CRLV because we did not have on hand the specific aphid vector (*Cavariella aegopodii*) of this virus (Murant et al. 1969; Elnagar and Murant 1978), whereas we did have the aphid vector (*Myzus persicae*) of TuYV as well as an active culture of TuYV maintained in *C. b-p.* plants. Our results show that CMoV appears to be a driver of symptom development when co-infected with TuYV and/or Sigma or ST9. CMoV also facilitated the systemic movement of all three tlaRNAs—albeit with differing efficiencies—in the absence of TuYV, corroborating the results of a recent study that demonstrated umbravirus-facilitated tlaRNA systemic movement in the tobacco bushy top disease (TBTD) complex (Chen et al. 2022).

CMoV could also facilitate mechanical transmission of Sigma and ST9 (but not Gamma) and TuYV; the transmission rate of TuYV from plants co-infected with only CMoV was very

low, however when co-infected with both CMoV and either Sigma or ST9, the transmission rate of TuYV greatly increased. This is the first report to demonstrate that umbravirus co-infection can impart mechanical transmissibility to tlaRNAs and that some tlaRNAs appear to increase the efficiency with which a co-infecting polerovirus can be mechanically transmitted from plants also co-infected with an umbravirus. Effects of co-infection on the ability of CMoV and the tlaRNAs to be co-aphid transmitted with TuYV, as well as effects on the accumulation of each of these viruses were also determined.

Materials and Methods

Establishing mixed infections

Combined aphid and *Agrobacterium tumefaciens*-mediated inoculations were used to generate the various single, double, and triple infections examined in this study which are listed in Table 1. For TuYV inoculation, non-viruliferous green peach aphids (*Myzus persicae*) were fed on TuYV infected *C.b-p* plants for 18-24 hours, after which they were transferred to 2-3 week old healthy *Nicotiana benthamiana* seedlings for a four day inoculation access period (IAP), after which aphids were killed by spraying with BioAdvanced 3-In-1 Insect, Disease, and Mite Control (Bayer). The plants were kept in an air conditioned room until they grew large enough for agro-inoculation (4-6 leaf stage).

For CMoV and tlaRNA inoculations, cultures of *A. tumefaciens* strain GV3101, transformed individually with infectious clones of each virus, were prepared as described by Erickson et al. (2022); cultures resuspended in infiltration buffer were adjusted to an optical density at 600 nm ($O.D._{600}$) of 1.0. The *A. tumefaciens* cultures were infiltrated using a needless syringe into 3-4 leaves of healthy or TuYV-inoculated *N. benthamiana* plants at the 4-6 leaf stage; for treatments including both CMoV and a tlaRNA, cultures were mixed 1:1 prior to

infiltration. The plants were maintained in the air conditioned room for 4-5 days post inoculation (dpi) then transferred to a growth chamber kept at 19 ℃, 70% relative humidity (RH), and 16:8 hour light:dark photoperiod. After 3 weeks post infection (wpi) tissue was collected and stored at -80 ℃ prior to RNA extraction and RT-qPCR analysis. For treatments without tlaRNAs, tissue was only collected from non-inoculated leaves; for treatments with a tlaRNA, tissue was collected from both inoculated and systemic leaves. The experiments were repeated twice.

Aphid transmission experiments

To determine how different infection combinations affected the ability of each of the viruses in this study to be aphid transmitted, aphid transmission experiments were conducted as described in the previous section, this time using as the inoculum source leaf tissue from healthy plants and plants infected with the various single and multi-virus combinations described above. For treatments with a tlaRNA alone, TuYV with any tlaRNA, or CMoV+Gamma, agroinoculated leaves were used as the inoculum source; for all other treatments non-inoculated leaf tissue was used. Inoculated plants were maintained under the same conditions as the plants described in the previous section. After 4 wpi symptoms were noted and leaf tissue was collected and stored at -80 ℃ prior to RNA extraction and RT-qPCR analysis. The experiments were repeated twice.

Mechanical transmission experiments

To determine how different infection combinations affected the ability of each of the viruses in this study to be mechanically transmitted, leaf tissue from healthy plants and plants harboring each of the described virus infection treatments was ground with a mortar and pestle in 0.03 M KPO_4 + 0.1% Na_2SO_3 (pH 7) buffer in a 1:6 ratio (w/v), with celite added as an abrasive. For treatments with tlaRNAs alone, TuYV+tlaRNAs, or CMoV+Gamma, infiltrated leaves were used as the inoculum source, for all other treatments non-inoculated leaves were used. Using a

sterile cotton swab, the homogenized plant sap was gently rubbed onto 3-4 leaves of healthy *N. benthamiana* plants at the 4-6 leaf stage. Plants were kept in a growth chamber held at 19 ℃, 70% relative humidity (RH), and 16:8 hour light:dark photoperiod. At about 3-4 wpi, symptoms were noted and leaf tissue was collected and stored at -80 ℃ prior to RNA extraction and RT-qPCR analysis. The experiments were repeated twice.

Multiplexed RT-qPCR assay validation

Primer and probe sequences specific to each virus used in this study were designed using the PrimerQuest Tool (www.idtdna.com/PrimerQuest/Home/Index). Standard curves were made using plasmids harboring cloned viral genome sequences of each virus to determine the amplification efficiency of each primer/probe set (without fluorophore); temperature gradient analysis was also performed to determine an optimal annealing temperature. The assays were performed on the CFX96 Touch Real-Time PCR Detection System (Bio-Rad), in a reaction mix containing 10 µl of SsoAdvanced Universal SYBR® Green Supermix (Bio-Rad) 0.6 µl of each primer (10 µM), 2 µl of template, and 6.8 µl of nuclease free water. The thermocycling conditions were 95 ℃ for 3 m followed by 40 cycles of 95 ℃ for 10 s and 55-65 ℃ for 30 s, and concluded with melt curve analysis; a shared optimal temperature of 60 ℃ was selected**.** Each primer set was tested against non-target virus plasmids to confirm primer specificity. Next, plasmids with each virus were pooled in equimolar amounts, and standard curve analysis was repeated to confirm the pooled sample had minimal effects on primer amplification efficiency. Primer and probes (with fluorophore) were validated —first individually, then in a multiplexed reaction—in the same manner (excluding temperature gradient and melt-curve analyses), using a reaction mix containing 10 µl of iQ Multiplex Powermix (Bio-Rad), 0.04 µl of each primer (100 µM), 0.02 µl of probe (100 µM), 2 µl of template, and nuclease free water to 20 µl, and the same

thermocycling conditions. The amplification efficiency of all sets was between 90-110%. All primers and probes used in this study are listed in Table S1.

RNA extraction and multiplexed RT-qPCR analysis

Total RNA was extracted from leaf tissue samples using TRIzol™ Reagent (Invitrogen) according to the manufacturer's protocol. For the initial experiments in which the different single and multi-virus infections were established, samples were treated with RQ1 RNase-Free DNase (Promega) and cleaned by phenol/chloroform extraction prior to cDNA synthesis; this was not done for samples from the aphid and mechanical transmission experiments. RNA was used as template with the iScript™ cDNA Synthesis Kit (Bio-Rad); the synthesized cDNA was diluted to 5 ng/µl with nuclease free water. The qPCR reaction contained 10 µl of iQ Multiplex Powermix, 0.04 µl of each primer (100 µM), 0.02 µl of each prober (100 µM), 2 µl (10 ng) of cDNA template, and nuclease free water to 20 µl, and the thermocycling conditions were as described in the previous section. The cytochrome C oxidase gene was used as a reference. Two technical replicates were performed for each sample. The $2^{-\Delta\Delta}$ Ct method was used to calculate the relative viral accumulation in the initial set of experiments establishing the different virus infection treatments.

Statistical analyses

Significant differences in viral accumulation between different single and mixed virus infections were determined using ANOVA using generalized linear models with the corresponding R packages in InfoStat v2008. Normality and homoscedasticity were checked and corrected when necessary and means were separated using Fisher's least significant difference test ($p<0.05$). Data was plotted in GraphPad Prism v.5.03.

Results

Symptom development

No notable symptoms were observed in plants singly infected with any of the viruses, in any plants doubly infected with TuYV and any of the tlaRNAs, or in plants infected with CMoV+Gamma (Figure 2). Plants co-infected with CMoV+Sigma or with CMoV+ST9 developed prominent leaf mosaic symptoms, which were more severe in CMoV+ST9 infected plants which displayed more prominent yellowing as well as mild leaf curling. Plants infected with TuYV+CMoV developed punctate necrotic spots on the leaves, along with mild mosaic symptoms. These same symptoms were observed in plants co-inoculated with TuYV+CMoV+Gamma. In plants co-inoculated with TuYV+CMoV+Sigma or +ST9, the observed symptoms appeared to be a combination of those that were observed in the CMoV+TuYV, CMoV +Sigma, and CMoV+ST9 plants, displaying dramatic leaf mosaic, chlorosis, and punctate necrotic lesion symptoms on leaves (Figure 3). For all non-symptomatic plants and plants co-inoculated with CMoV +Sigma or +ST9, no prominent differences in overall growth were observed (Figure 4a). However, plants co-inoculated with TuYV+CMoV, and TuYV+CMoV +Sigma or +ST9 were severely stunted, and this effect was most severe in the TuYV+CMoV+ST9 co-infected plants (Figure 4b).

Systemic trafficking of tlaRNAs

In plants singly infected with each tlaRNA, none of the tlaRNAs could be detected in the upper non-inoculated leaves, despite being detected in the inoculated leaves. This was also true for plants harboring co-infections of TuYV+Gamma or TuYV+Sigma. In a few plants, while TuYV was detected in non-inoculated leaves, it was not detected in leaves agroinoculated with the tlaRNA, which may explain the lack of tlaRNA systemic movement in these plants.

However, in the majority of the plants tested both TuYV and the tlaRNAs were detected in inoculated leaves, while only TuYV was detected in the upper non-inoculated indicating that, under the conditions used in this study, TuYV did not support systemic trafficking of these tlaRNAs. However, in plants co-infected with TuYV+ST9 both viruses were detected in the upper non-inoculated leaves of three plants (and in the inoculated leaves of all eight plants tested).

In plants infected with CMoV in combination with each of the tlaRNAs, all of the tlaRNAs could be detected in the upper non-inoculated leaves, although this interaction occurred with differing frequencies for the different tlaRNAs. In CMoV+Sigma and CMoV+ST9 co-infected plants, both tlaRNAs were systemically trafficked 100% of the time, however, in CMoV+Gamma co-infected plants, systemic trafficking of Gamma was only observed 50% of the time. Similar results were observed for plants co-infected with TuYV, CMoV, and each of the tlaRNAs. These results are summarized in Table 2.

Relative viral accumulation

The only co-infection treatments which were associated with a significant increase in TuYV accumulation relative to plants infected with TuYV alone were co-infections of TuYV+CMoV (5.50-fold increase), TuYV+CMoV+Gamma (7.84-fold increase in non-inoculated leaves (NILs)), and by far the most dramatic increase (172.66-fold) was observed in the NILs of TuYV+CMoV+ST9 infected plants. All other co-infection treatments resulted in non-significant changes in TuYV accumulation (Figure 5a). CMoV accumulation increased significantly in the inoculated leaves (ILs) (17.08-fold and 10.10-fold) and NILs (22.36-fold and 39.48-fold) of CMoV+ST9 and TUYV+CMoV+ST9 inoculated plants, respectively. All other

infection treatments produced minimal, non-significant changes in CMoV accumulation with respect to accumulation levels in plants inoculated with only CMoV (Figure 5b).

Gamma accumulation levels increased signficantly in the ILs of TuYV+Gamma, CMoV+Gamma, and TuYV+CMoV+Gamma inoculated plants by 3.00-, 25.35-, and 37.25-fold, respectively. Interestingly in the NILs of CMoV+Gamma and TuYV+CMoV+Gamma, Gamma accumulation levels (1.45-fold and 2.15-fold, respectively) did not vary significantly from that in the ILs of plants inoculated with Gamma alone (Figure 5c). Among the tlaRNAs tested in this study, Sigma accumulation varied the most in co-infected plants, relative to that in the ILs of plants inoclated with Simga alone. While Sigma accumulation did not change significantly in the ILs of TuYV+Sigma infected plants (0.55-fold), it increased signficantly both in the ILs (10.47-fold and 7.9-fold) and the NILs (48.66-fold and 30.16-fold) of CMoV+Sigma and TuYV+CMoV+Sigma co-infected plants, respectively (Figure 5d). ST9 accumulation levels were not significantly altered in the ILs of TuYV+ST9 infected plants, and only varied significantly in the ILs of CMoV+ST9 inoculated plants (1.76-fold increase), however a noticeable but non-signficant increasing trend was observed in the NILs of these plants (4.96-fold), as well as in the ILs (5.68-fold) and NILs (5.13-fold) of TuYV+CMoV+ST9 inoculated plants (Figure 5e). It is interesting to note that in some co-infections with ST9, TuYV and CMoV accumulations both dramatically increased, but a compensatory increase in ST9 accumulation was not observed.

Effects of co-infection on mechanical transmission

As expected, when *N. benthamiana* plants were inoculated using tissue from plants infected with any of the viruses in this study not known to be independently mechanically transmissible (TuYV and tlaRNAs), systemic infections were not observed by any of these

viruses; when the rub-inoculated leaves were tested for these viruses, low level amplification of all but Gamma could be detected. This low level detection may simply be attributed to residual inoculum, or it may suggest that some cells could become infected with these viruses by rub inoculation but that the viruses could not move beyond the inoculated cells (data not shown); these results coincide with those from early studies on ST9 in rub inoculated *C. b-p* leaves (Passmore et al., 1993). CMoV was mechanically transmitted and initiated a systemic infection in 100% of the rub-inoculated plants, regardless of whether the inoculum source was infected with CMoV alone or in combination with any of the other viruses. Somewhat unexpectedly, Sigma and ST9 were both efficiently mechanically transmitted (and established systemic infections) from plants co-infected with either of these tlaRNAs and CMoV, and plants co-infected with TuYV+CMoV and either of these tlaRNAs; Sigma was transmitted to 100% and 69%, respectively, of plants when tissue from CMoV+Sigma and TuYV+CMoV+Sigma co-infected plants were used as the inoculum source, and ST9 was transmitted to 100% and 62%, respectively, of plants when tissue from CMoV+ST9 and TuYV+CMoV+ST9 co-inoculated plants, were used as the inoculum source. Gamma could not be detected in the ILs or NILS of any rub inoculated plants, regardles of whether tissue from CMoV+Gamma or TuYV+CMoV+Gamma infected plants was used as the inoculum source. TuYV was transmitted with very low efficiency (11%) from TuYV+CMoV co-infected plants. Interestingly, the efficiency with which TuYV was mechanically transmitted increased markedly from plants co-infected with TuYV+CMoV and either Sigma or ST9. When TuYV+CMoV+Sigma infected plants were used as the inoculum, the transmission rate of TuYV increased to 54%, and when TuYV+CMoV+ST9 infected plants were used as the inoculum source it increased to 77%. This data is summarized in Table 3.

Effects of co-infection on aphid transmission

As expected, none of the viruses in this study not known to be independently aphid transmitted (CMoV and tlaRNAs) could be detected in aphid inoculated plants, when tissue from plants infected singly or in combination with any of these viruses was used as the inoculum. Co-infection with TuYV did facilitate aphid transmission of CMoV when plants co-infected with TuYV+CMoV, TuYV+CMoV+Gamma, and TuYV+CMoV+ST9 were used as the inoculum source—CMoV was transmitted to 42%, 43%, and 64% of recipient plants, resepectively, and TuYV was respectively transmitted to 100%, 77%, and 77% of recipient plants. Neither Gamma nor Sigma became aphid transmissible when co-infected with TuYV, despite TuYV being transmitted to 100% and 92% of recipient plants from these inoculum sources. Triple infections of each of these tlaRNAs with TuYV and CMoV did not yield different results, despite TuYV transmission efficiency remaining high (100% and 77%, respectively). Conversely ST9 was succesffully aphid transmitted with low efficiency (10%) to a single recipient plant from plants co-infected with TuYV+ST9, and was aphid transmitted to 7% of recipient plants when the inoculum source came from plants also infected with TuYV+CMoV. Transmission efficiencies of TuYV in these treatments were 100% and 77% respectively. These results are summarized in Table 4.

Discussion

While there are many studies on polerovirus-tlaRNA and polerovirus-umbravirus interactions in disease complexes harboring various combinations of these viruses, there exist only two recent studies that have begun to touch upon umbravirus-tlaRNA interactions (Yoshida 2020; Chen et al. 2022). While we investigated the effects of co-infection in all possible co-infection combinations of the polerovirus TuYV, the umbravirus CMoV, and the tlaRNAs

Gamma, Sigma, and ST9—with respect to single infections of each of these viruses—perhaps the most intriguing findings we uncovered were those concerning interactions involving CMoV and tlaRNAs.

With respect to symptom development in *N. benthamiana* plants, the most interesting result we found was that almost all co-infections that included CMoV (with the exception of CMoV+Gamma) induced enhanced symptom development in inoculated plants relative to those infected with any virus alone or plants co-infected with TuYV and any tlaRNA. Additionally, there were noticeable differences in symptom presentation depending on if CMoV was co-infected with TuYV (dispersed, punctate, necrotic lesions on leaves) or with either Sigma or ST9 (mosaic symptoms on leaves). There were also notable differences in the severity of leaf mosaic symptoms between co-infections that included Sigma (less severe) and those that included ST9 (more severe), both in double infections with CMoV and in triple infections with TuYV and CMoV. These results suggest that, in this model host and disease complex system, CMoV is the key driver of symptom development since symptoms only occured in co-infections in which it was present. These results also demonstrate marked differences in symptom development with respect to each each of the tlaRNAs; as more of these tlaRNAs are being regularly discovered, it will be interesting to further uncover the various ways they differ in the effects they have on symptom development and interactions they have with co-infecting viruses in these unique disease complexes.

Until recently, it was thought that only poleroviruses were responsible for systemically trafficking tlaRNAs in these disease complexes. However, a recent study by Naoto Yoshida (2020) found that after attempting to aphid transmit CRLV, CMoV, and a CRLVaRNA from CMD affected carrot plants harboring all three of these viruses to Japanese parsley (*Cryptotaenia*

canadensis subsp. *Japonica*), only CMoV and the CRLVaRNA could be detected in the recipient plant, making this the first reported evidence that an umbravirus may support tlaRNA systemic movement in the absence of a co-infecting polerovirus, although these results could also have other potential explanations. In another recent study by Chen at al. (2022), after co-agroinoculation of infectious clones of the umbravirus tobacco bushy top virus (TBTV) with the tobacco vein distorting virus associated RNA (TVDVaRNA) the authors could detect the TVDVaRNA along with TBTV in the distal non-inoculated leaves, thereby confirming an umbravirus could independently support tlaRNA systemic movement. Here, we present data demonstrating that CMoV was able to support systemic movement of all three tlaRNAs (Gamma, Sigma, ST9), however this interaction appeared to be less efficient in co-infections with Gamma, suggesting some degree of specificity in these umbravirus-tlaRNA interactions.

Since neither Gamma nor Sigma moved systemically when co-infected with TuYV alone, it is possible there exists a degree of specificity in polerovirus-tlaRNA interactions. However, in TuYV+ST9 co-infected *N. benthamiana* plants, ST9 only moved systemically 38% of the time, which was odd as these viruses are known to naturally co-occur and form a strong helper-dependence relationship in *Capsella bursa-pastoris* plants (Passmore et al. 1993; Falk and Duffus 1984; Sanger et al. 1994). We speculated this discrepancy might result from combined aphid inoculation of TuYV and agroinoculation of ST9 effectively failing to introduce these two viruses into the same cells. To address this we conducted preliminary experiments in which we coinfiltrated each of the tlaRNAs with an infectious clone of another polerovirus (barley virus G (BVG)) that we had on hand (Erickson et al. 2023). Interestingly, ST9 could be detected along with BVG in the upper NILs in 100% of co-infected plants; neither Gamma nor Sigma were

detected in the upper non-inoculated leaves, suggesting that potential specificity in polerovirus+tlaRNA interactions may be driven by the tlaRNA (Figure S1).

In several of these virus disease complexes, it has been found that co-infection increases viral RNA accumulation of one or more of the co-infecting viruses (Sanger et al. 1994; Yoshida 2020; Chen et al. 2022). Our results shows that tlaRNA ST9 appears to have a significant impact on CMoV accumulation, both in CMoV+ST9 and TuYV+CMoV+ST9 co-infections, and on TuYV accumulation in TUYV+CMoV+ST9 co-infected plants. These dramatic increases in CMoV and TuYV accumulation could potentially explain why symptom development was most severe in plants harboring these co-infection combinations. Surprisingly, TuYV+ST9 co-infection in *N. benthamiana* plants did not stimulate a significant increase in TuYV accumulation, which was again unexpected given that in natural TuYV+ST9 co-infections in *C. bursa-pastoris*, the accumulation of both TuYV genomic RNAs and capsid proteins significantly increased (Passmore et al. 1993; Falk and Duffus 1984; Sanger et al. 1994). This discrepancy may again indicate a requirement for certain host factor(s) to facilitate TuYV+ST9 interactions.

Interestingly, the relative accumulation of Gamma increased significantly in the ILs of CMoV+Gamma and TuYV+CMoV+Gamma co-infected plants, but minimal differences in Gamma accumulation were observed in the NILs. A somewhat similar effect was observed for ST9 in CMoV+ST9 infected plants, wherein a significant increase was observed in ILs but not in NILs of CMoV+ST9 inoculated plants, however there was a notable increasing trend of ST9 in the NILs. The opposite was observed for Sigma, wherein a non-significant increasing trend in Sigma accumulation was observed in the ILs of CMoV+TuYV and TuYV+CMoV+ST9 inoculated plants, while a significant increase was observed in the NILs; this overall increase in

accumulation of Sigma may partially explain the enhanced mosaic leaf symptoms observed in these co-infected plants.

The mechanisms responsible for increased accumulation of some viruses as a result of co-infection aren't precisely known, however there are three main ways this is thought—and in some instances has been demonstrated—to occur (Alcaide et al. 2020; Latham and Wilson 2008; Rochow 1972; Syller 2012). One is that co-infection functions to increase the replication of one or more co-infecting viruses, resulting in more viral copies per cell, as has been found in co-infections of the plant infecting reoviruses southern rice-black streaked dwarf virus (SRBSDV) and rice ragged stunt virus (RRSV), and for TuYV and ST9 in *C. b-p.* plants (Passmore et al. 1993; Li et al. 2017). Another possibility is that umbravirus encoded movement proteins interact with co-infecting heterologous viral RNAs to impart them with cell-to-cell and systemic movement within the plant thereby resulting in more cells being infected with the dependent virus, as has been observed in co-infections of the polerovirus potato leafroll virus (PLRV) with the umbravirus pea enation mosaic virus 2 (PEMV2) (Ryabov et al. 2001a). This could explain the increase of TuYV accumulation in the presence of CMoV, since on its own TuYV is phloem limited and co-infection may help it break this phloem limitation. Weak interactions between Gamma RNAs and CMoV movement protetins may explain the differences in accumulation of Gamma between the ILs and NILs of plants co-infected with CMoV, as well as the reduced efficiency of systemic transport of Gamma. A third possibility is that one or more of the co-infecting viruses have different host defense mechanisms that can supress host defense systems against which the other co-infecting virus(es) may be susceptible. For example, the P0 protein of some poleroviruses, including TuYV, functions as a supressor of the RNA interference (RNAi) system of the host plant (Csorba et al. 2010; Bortolamiol et al. 2007; Baumberger et al. 2007).

TlaRNA ST9 was found to have a structural feature in the 3' untranslated region (UTR) of its genomic RNA that functions to stall host XRN1 degradation (Campbell et al. 2022), which may explain the dramatic effect ST9 appeared to have on TuYV and CMoV accumulation in co-infected plants. The long distance movement protein (encoded by ORF3) of umbraviruses has been shown to form protective ribonucleoprotein complexes with both umbravirus and heterologous virus RNAs (Ryabov et al. 2001b; Taliansky et al. 2003), and has also been shown in PEMV2 to protect viral RNAs from the host nonsense mediated decay (NMD) degradation pathway (May et al. 2020). Perhaps the combined effects of the TuYV P0 RNAi silencing suppressor (RSS) activity, putative CMoV derived NMD resistance, and stalling of XRN1 degradation by ST9 could explain the drastic increases of TuYV and CMoV in co-infections of these three viruses and the severe symptom development. It is likely that a combination of these these various viral functions interplay to produce the variable effects on viral accumulation and disease presentation observed in the different co-infections of the viruses used in this study.

There are multiple examples of umbraviruses conferring mechanical transmissibility to a co-infecting polerovirus. Falk et al. (1979) showed that TuYV (formerly referred to as beet western yellows virus (BWYV) was occasionally mechanically transmitted from plants co-infected with the umbravirus, lettuce speckles mottle virus (LSMV), and PLRV has been observed to gain mechanical transmissibility as a result of co-infection with PEMV2 (Ryabov et al. 2001a; Falk and Duffus 1979). In the latter study, it was also found that PLRV became mechanically transmissible when co-infected with a cucumber mosaic virus (CMV) vector engineered to express the GRV ORF4 protein, suggesting that this protein likely plays an important mechanistic role in mechanical transmission. However, when PLRV was coinoculated with a GRV-ORF4 expressing CMV vector that had a defective 2b RSS, mechanical

transmissibility of PLRV was lost, further highlighting the likely role virus encoded host defense suppressors may play in such interactions. However, there are other examples of polerovirus-umbravirus co-infections that did not confer mechanical transmissibility to the polerovirus, as has been observed in co-infections of tobacco bushy top virus (TBTV) and tobacco vein distorting virus (TVDV) (Chen et al. 2022). While it has been speculated, no studies have been pulished on whether an umbravirus can confer mechanical transmissibility to a tlaRNA, until now. In this study, we found that both Sigma and ST9 could be mechanically transmitted from plants co-inoculated with CMoV; Gamma, conversely, did not gain mechanical transmissibility.

When TuYV was co-infected with CMoV alone, it became mechanically transmissible, but with extremely low efficiency (11%). However, when TuYV was co-inoculated with CMoV and either Sigma or ST9, the efficiency of TuYV mechanical transmission greatly increased. The observed increase in TuYV accumulation in these plants may partially explain the increased rate of mechanical transmission of TuYV. Conversely, the low accumulation of Gamma may help to explain why this tlaRNA could not be mechanically co-transmitted with CMoV.

We also found that CMoV became aphid transmissible when co-infected with TuYV, except from plants co-infected with TuYV+CMoV+Sigma. This supports similar findings that demonstrate CMoV could be transmitted by *M. persicae* aphids when co-infected with either of the poleroviruses potato leaf roll virus (PLRV) or beet western yellows virus (BWYV), along with other examples of compatible interactions betwe non-naturally co-occurring poleroviruses and umbraviruses, which could have important epidemiological implications for the development of novel disease complexes or transmission of umbraviruses to novel hosts (Zhou et al. 2017; Abraham et al. 2014). CMoV was transmitted with the greatest efficiency (64%) from plants co-infected with TuYV+CMoV+ST9. Whether this increase in CMoV co-transmission rate in the

presence of ST9, or the lack of CMoV co-transmission observed when Sigma was present, are indicative of potential syngeristic and antagonistic effects, respectively, requires further investigation. Similar to other findings in this study, while ST9 did become aphid transmissible when co-infected with TuYV, the transmission rate was lower than expected, again highlighting the potential need of host specific factors for this interaction.

Together, these findings add to the growing body of knowledge on disease complexes involving these types of viruses and provide novel insights into the virus-virus interactions that occur. Such information could potentially be employed in programs aimed at preventing or controlling outbreaks of such disease complexes and perhaps could be used in the development of novel virus-based gene delivery systems.

Acknowledgements

We thank Dr.s Yen-Wen Kuo and Jun Jiang for their valuable input and advice on the mechanical transmission experiments and data presentation, respectively. This work was supported in part by the University of California, Davis.

References

Abraham, Adane D., Wulf Menzel, Berhanu Bekele, and Stephan Winter. 2014. "A Novel Combination of a New Umbravirus, a New Satellite RNA and Potato Leafroll Virus Causes Tobacco Bushy Top Disease in Ethiopia." *Archives of Virology* 159 (12): 3395–99. https://doi.org/10.1007/s00705-014-2202-4.

Alcaide, Cristina, M. Pilar Rabadán, Manuel G. Moreno-Pérez, and Pedro Gómez. 2020. "Implications of Mixed Viral Infections on Plant Disease Ecology and Evolution." *Advances in Virus Research* 106 (0065–3527): 145–69. https://doi.org/10.1016/bs.aivir.2020.02.001.

Barker, H. 1989. “Specificity of the Effect of Sap-Transmissible Viruses in Increasing the Accumulation of Luteoviruses in Co-Infected Plants.” *Annals of Applied Biology* 115 (1): 71–78. https://doi.org/10.1111/j.1744-7348.1989.tb06813.x.

Baumberger, Nicolas, Ching-hsui Tsai, Miranda Lie, and Ericka Havecker. 2007. “Report The Polerovirus Silencing Suppressor P0 Targets ARGONAUTE Proteins for Degradation.” *Current Biology* 17 (18): 1609–14. https://doi.org/10.1016/j.cub.2007.08.039.

Bortolamiol, Diane; Pazhouhandeh, Maghsoud; and Veronique Marrocco, Katia; Genschik, Pascal; Ziegler-Graff. 2007. “The Polerovirus F Box Protein P0 Targets ARGONAUTE1 to Suppress RNA Silencing.” *Current Biology* 17 (18): 1615–21. https://doi.org/10.1016/j.cub.2007.07.061.

Brault, V., J. F. J. M. van den Heuvel, M. Verbeek, V. Ziegler-Graff, A. Reutenauer, E. Herrbach, J.-C. Garaud, H. Guilley, K. Richards, and G. Jonard. 1995. “Aphid Transmission of Beet Western Yellows Luteovirus Requires the Minor Capsid Read-through Protein P74.” *The EMBO Journal* 14 (4): 650–59. https://doi.org/10.1002/j.1460-2075.1995.tb07043.x.

Campbell, A. J., Anna Erickson, Evan Pellerin, Nidá Salem, Xiaohan Mo, Bryce W. Falk, and Inmaculada Ferriol. 2020. “Phylogenetic Classification of a Group of Self-Replicating RNAs That Are Common in Co-Infections with Poleroviruses.” *Virus Research* 276 (January). https://doi.org/10.1016/J.VIRUSRES.2019.197831.

Campbell, A. J., John R. Anderson, and Jeffrey Wilusz. 2022. “A Plant-Infecting Subviral RNA Associated with Poleroviruses Produces a Subgenomic RNA Which Resists Exonuclease XRN1 in Vitro.” *Virology* 566: 1–8. https://doi.org/10.1016/j.virol.2021.11.002.

Chen, Xiaojiao, Hengming Luo, Jingyi Zhang, Yan Ma, Kehua Li, Feng Xiong, and and Fan Li Yahui Yang, Jiazhen Yang, Pingxiu Lan, Taiyun Wei, Yi Xu, Hairu Chen. 2022. “Synergism

Among the Four Tobacco Bushy Top Disease Casual Agents in Symptom Induction and Aphid Transmission." *Frontiers in Microbiology* 13. https://doi.org/10.3389/fmicb.2022.846857.

Csorba, Tibor, Rita Lózsa, György Hutvágner, and József Burgyán. 2010. "Polerovirus Protein P0 Prevents the Assembly of Small RNA-Containing RISC Complexes and Leads to Degradation of ARGONAUTE1." *Plant Journal* 62 (3): 463–72. https://doi.org/10.1111/j.1365-313X.2010.04163.x.

Elnagar, S., and A. F. Murant. 1978. "Relations of Carrot Red Leaf and Carrot Mottle Viruses with Their Aphid Vector, Cavariella Aegopodii." *Annals of Applied Biology* 89 (2): 237–44. https://doi.org/10.1111/j.1744-7348.1978.tb07695.x.

Erickson, Anna, Jun Jiang, Yen-wen Kuo, and Bryce W. Falk. 2023. "Construction and Use of an Infectious CDNA Clone to Identify Aphid Vectors and Susceptible Monocot Hosts of the Polerovirus Barley Virus G." *Virology* 579: 178–85. https://doi.org/10.1016/j.virol.2023.01.011.

Falk, B.W., J.E. Duffus, and T.J. Morris. 1979. "Transmission, Host Range, and Serological Properties of the Viruses That Cause Lettuce Speckles Disease." *Phytopathology* 69: 612–17.

Falk, B. W. andDuffus, J. E. 1984. "Identification of Small Single- and Double-Stranded RNAs Associated with Severe Symptoms in Beet Western Yellows Virus-Infected Capsella Bursa-Pastoris." *Phytopathology* 74 (10): 1224–29. https://doi.org/10.1094/phyto-74-1224.

Hoffman, K., M. Verbeek, A. Romano, A.M. Dullemans, J.F.J.M. van den Heuvel, F. van der Wilk. 2001. "Mechanical Transmission of Poleroviruses." *Journal of Virological Methods* 91 (2): 197–201. https://doi.org/10.1016/S0166-0934(00)00256-1.

Hull, R., and A. N. Adams. 1968. “Groundnut Rosette and Its Assistor Virus.” *Annals of Applied Biology* 62 (1): 139–45. https://doi.org/10.1111/j.1744-7348.1968.tb03857.x.

Kim, Sang Hyon, Stuart Macfarlane, Natalia O Kalinina, Daria V Rakitina, Eugene V Ryabov, Trudi Gillespie, Sophie Haupt, John W. S. Brown, and Michael Taliansky. 2007. “Interaction of a Plant Virus-Encoded Protein with the Major Nucleolar Protein Fibrillarin Is Required for Systemic Virus Infection.” *PNAS* 104 (26): 11115–20. https://doi.org/10.1073/pnas.0704632104.

Latham, Jonathan R., and Allison K. Wilson. 2008. “Transcomplementation and Synergism in Plants: Implications for Viral Transgenes?” *Molecular Plant Pathology* 9 (1): 85–103. https://doi.org/10.1111/j.1364-3703.2007.00441.x.

Li, Shu, Tong Zhang, Yingzhi Zhu, and Guohui Zhou. 2017. “Co-Infection of Two Reoviruses Increases Both Viruses Accumulation in Rice by up-Regulating of Viroplasm Components and Movement Proteins Bilaterally and RNA Silencing Suppressor Unilaterally.” *Virology Journal* 14 (1): 1–8. https://doi.org/10.1186/s12985-017-0819-0.

May, Jared P., Philip Z. Johnson, Muhammad Ilyas, Feng Gao, and E. Simon. 2020. “The Multifunctional Long-Distance Movement Protein of Pea Enation Mosaic Virus 2 Protects Viral and Host Transcripts from Nonsense-Mediated Decay.” *MBio* 11 (2): 1–16.

Mayo, M. A., and V. Ziegler-Graff. 1996. “Molecular Biology of Luteoviruses.” *Advances in Virus Research* 46: 413–60. https://doi.org/10.1016/S0065-3527(08)60077-9.

Murant, A. F., R. Rajeshwari, D. J. Robinson, and J. H. Raschki. 1988. “A Satellite RNA of Groundnut Rosette Virus That Is Largely Responsible for Symptoms of Groundnut Rosette Disease.” *J. Gen. Virol* 69 (7): 1479–86. https://doi.org/10.1099/0022-1317-69-7-1479.

Murant, A. F. 1990. “Dependence of Groundnut Rosette Virus on Its Satellite RNA as Well as on

Groundnut Rosette Assistor Luteovirus for Transmission by Aphis Craccivora." *Journal of General Virology* 71 (9): 2163–66. https://doi.org/10.1099/0022-1317-71-9-2163.

Murant, A. F., R. A. Goold, I. M., Roberts, and J. Cathro. 1969. "Carrot Mottle-a Persistent Aphid-Borne Virus with Unusual Properties and Particles." *J. Gen. Virol.* 4: 329–41. https://doi.org/10.1099/0022-1317-4-3-329.

Murant, A. F., P. M. Waterhouse, J. H. Raschki~, and D. J. Robinson. 1985. "Carrot Red Leaf and Carrot Mottle Viruses: Observations on the Composition of the Particles in Single and Mixed Infections." *J. Gen. Virol*. Vol. 66. https://doi.org/10.1099/0022-1317-66-7-1575.

Naidu, R. A., H. Bottenber, P. Subrahmanyam, F. M. Kimmins, D. J. Robinson, and J. M. Thresh. 1998. "Epidemiology of Groundnut Rosette Virus Disease: Current Status and Future Research Needs." *Annals of Applied Biology* 132 (3): 525–48. https://doi.org/10.1111/j.1744-7348.1998.tb05227.x.

Nurkiyanova, Kulpash M., Eugene V. Ryabov, Natalia O. Kalinina, Yongchang Fan, Igor Andreev, Alexander G. Fitzgerald, Peter Palukaitis, and Michael Taliansky. 2001. "Umbravirus-Encoded Movement Protein Induces Tubule Formation on the Surface of Protoplasts and Binds RNA Incompletely and Non-Cooperatively." *Journal of General Virology* 82 (10): 2579–88. https://doi.org/10.1099/0022-1317-82-10-2579.

Pagán, Israel, and Edward C. Holmes. 2010. "Long-Term Evolution of the Luteoviridae : Time Scale and Mode of Virus Speciation." *Journal of Virology* 84 (12): 6177–87. https://doi.org/10.1128/jvi.02160-09.

Passmore, Boni K., Margaret Sanger, Lih-Shen Chin, Bryce W. Falk, and George Bruening. 1993. "Beet Western Yellows Virus-Associated RNA: An Independently Replicating RNA That Stimulates Virus Accumulation." *Proceedings of the National Academy of Sciences of*

the United States of America 90 (21): 10168–72. https://doi.org/10.1073/PNAS.90.21.10168.

Peter, K. A., F. Gildow, P. Palukaitis, and S. M. Gray. 2009. "The C Terminus of the Polerovirus P5 Readthrough Domain Limits Virus Infection to the Phloem." *Journal of Virology* 83 (11): 5419–29. https://doi.org/10.1128/JVI.02312-08.

Rochow, W. F. 1972. "The Role of Mixed Infections in the Transmission of Plant Viruses by Aphids." *Annual Review of Phytopathology* 10 (1): 101–24. https://doi.org/10.1146/annurev.py.10.090172.000533.

Ryabov, Eugene V., Gillian Fraser, Mike A. Mayo, Hugh Barker, and Michael Taliansky. 2001a. "Umbravirus Gene Expression Helps Potato Leafroll Virus to Invade Mesophyll Tissues and to Be Transmitted Mechanically Between Plants." *Virology* 286 (2): 363–72. https://doi.org/10.1006/viro.2001.0982.

Ryabov, Eugene V., David J. Robinson, and Michael Taliansky. 2001b. "Umbravirus-Encoded Proteins Both Stabilize Heterologous Viral RNA and Mediate Its Systemic Movement in Some Plant Species." *Virology* 288 (2): 391–400. https://doi.org/10.1006/viro.2001.1078.

Sanger, Margaret, Boni Passmore, Bryce W. Falk, George Bruening, Biao Ding, and William J. Lucas. 1994. "Symptom Severity of Beet Western Yellows Virus Strain ST9 Is Conferred by the ST9-Associated RNA and Is Not Associated with Virus Release from the Phloem." *Virology* 200 (1): 48–55. https://doi.org/10.1006/viro.1994.1161.

Storey, H. H., and A. K. Ryland. 1955. "Transmission of Groundnut Rosette Virus." *Annals of Applied Biology* 43 (3): 423–32. https://doi.org/10.1111/j.1744-7348.1955.tb02492.x.

Syller, Jerzy. 2012. "Facilitative and Antagonistic Interactions between Plant Viruses in Mixed Infections." *Molecular Plant Pathology* 13 (2): 204–16. https://doi.org/10.1111/J.1364-

3703.2011.00734.X.

Taliansky, M. E., D. J. Robinson, and A. F. Murant. 1996. “Complete Nucleotide Sequence and Organization of the RNA Genome of Groundnut Rosette Umbravirus.” *Journal of General Virology* 77 (9): 2335–45. https://doi.org/10.1099/0022-1317-77-9-2335.

Taliansky, Michael E., D. J. Robinson, and A. F. Murant. 2000. “Groundnut Rosette Disease Virus Complex: Biology and Molecular Biology.” *Advances in Virus Research*. Vol. 55. https://doi.org/10.1016/S0065-3527(00)55008-8.

Taliansky, Michael E., and David J. Robinson. 2003. “Molecular Biology of Umbraviruses: Phantom Warriors.” *Journal of General Virology*. Microbiology Society. https://doi.org/10.1099/vir.0.19219-0.

Taliansky, Michael, Ian M. Roberts, Natalia Kalinina, Eugene V. Ryabov, Shri Krishna Raj, David J. Robinson, and Karl J. Oparka. 2003. “An Umbraviral Protein, Involved in Long-Distance RNA Movement, Binds Viral RNA and Forms Unique, Protective Ribonucleoprotein Complexes.” *Journal of Virology* 77 (5): 3031–40. https://doi.org/10.1128/jvi.77.5.3031-3040.2003.

Waterhouse, P. M., and A. F. Murant. 1983. “Further Evidence on the Nature of the Dependence of Carrot Mottle Virus on Carrot Red Leaf Virus for Transmission by Aphids.” *Annals of Applied Biology* 103 (3): 455–64. https://doi.org/10.1111/j.1744-7348.1983.tb02783.x.

Watson, M. andSerjeant, E.P. 1964. “The Effect of Motley Dwarf Virus on Yield of Carrots and Its Transmission in the Field by Cavariella Aegopdiae Scop.” *Annals of Applied Biology* 53 (1): 77–93. https://doi.org/10.1111/j.1744-7348.1964.tb03782.x.

Watson, M. T., and B. W. Falk. 1994. “Ecological and Epidemiological Factors Affecting Carrot Motley Dwarf Development in Carrots Grown in the Salinas Valley of California.” *Plant*

Disease. https://doi.org/10.1094/PD-78-0477.

Watson, Marion, E. P. Serjeant, and E. A. Lennon. 1964. "Carrot Motley Dwarf and Parsnip Mottle Viruses." *Annals of Applied Biology* 54 (2): 153–66. https://doi.org/10.1111/j.1744-7348.1964.tb01179.x.

Watson, Michael T., Tongyan Tian, Elizabeth Estabrook, and Bryce W. Falk. 1998. "A Small RNA Resembling the Beet Western Yellows Luteovirus ST9-Associated RNA Is a Component of the California Carrot Motley Dwarf Complex." *Phytopathology*. Vol. 88. https://doi.org/10.1094/PHYTO.1998.88.2.164.

Yoshida, Naoto. 2020. "Biological and Genetic Characterization of Carrot Red Leaf Virus and Its Associated Virus/RNA Isolated from Carrots in Hokkaido Japan." *Plant Pathology* 69 (7): 1379–89. https://doi.org/10.1111/ppa.13202.

Zhou, Cui-Ji;, Xiao-Yan Zhang, Song-Yu Liu, Ying Wang, Da-Wei Li, Jia-Lin Yu & Cheng-Gui Han. 2017. "Synergistic Infection of BrYV and PEMV 2 Increases the Accumulations of Both BrYV and BrYV-Derived SiRNAs in Nicotiana Benthamiana." *Scientific Reports* 7 (45132): 1–13. https://doi.org/10.1038/srep45132.

Table 1: Single and mixed virus infections investigated in this study

Single	Double	Triple
TuYV	TuYV+CMoV	TuYV+CMoV+Gamma
CMoV	TuYV+Gamma	TuYV+CMoV+Sigma
Gamma	TuYV+Sigma	TuYV+CMoV+ST9
Sigma	TuYV+ST9	
ST9	CMoV+Gamma	
	CMoV+Sigma	
	CMoV+ST9	

TuYV is the polerovirus, turnip yellows virus, CMoV is the umbravirus, carrot mottle virus, and Gamma, Sigma, and ST9 refer to the specific tombusvirus-like associated RNAs (tlaRNAs).

Table 2: Summary of symptom development and tlaRNA systemic movement in the various single and mixed virus infections established in *Nicotiana benthamiana*

		Single Infection					Double Infection							Triple Infection		
Infecting viruses		TuYV	CMoV	Gamma	Sigma	ST9	TuYV+ Gamma	TuYV+ Sigma	TuYV+ ST9	TuYV+ CMoV	CMoV+ Gamma	CMoV+ Sigma	CMoV+ Gamma	TuYV+ CMoV+ Gamma	TuYV+ CMoV+ Sigma	TuYV+ CMoV+ ST9
Symptoms		No	No	No	No	No	No	No	No	Yes	No	Yes	Yes	Yes	Yes	Yes
tlaRNA systemic movement		-	-	0/10	0/8	0/8	0/10	0/7	3/8	-	4/10	8/8	8/8	4/10	8/8	8/8
No. of plants infected	**TuYV**	22/23	-	-	-	-	10/10	7/7	8/8	22/23	-	-	-	10/10	8/8	8/8
	CMoV	-	21/23	-	-	-	-	-	-	23/23	9/10	8/8	8/8	10/10	8/8	8/8
	tlaRNA	-	-	10/10	8/8	8/8	10/10	7/7	8/8	-	10/10	8/8	8/8	10/10	8/8	8/8

The top row of the table indicates the infecting virus(es), the second row indicates whether symptoms were observed in plants infected with the respective single and co-infection treatments, and the third row indicates the number of plants in which the coinfecting tlaRNA could be detected in the upper non-inoculated leaves. The bottom three rows of the table indicate the infection rates (number of plants infected/number of plants inoculated) for all of the viruses in each treatment.

Table 3: Summary of the mechanical transmission rates of TuYV, CMoV, and tlaRNAs from *N. benthamiana* plants infected with different combinations of each of these viruses.

		Single-virus Infection					Double-virus Infection							Triple-virus Infection		
Viruses in Inoculum		TuYV	CMoV	Gamma	Sigma	ST9	TuYV+ Gamma	TuYV+ Sigma	TuYV+ ST9	TuYV+ CMoV	CMoV+ Gamma	CMoV+ Sigma	CMoV+ ST9	TuYV + CMoV + Gamma	TuYV+ CMoV+ Sigma	TuYV+ CMoV+ ST9
No. of plants infected (%)	**TuYV**	0/18	-	-	-	-	0/23	0/23	0/23	2/18	-	-	-	0/15	7/13	10/13
		0%					0%	0%	0%	11%				0%	54%	77%
	CMoV	-	-	-	-	18/18	-	-	-	18/18	15/15	13/13	13/13	15/15	13/13	13/13
						100%				100%	100%	100%	100%	100%	100%	100%
	tlaRNA	-	0/23	0/23	0/23	-	0/23	0/23	0/23	-	0/15	13/13	13/13	0/15	9/13	8/13
			0%	0%	0%		0%	0%	0%		0%	100%	100%	0%	69%	62%

The top row of the table indicates which viruses were present in the inoculum tissue used for rub inoculation, and the succeeding rows indicate the transmission rate of each virus in each treatment in terms of number of plants infected / number of plants inoculated (white row) and in percentage of plants infected (grey row).

Table 4: Summary of the aphid transmission rates of TuYV, CMoV, and tlaRNAs from *N. benthamiana* plants infected with different combinations of each of these viruses.

		Single-virus infection					Double-virus infection							Triple-virus infection		
Viruses in Inoculum		TuYV	CMoV	Gamma	Sigma	ST9	TuYV+ Gamma	TuYV+ Sigma	TuYV+ ST9	TuYV+ CMoV	CMoV+ Gamma	CMoV+ Sigma	CMoV+ ST9	TuYV+ CMoV+ Gamma	TuYV+ CMoV+ Sigma	TuYV+ CMoV+ ST9
No. of plants infected (%)	**TuYV**	20/25	-	-	-	-	13/13	11/12	10/10	22/24	-	-	-	14/14	10/13	13/14
		80%					100%	92%	100%	92%				100%	77%	77%
	CMoV	-	-	0/25	-	-	-	-	-	10/24	0/15	0/15	0/14	6/14	0/13	9/14
				0%						42%	0%	0%	0%	43%	0%	64%
	tlaRNA	-	0/15		0/14	0/15	0/13	0/12	1/10	-	0/15	0/15	0/14	0/14	0/13	1/14
			0%		0%	0%	0%	0%	10%		0%	0%	0%	0%	0%	7%

The top row of the table indicates which viruses were present in the inoculum tissue used for aphid inoculation, and the succeeding rows indicate the transmission rate of each virus in each treatment in terms of number of plants infected / number of plants inoculated (white row) and in percentage of plants infected (grey row).

Table S1: Primers used for multiplexed RT-qPCR detection and relative quantification of viruses used in this study

Target	Primer/probe name	Sequence	Fluorophore
TuYV	TuYV_qF	GGAAGGACTGTTAGGCTGTAAA	
	TuYV_qR	TAACCCAGCCATCTCTCTCA	
	TuYV_qP	TGCTTTGCACTTTGCTAGGTTGGC	Fam
CMoV	CMoV_qF	GTTAATCACCCAGGAGAGGATG	
	CMoV_qR	CATACTGGGCAACTGGTATGT	
	CMoV_qP	TCTCTGTTGAGCATGAGCGTTGGT	Cy5
Gamma	Gam_qF	GAGCATGTGGGTCTTCTAGTTT	
	Gam_qR	CTCCACCATCTGGTTTCATCTT	
	Gam_qP	TAGTGCGCTCAGCTCCACATCAAA	Texas red
Sigma	Sig_qF	ATGCAAGGAGGGCACATAC	
	Sig_qR	TCACAAACCACCCTCGTAATC	
	Sig_qP	TGTCACTATCGCCGGAACATCTGC	Texas red
ST9	ST9_qF	CGCATCTGGTTGAGGATAGTATAG	
	ST9_qR	GTAGACTGGACTCCCACAATTC	
	ST9_qP	AAACTGTGCTGGAGGTAGACGACC	Texas red
Cytochrome C Oxidase	Cox_qF	CGTCGCATTCCAGATTATCCA	
	Cox_qR	CAACTACGGATATATAAGRRCCRRAAC	
	Cox_qP	AGGGCATTCCATCCAGCGTAAGCA	Hex

Listed are the target viruses and corresponding primer names, sequences, and respective fluorophores used for the multiplexed RT-qPCR assay used in this study.

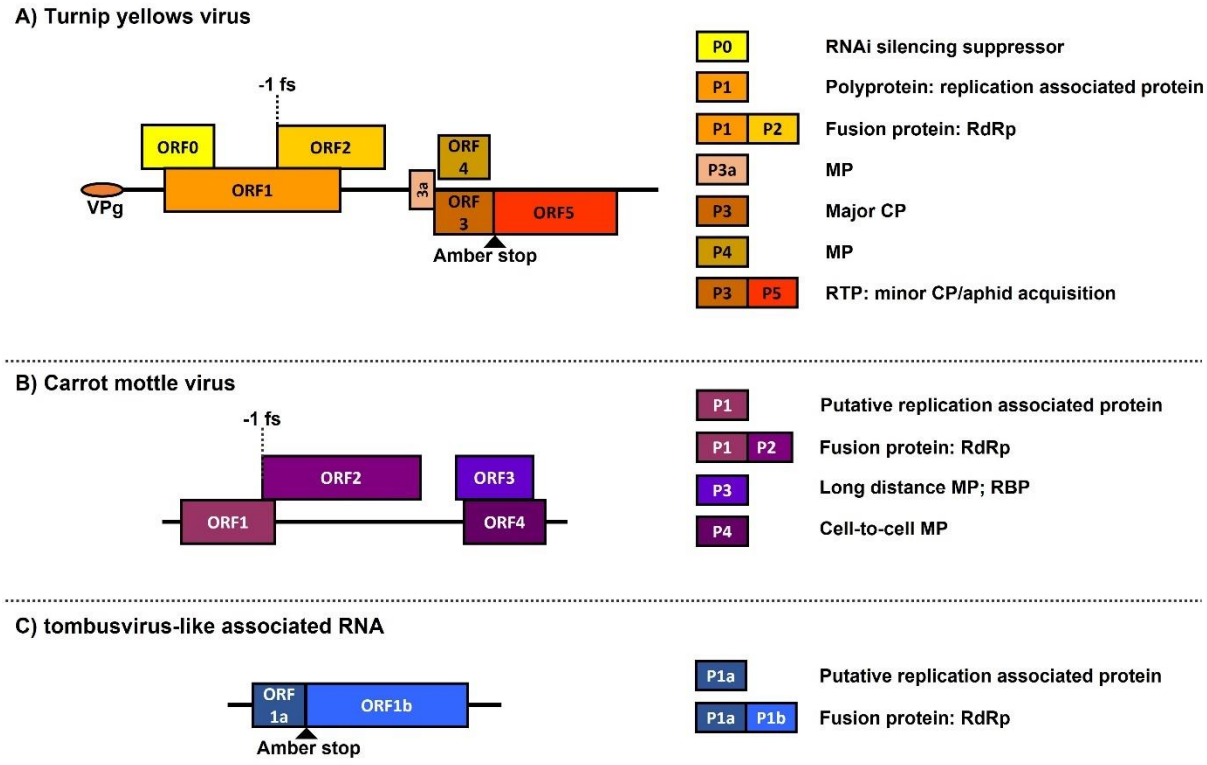

Figure 1. Genome maps of viruses used in this study.

Depicted are graphical representations of: (A) the polerovirus turnip yellows virus (TuYV); (B) the umbravirus carrot mottle virus (CMoV); and (C) a general representation of tombusvirus-like associated RNA (tlaRNA) genome structure. Diagrams are drawn to scale. Solid black lines depict the length of the viral RNA genome. Boxes indicated the open reading frames (ORFs) encoded by each virus, and their positions in relation to the solid black line indicate in which reading frame register (RFR) they occur (Above the line: RFR1; on the line: RFR2; beneath the line: RFR3). Key translation features such as amber stop codons used for translational readthrough and -1 frameshift sites are depicted. The boxes to the right of the genome indicate the known functions of proteins encoded by the corresponding ORFs depicted in the viral genomes. RNAi: RNA interference; RdRp: viral replicase protein; MP: movement protein; CP: capsid protein: RTP: readthrough protein; RBP: RNA binding protein.

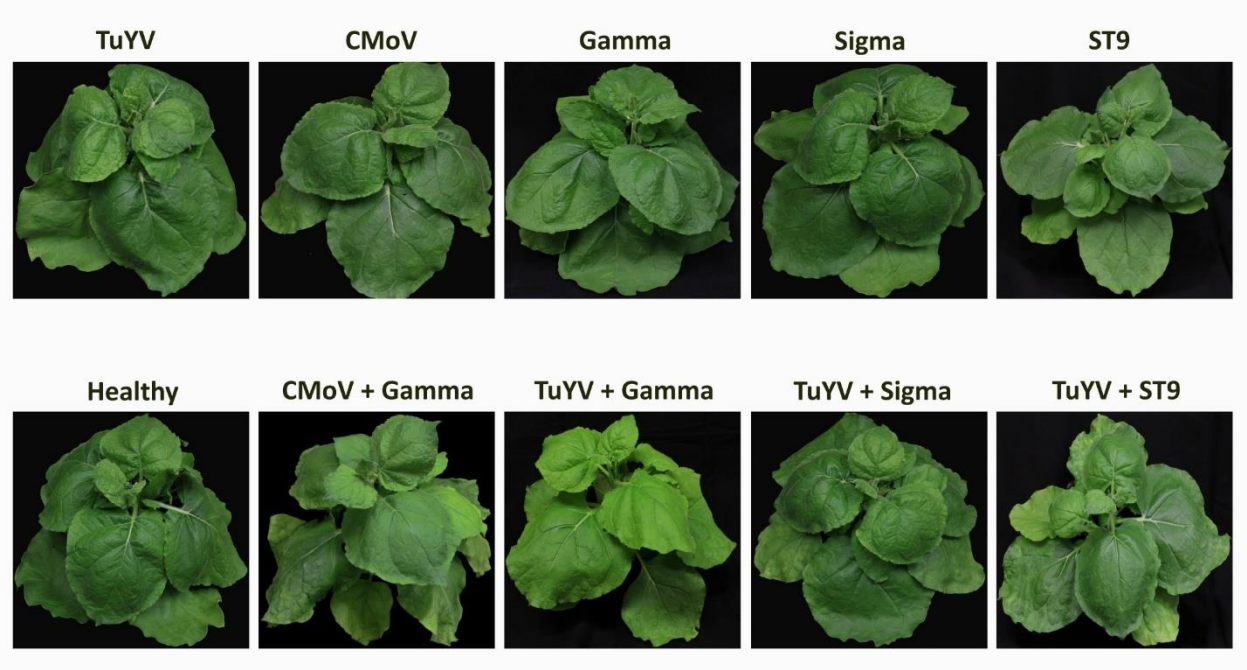

Figure 2. Asymptomatic virus infections in *Nicotiana benthamiana plants*

Depicted are asymptomatic *N. benthamiana* plants that have been inoculated singly with TuYV, CMoV, and tlaRNAs Gamma, Sigma, or ST9, doubly with TuYV and each of the tlaRNAs, and inoculated with CMoV+Gamma, along with a healthy, non-inoculated plant for comparison. Labels above each plant picture indicate the virus infection treatment. Photos were taken 3 wpi.

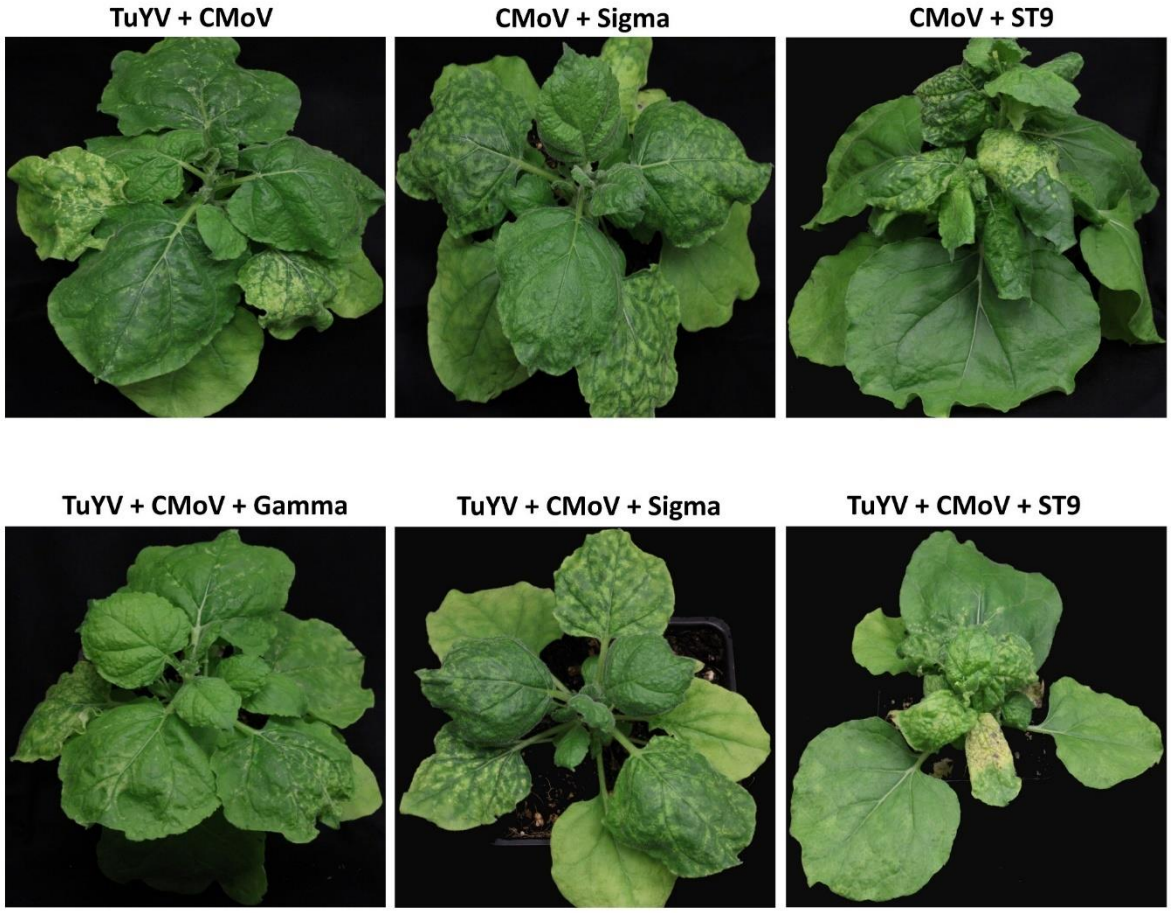

Figure 3. Symptomatic virus infections in *Nicotiana benthamiana* plants

Depicted are asymptomatic plants doubly infected with CMoV and either Sigma or ST9, or CMoV and TuYV, and plants triply infected with TuYV, CMoV, and either Sigma or ST9. Labels above each plant picture indicate the virus infection treatment. Photos were taken 3 wpi.

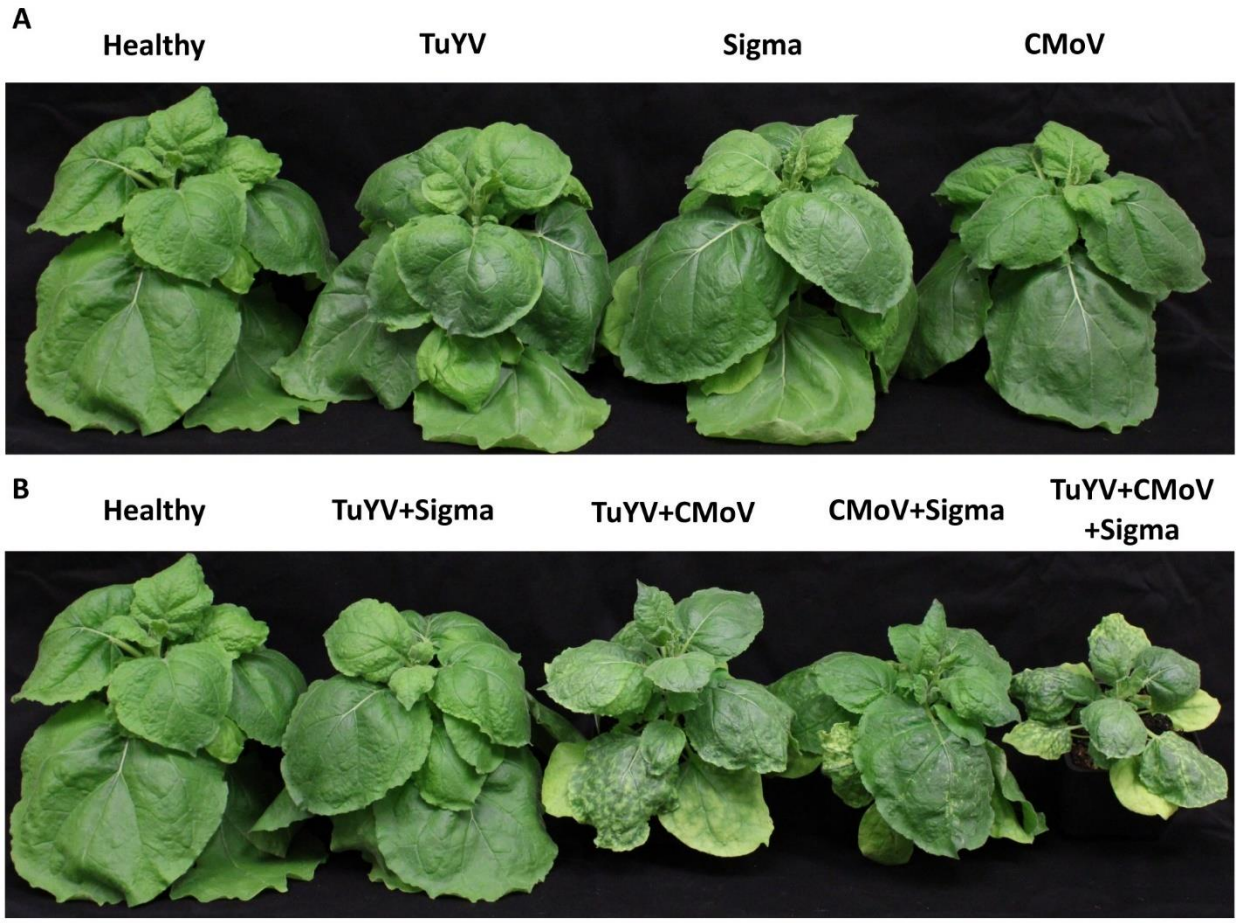

Figure 4: Lineup of virus inoculated *Nicotiana benthamiana* plants

Depicted are *Nicotiana benthamiana* plants harboring single or multi-virus infections of TuYV, CMoV, and/or Sigma. **A)** Asymptomatic virus infections; little to no difference in plant stature was observed between the different virus treatments represented. **B)** Symptomatic virus infections; notable stunting can be seen in plants infected with 2 or more viruses, relative to a healthy control. A similar, albeit more severe, effect was observed for plants harboring co-infections including ST9, whereas this effect was not observed in plants harboring co-infections including Gamma. Labels above each plant picture indicate the virus infection treatment. Photos were taken 3 wpi.

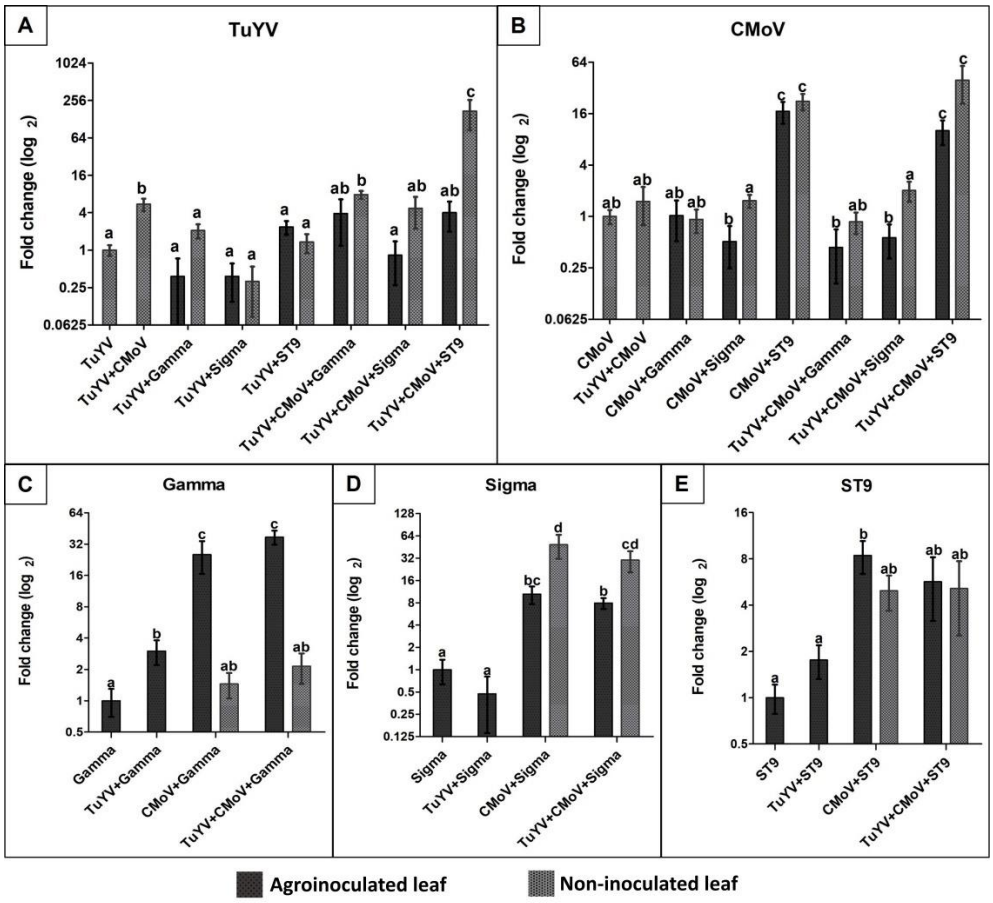

Figure 5. Relative accumulation of TuYV, CMoV, and tlaRNAs Gamma, Sigma, and ST9 as a function of co-infection

Graphs depict $\log_2$ changes in viral accumulation of (**A**) TuYV, (**B**) CMoV, and the tlaRNAs (**C**) Gamma, (**D**) Sigma, and (**E**) ST9 in mixed infections relative to accumulation of each of these viruses in single infections; the y-axis. Virus accumulation was quantified using RT-qPCR and calculated using the $2^{-\Delta\Delta}$ Ct method. Black and grey bars represent relative viral accumulation in agroinoculated and non-inoculated leaves, respectively. Graphs depict the means ± SEs. Significant differences between treatments were determined using ANOVA with a significance value of $p<0.05$; different letters indicate significant differences between treatments, whereas shared letters indicate there was not a significant difference between treatments.

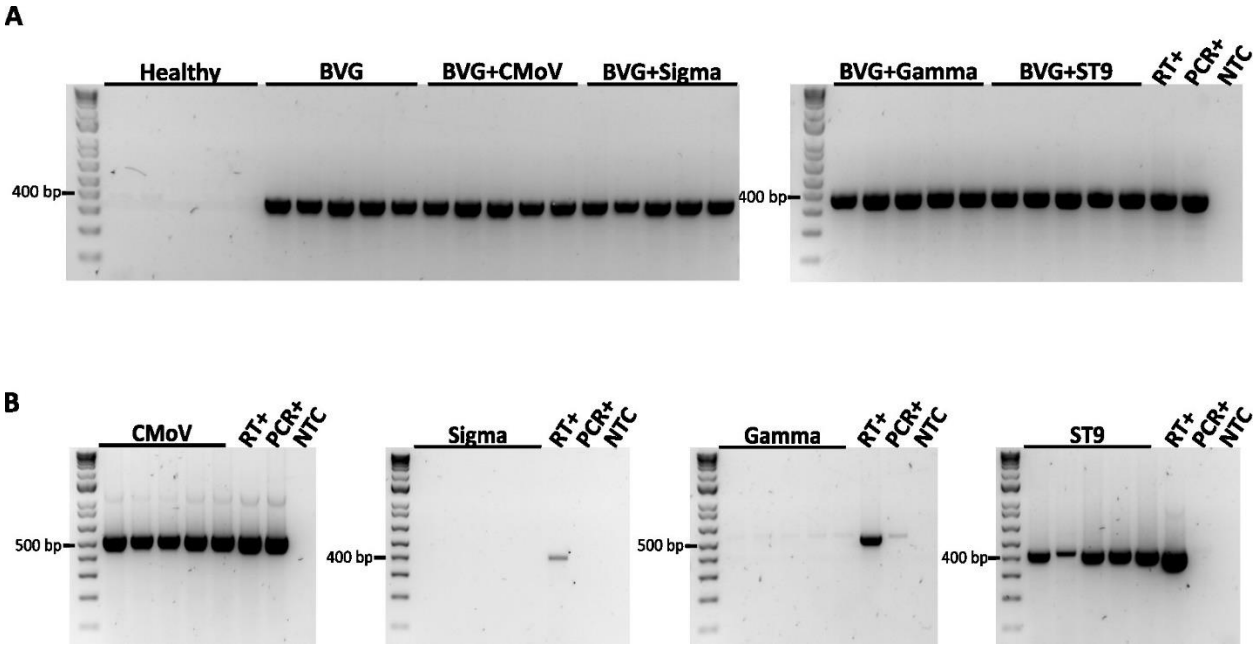

Figure S1. RT-PCR data of from BVG + tlaRNA co-inoculation experiments

Panel **A** shows the products obtained from RT-PCR based detection of BVG in *Nicotiana benthamiana* plants that were agroinoculated with BVG alone, or co-inoculated with BVG and CMoV, or BVG and tlaRNAs Gamma, Sigma, or ST9. Expected product size for BVG is 390 bp. Panel **B** shows products from RT-PCR based detection of CMoV, Gamma, Sigma, and ST9 in *N. benthamiana* plants co-inoculated with BVG and each of these viruses. Expected product sizes are as follows: CMoV=532 bp; Gamma=534 bp; Sigma=399 bp; ST9=430 bp. We suspect the faint bands in the gel image for Gamma detection are likely from minor cross contamination or nonspecific primer binding. RT+: reverse transcription positive control; PCR+: plasmids used as PCR positive controls – some of these did not amplify, we suspect too much plasmid was used in the reaction; NTC: no template control.

Chapter 3

Transcriptome sequencing of apiaceous plants exhibiting symptoms of carrot motley dwarf disease reveals two poleroviruses and a tlaRNA new to the United States, a putative new recombinant polerovirus, and highlights the plasticity and complexity of mutli-virus disease complexes

Anna Erickson[1], Anneliek M. ter Horst[1], Curtis R. Carlson[1], Bryce W. Falk[1]

[1]Department of Plant Pathology, University of California, Davis, CA, 95616, USA

Abstract

In 2020 and 2021 carrot samples from Washington, United States, and flat and curly leaf parsley, and cilantro samples from California, U.S., exhibiting typical symptoms of carrot motley dwarf (CMD) disease were submitted to our lab for diagnosis. Initial RT-PCR based diagnostic assays identified all three of the viruses known to be associated with CMD—the polerovirus Carrot red leaf virus (CRLV), the umbraviruses Carrot mottle virus (CMoV) and/or Carrot mottle mimic virus (CMoMV), and tombusvirus-like associated RNAs (tlaRNAs)—in the carrot samples from Washington, however only the associated umbraviruses and tlaRNAs were detected in the parsley and cilantro samples. The umbraviruses CMoV/CMoMV and tlaRNAs are known to be reliant on CRLV for aphid transmission to new host plants, therefore we subjected these samples to another RT-PCR assay designed for the generic detection of poleroviruses, and recovered products of the expected size. Sanger sequencing of these PCR products returned results for the putative polerovirus Torilis crimson leaf virus (TorCLV) in the parsley samples from the 2020-2021 and the 2020 cilantro sample, and the putative polerovirus Fennel mottle virus (FMV) in the 2021 cilantro sample. These results inspired us to subject these, and the Washington carrot samples, to RNA sequencing analysis to confirm these initial diagnostic results and determine if any other emergent polerovirus, umbravirus, or tlaRNA species were present. In addition to confirming the presence of TorCLV and the classic CMD associated viruses, we found another recently described polerovirus, two recently described umbravirus species that we determined to likely be divergent strains of CMoV, a recently described tlaRNA, and a putative novel polerovirus that appears to be a recombinant between TorCLV and an unknown polerovirus that is closely related to another recently described polerovirus,

Trachyspermum ammi polerovirus (TaPV). This work highlights the diversity and modularity of these complexed viral species associated with CMD.

Introduction

Carrot motley dwarf (CMD) is a multi-virus disease complex composed of a polerovirus in combination with an umbravirus and/or one of several tombusvirus-like associated RNAs (tlaRNAs), all of which are positive sense, single stranded RNA viruses (+ssRNA) (Watson et al. 1998; Murant et al. 1969; Syller 2003; Taliansky and Robinson 2003; Halk et al. Murant 1979; Campbell et al. 2020; LaTourrette et al. 2021; Huang et al. 2005; Delfosse et al., 2021) Viruses currently known to be associated with CMD include the polerovirus carrot red leaf virus (CRLV), the umbraviruses carrot mottle virus (CMoV) and carrot mottle mimic virus (CMoMV), and a multitude of tlaRNAs—carrot red leaf virus associated RNAs (CRLVaRNAs) a8, a25, alpha, beta, gamma, sigma, SN, and HK (Watson et al., 1964; Gibbs et al. 1996; Murant et al. 1985; Waterhouse and Murant 1981; Murant and Roberts 1979). In addition to its namesake, carrots (*Daucus carota*), CMD can affect a variety of other plants within the *Umbilliferae* (*Apiaceae*) family including coriander/cilantro (*Coriandrum sativum*), chervil (*Anthriscus cerefolium*), cumin (*Cuminum cyminum*), and parsley (*Petroselinum crispum*) (Yoshida 2020; Tang et al., 2009; Watson and Serjeant, 1964; Gibbs et al.1996). CMD can be found throughout the world wherever carrots are grown. While sporadic, outbreaks of CMD can cause severe losses in carrot crops, the severity of symptoms is highly dependent on the carrot cultivar, plant age at the time of infection, environmental conditions—cool temperatures and low-light conditions are more conducive—and the number of co-infecting viruses contributing to the disease.

Experimental inoculations of CRLV and CMoV or CMoMV via aphid and mechanical inoculation methods, respectively, have determined that symptoms caused by individual infections of these viruses are relatively mild to absent, whereas those composed of double infections of CRLV with either CMoV or CMoMV, or CRLV with a CRLVaRNA become more severe, and infections composed of all three types of viruses—CRLV, CMoV or CMoMV, and a CRLVaRNA—produce the most severe symptoms hallmarked by vibrant yellow to red mottled discoloration and browning of leaf tips and margins, and severe stunting (Watson et al., 1964; Gibbs et al. 1996; Watson and Falk 1994; Yoshida 2020; Watson and Serjeant, 1964; Erickson and Falk, 2023 (in review)). However, in natural settings single infections of the associated umbraviruses or CRLVaRNAs have not been observed in the field (Elnagar and Murant, 1978; Waterhouse and Murant, 1983). This is due to the unique nature of disease complexes caused by co-infection of a polerovirus, umbravirus, and/or tlaRNAs, wherein, despite each virus being able to replicate autonomously, umbraviruses and tlaRNAs both rely on interactions with a compatible co-infecting polerovirus to gain necessary functions for them to complete the infection cycle. Poleroviruses are completely autonomous, phloem limited viruses that encode their own capsid proteins which allow them to move systemically within a plant and be transmitted between hosts by aphid vectors in a persistent, non-propagative manner (Delfosse et al., 2021; Rochow, 1972; Cilia et al., 2014). While umbraviruses can move both systemically in the phloem and locally between mesophyll cells (cell-to-cell movement), and can be mechanically transmitted—though this is not known to be a primary means of transmission in the field—they do not encode their own capsid proteins and are thus dependent on co-infection with a polerovirus wherein their genomic RNAs can be transcapsidated by polerovirus capsid proteins and become aphid transmissible (Elnagar and Murant, 1978; Waterhouse and Murant 1983;

Taliansky and Robinson 2003; Elnagar and Murant 1978; Murant et al. 1969). TlaRNAs only encode a replicase protein, and are therefore dependent on a co-infecting polerovirus and/or umbravirus for within host movement and to gain aphid or mechanical transmissibility (Campbell et al. 2020; Erickson and Falk, 2023 (in review)).

In the spring and summer of 2020, carrot samples collected in western (Jefferson county) and central (Grant county) Washington, USA, curly and flat leaf parsley samples collected in Ventura county, CA, USA, and a cilantro sample collected in Yolo, county CA, USA, exhibiting typical CMD symptoms were submitted to our lab for diagnosis. We tested these samples for CRLV, CMoV/CMoMV, and CRLVaRNAs using generic RT-PCR based assays as described (Vercruysse et al. 2000; Campbell et al. 2020). The carrot samples tested positive for all three suspected CMD associated viruses. However, while the parsley and cilantro samples tested positive for CMoV/CMoMV and/or CRLVaRNAs, in varying combinations, none of these samples tested positive for CRLV. Given the dependency of umbraviruses and tlaRNAs on a co-infecting polerovirus for aphid transmission, we retested these samples using degenerate primers for polerovirus detection, as described (Lotos et al. 2014), which yielded positive results. Sanger sequencing of these PCR products identified the unknown polerovirus as Torilis crimson leaf virus (TorCLV) (GenBank accession: LT595017.1)

These results inspired us to conduct an exploratory RNA sequencing (RNAseq) based analysis of these samples, along with the carrot samples from Washington, and additional parsley samples (Ventura county, CA) and a cilantro sample (Yolo county, CA) collected in 2021 to confirm the presence of TorCLV and look for other emergent polerovirus, umbravirus, or tlaRNA species, and combinations thereof, that could potentially contribute to CMD disease. In this study we describe the detection of the classically known CMD associated viruses, plus two recently

described poleroviruses, two putatively divergent strains of CMoV, one tlaRNA species not previously detected in the United States, and one potentially new polerovirus species that appears to be a recombinant of TorCLV and another unidentified putative polerovirus. Not only does this study shed light on the complexity of known and emergent viruses that may contribute to CMD in parsley and cilantro plants, it also highlights the ongoing utility of using high throughput sequencing (HTS) technologies in the discovery of emergent, and potentially economically important, plant viruses.

Materials and methods

Plant material and diagnostics

Descriptive details about the carrot, parsley, and cilantro samples used for RNAseq analysis in this study, including the library IDs and number of sequencing reads obtained per sample, can be found in Table 1. From the different carrot, parsley, and cilantro sample sets submitted to our lab for diagnosis, individual samples exhibiting the most obvious potential symptoms of CMD were selected for testing. A portion of each sample was cut into small pieces, the cut tissue was split into two aliquots, one of which was flash frozen in liquid nitrogen and stored at -80 ℃ and the other vacuum dried for 4 days then stored at -20 ℃ for future use.

The remaining sample tissues were pooled according to location of origin, and total RNA was extracted using TRIzol™ Reagent (Invitrogen) according to the manufacturer's protocol and used as template for cDNA synthesis using the SuperScript™ III Reverse Transcriptase kit (Invitrogen). RT-PCR was performed using the GoTaq® Flexi DNA Polymerase kit (Promega) in a 25 µl reaction containing 5 µl of 5X Green GoTaq® Flexi Buffer, 1.5 µl of 25 mM $MgCl_2$, 1.25 µl of each primer (10 µM), 0.5 µl of 10 mM dNTPs, 0.125 µl of Taq polymerase, 2 µl of cDNA, and 14.375 µl of nuclease free water. The primers and thermocycling conditions used for CMoV

and CRLV are detailed in Vercruysse et al. 2000 and Campbell et al., 2020, respectively. PCR products were visualized by electrophoresis through a 2% agarose gel, and PCR products of the expected molecular weight were excised and purified using the NucleoSpin Gel and PCR Clean-up kit (Takara Bio) and sent for Sanger sequencing (genewiz.com). CMoV and tlaRNAs were detected in parsley and cilantro samples in various combinations, however CRLV was not. Therefore, these samples were subjected to a subsequent RT-PCR assay designed for the generic detection of poleroviruses, as described (Lotos et al. 2014). All primers used in this study are listed in Table S1.

Sample preparation for RNA sequencing (RNA-seq)

Tissue from the individual plant samples stored at -80 ℃, as well as from healthy flat and curly leaf parsley, cilantro, and carrot plants grown from seed in a growth chamber, were used for total RNA extraction using the RNeasy Plant Mini Kit (Qiagen) according to the "Purification of Total RNA from Plant Cells and Filamentous Fungi" protocol in the user's manual. RNA samples were DNase treated with RQ1 RNase-Free DNase (Promega) and cleaned using the "RNA Cleanup" protocol from the same extraction kit. The concentration and integrity of RNA samples were checked using the Qubit 4 Fluorometer (ThermoFisher Scientific) and the Experion™ Automated Electrophoresis System bioanalyzer. RNA samples were submitted to the DNA Technologies and Expression Analysis Core Laboratory at the UC Davis genome center for ribodepletion, library preparation, and transcriptome sequencing on the NovaSeq 6000 platform (Illumina). Aliquots of each RNA sample were retained for RT-PCR validation of viral sequences obtained by RNAseq.

Bioinformatic analysis

The returned raw read data was processed and analyzed according to a previously established pipeline for detecting viral RNAs in plant samples (ter Horst, 2021). In brief, the raw read data was quality checked using FastQC v0.11.9 (Ewels, et al., 2016), adapter sequences and low quality reads were removed using Trimmomatic v0.40 (Bulger, et al., 2014), and the clean read data was quality checked again. Clean reads were assembled with MEGAHIT v1.02 (Li, et al., 2015) using default settings with a minimum contig length of 200 bp. Prodigal v2.6.3 (Hyatt et al., 2010) was used to predict protein coding sequences from the assembled contiguous sequences (contigs), the output of which was then subjected to analysis with HMMR v3.3.2 (Finn et al., 2011) to search for viral RdRp-like sequences using the protocols and HMM profiles established by Wolf et al., 2018, with the default E-value cutoff. Returned RdRp-like contigs were compared against the NCBI nucleotide (nt) database using BLASTn, and predicted protein coding sequences were used as query in a search against the NCBI non-redundant (nr) protein database using BLASTp.

The BLASTn and BLASTp results were then manually curated. Sequencing reads were mapped back against selected virus contigs of interest using Samtools v1.11 software, and coverage tables were generated with coverM v0.6.1 software using the mean method to determine the mean number of aligned reads that overlapped each position of the contig. Viral contigs >1000 nt in length, represented by >1% of total virus reads, with >100x average genome coverage and sharing homology with putative poleroviruses, umbraviruses, and tlaRNAs were selected for manual inspection. In some of the retrieved viral contigs of interest, contaminating host sequences were found, these were manually trimmed prior to further analysis. Contigs of interest were aligned with reference virus genomes obtained from the NCBI Genbank database that were indicated in the BLASTn and BLASTp outputs using SnapGene software

(www.snapgene.com). Viral contigs that did not align with the selected viruses were subjected to BLASTn and/or BLASTx analysis to identify the nearest virus relative.

Phylogenetic classification and percent pairwise identity analysis

To determine the relative taxonomic positions of the poleroviruses, umbraviruses, and tlaRNAs identified in this study to those of previously described viruses, phylogenetic analyses were performed. According to the International Committee on Taxonomy of Viruses (ICTV), the species demarcation for poleroviruses is a >10% difference in shared amino acid sequence identity for any of the encoded gene products (Walker et al. 2022). Umbravirus species are demarcated by <70% shared nucleotide sequence identity of the entire genome and/or <75% identity with the RdRp (P2) or cell-to-cell movement protein (P4) amino acid sequences. As they are currently unclassified, there is no set species demarcation criteria for tlaRNAs. For poleroviruses, we used near to full length P1 (replication associated protein; Rap) and P3 (capsid protein; CP) translated amino acid sequences for phylogenetic and pairwise identity analyses; comparisons using P2 (RdRp) translated amino acid sequences were also made, but due to the RdRp sequence being highly conserved among poleroviruses, this did not show as clear of a demarcation between the different polerovirus species as did the other amino acid sequences (Figure S1). For the identified umbraviruses we used nearly full length genome sequences, as well as near to full length P2 and P4 translated amino acid sequences for analysis, and for tlaRNAs we used nearly full length translated amino acid sequences of the combined P1a+P1b (RdRp) predicted readthrough protein.

For phylogenetic analyses, the selected amino acid and nucleotide sequences of the viruses identified in this study by RNAseq, along with those of reference virus isolates, were aligned with the MUSCLE algorithm using MEGA11 software (Tamura et al., 2021), and the

unaligned ends were manually trimmed; redundant sequences were removed to reduce processing time. Maximum likelihood (ML) phylogenetic analyses were performed after identifying the most appropriate substitution models for each of the targets using the MEGA11 model selection tool details of the substitution models used for each target are listed in Table S2. Pairwise identity comparisons for each of the individual targets were calculated using SDT v1.2 (Muhire, Varsani, and Martin 2014); the results were imported into Excel and the percent shared identities for each group of viruses were averaged, except for reference isolates and a couple virus isolates from this study that appeared to stand out from the group. The phylogenetic tree and averaged shared percent identity matrices were edited using Inkscape v1.2 software (https://inkscape.org/).

Recombination analysis

Three putative virus sequences obtained in this study appeared to be potential recombinants of two different *Polerovirus* species, TorCLV and TaPV. Alignments of these putative recombinant sequences with TorCLV and TaPV reference isolate sequences were made using the MUSCLE algorithm in MEGA11 and the unaligned terminal sequences were trimmed; one of the recombinants (contig 110527) was found to have very large gaps in relation to the other viruses and therefore was excluded from the analysis. The alignments were then subjected to recombination analysis using the full suite of available test options using the Recombination Detection Program 4 (RDP4; Martin et al., 2015) software.

RT-PCR validation

Primers were designed using SnapGene v6.1 software (www.snapgene.com) to amplify nearly full length genomic sequences of the selected viruses identified by RNAseq. Primer specificity was checked by attempting to align each primer set against each virus target. Among

the tlaRNAs detected, most shared so much sequence homology that finding primer binding sites that would be specific for each one was challenging, so primers were designed to detect any of these tlaRNAs; CRLVaRNA sigma and arracacha latent virus associated RNA (ALVaRNA) were dissimilar enough that specific primers could be designed.

Aliquots of the same RNA samples that were submitted for RNA-seq analysis were used as templates for cDNA synthesis using the SuperScript™ IV Reverse Transcriptase kit (Invitrogen). PCR was performed using CloneAmp HiFi PCR Premix (Takara) in 25 µl reactions containing 12.5 µl of premix, 1 µl of each primer (10 µM), 1 ul of cDNA, and 9.5 µl of nuclease free water; thermocycling conditions were as follows: 95 ℃ for 1 min, followed by 40 cycles of 98 ℃ for 10 s, 50-55 ℃ (depending on primer set, see Table S1), 72 ℃ for 40-70 s (depending on expected product size, see Table S1), and a final extension at 72 ℃ for 5 min. PCR products were visualized by electrophoresis through a 1% agarose gel. PCR products were purified using the NucleoSpin Gel and PCR Clean-up (Takara Bio), then cloned into the pCR-XL-2-TOPO vector using the TOPO™ XL-2 Complete PCR Cloning Kit (Invitrogen) and transformed into *E. coli* strain DH5α cells. Plasmids from positive colonies were extracted using the QIAprep Spin Miniprep Kit, and sent to Eurofins genomics for whole plasmid Nanopore sequencing, to confirm the sequences obtained by RNAseq.

Results

Detection of CMD viruses in plant samples submitted for diagnosis

After performing initial RT-PCR based diagnostic assays (Campbell et al., 2020; Vercruysse et al., 2000) on flat and curly leaf parsley, carrot, and cilantro samples exhibiting typical symptoms of CMD (Figure 1) submitted to our lab, we found that all of the known CMD-associated viruses were present in the carrot samples (Figure 2a). Unexpectedly however, only

umbraviruses (CMoV and/or CMoMV) and tlaRNAs were detected in the parsley and cilantro samples in the absence of the known helper polerovirus, CRLV (Figure 2b). Given the dependence of umbraviruses and tlaRNAs on a coinfecting polerovirus for aphid transmission between hosts, we suspected the presence of a different polerovirus. After retesting these samples using a different RT-PCR based assay for generic polerovirus detection (Lotos et al., 2013), we obtained PCR products of the expected size (~600 bp), which we submitted for Sanger sequencing. BLASTn analysis determined the amplicon sequences shared 95.7% nt sequence identity with a recently deposited polerovirus sequence, Torilis crimson leaf virus (TorCLV; accession LT595016.1), thereby confirming our suspicions. Additional parsley and cilantro samples received in the following year were tested using this assay; the parsley samples again tested positive for TorCLV in various combinations with CMoV/CMoMV and/or CRLVaRNAs, however, the amplicon sequence from the cilantro sample was found to share 89.8% identity with a different polerovirus, Fennel motley virus (FMV; accession LT595018.1). Given these results we selected a subset of these samples for RNA sequencing (RNAseq) to confirm the presence of these newly described viruses in these samples and determine if other new or recently discovered umbraviruses and/or tlaRNAs were present; several of the Washington carrot samples were also included.

General summary of RNA sequencing results

In total 18 parsley (seven flat leaf and 11 curly leaf), two cilantro, and 12 carrot samples were selected for RNA sequencing. Descriptions of the samples submitted for RNAseq analysis—including the sample group, collection year, county and state of origin, library IDs, and sequencing reads obtained for each library—are detailed in Table 1. After removing adapter sequences and low quality reads, 8.9 to 19.6 million paired end reads approximately 150 (bp) in

length were returned. In total, 545 predicted plant viral contiguous sequences (contigs) represented by 10 families, 15 genera, and 35 species were assembled, ranging in length from 240 to 14,036 nt (Table 2). 338 mycovirus, 36 arthropod virus, and four miscellaneous virus contigs were also retrieved, these results are summarized in Table S3. Among the putative virus contigs returned, polerovirus, umbravirus, and tlaRNA contigs predominated. Virus contigs >1000 nt long, represented by >1% of viral reads, and having greater than 100x average genome coverage were selected for further analysis. Table 3 details the number and percentage of sequencing reads that mapped back to the polerovirus, umbravirus, and tlaRNAs contigs, along with their average genome coverages.

Polerovirus sequence identification

In total, five polerovirus sequences were identified by RNAseq analysis (Table 2), however only three of these—CRLV, TorCLV, and wild carrot red leaf virus (WCRLV)—were represented by contigs meeting the cutoff criteria described in section 3.2; the other two polerovirus sequences (Parsley mottle virus and Parsley mottle mimic virus) were excluded from further analysis. CRLV contigs covering essentially the entire length of the ~5.7 kb reference genome and sharing a high percent nt sequence identity (>98%) with CRLV accessions in the NCBI GenBank database, were present in eleven of the 12 sequenced carrot samples, but none of the tested parsley or cilantro samples. TorCLV was present in 16 out of the 18 tested parsley samples and in the cilantro sample collected in 2020, with several (5) contigs covering nearly 100% of the ~5.6 kb and sharing>95% identity with the single reference isolate in the GenBank database. TorCLV was not found in the cilantro sample collected in 2021 or in any of the tested carrot samples. Together, these results support our findings of these viruses in the initial diagnostic assays.

Upon closer analysis of the polerovirus sequences designated as WCRLV by the RNAseq results, we encountered unexpected results. According to manual BLASTn analysis of each of these contigs, none, were found to be WCRLV. Of the nine contigs misidentified as WCRLV, five were found to be most closely related to a recently described polerovirus, Trachyspermum ammi polerovirus (TaPV; BK059374.1). The longest of these contigs was ~3.9 kb, covering only 68.5% of the ~5.7 kb of the reference genome and sharing only 86.7% nt identity with the reference genome; these sequences were present in four of the 18 parsley samples. In the cilantro sample collected in 2021, which was thought to have FMV according to the initial diagnostic assays, the single ~5.1 kb polerovirus contig present was identified by BLASTn analysis as another recently described polerovirus, Foeniculum vulgare polerovirus (FvPV; BK059375.1), sharing 94% identity with the reference isolate. The sequence of the FvPV isolate found in this study was slightly longer than that of the partial genome sequence uploaded for the reference isolate (~4.3 kb). FvPV sequences were found in no other samples.

Interestingly, for the remaining three contigs misidentified as WCRLV—which ranged in length from ~4.4 kb to ~5.2 kb—found in 3 separate parsley samples, the BLASTn results returned hits for both TaPV and ToRCLV, both with rather low query coverage (79% with TaPV and 85% with TorCLV) and percent shared identity scores (86.24% with TaPV and 84.47% with TorCLV), with these reference isolates. Visual assessment of alignments of the TaPV and TorCLV reference sequences with these three contigs revealed they all aligned more closely with TaPV in the first 5’ 2/3 of their genomes (covering ~3-4 kb, of the total contig length), whereas the remaining 3’ 1/3 of their genomes aligned more closely with TorCLV (covering ~2.4 kb). The TaPV aligned sequence covered ORFs 0, 1, and 2 of the genome (5’ gene block), the TorCLV aligned sequence covered ORFs 3 ,4, and 5 (3’ gene block), and both alignments appeared to

overlap in the intergenic region between the 5' and 3' gene blocks (Figure 3). Given these results we suspected these contigs to be representative of a putative new recombinant virus related to both TaPV and TorCLV. For simplicity, we will refer to these putative recombinant poleroviral sequences as 'hybrid' sequences.

Phylogenetic and pairwise identity comparisons of identified polerovirus sequences

The species demarcation for poleroviruses is a >10% difference in amino acid sequence identity of any of the six ORF encoded proteins. To compare the phylogenetic and sequence similarity relationships of the poleroviruses identified in this study, we constructed maximum likelihood phylogenetic trees and average percent identity matrices using translated amino acid sequences of the P1 (Rap) protein coding sequences from the 5' have of the genome and the P3 (CP) protein coding sequence from the 3' half of the genome. The cereal infecting polerovirus, Barley virus G (BVG), was used as an outgroup and WCRLV (LT615231.1) was also included in the analysis.

Of particular interest, are the phylogenetic and average amino acid comparisons of the putative hybrid sequences with those of TorCLV and TaPV sequences. It should be noted that since only partial sequences were obtained for the non-hybrid putative TaPV-like sequences these contigs could not be included in the comparative analyses of the P3 (CP) protein as this region was not covered; two contigs did, however, cover the P1 (Rap) gene region and were therefore included in the analyses for this protein. In phylogenetic comparisons of the P1 amino acid sequences, the hybrid sequences clustered in the same clade as the TaPV reference isolate (Figure 4a), and these viruses shared 83% ID with one another (Figure 4b). The truncated TaPV-like sequences also only shared 83% ID with the TaPV reference isolate and clustered with the hybrid sequences in the same clade as TaPV. Conversely, the TaPV-like and putative hybrid P1

sequences shared only 57% and 56% ID with the TorCLV reference isolate sequence TorCLV sequences obtained in this study, respectively. Both the TorCLV reference sequences and those from this study shared greater identity (59% and 58%, respectively) with the TaPV reference isolate, indicating these sequences are more closely related to TaPV than are the putative hybrid virus sequences.

Comparisons of the P3 amino acid sequences conversely placed the putative hybrid virus sequences in the same lineage as TorCLV (Figure 4c), and shared 98% and 99% ID, respectively, with the TorCLV reference isolate and the isolates obtained in this study (Figure 4d). With respect to the TaPV reference isolate, the hybrid sequences only shared 74% identity. Altogether, these results demonstrate that the 5' and 3' gene blocks of the putative hybrid viruses vary dramatically in their respective lineages, with the P3 (CP) sequence from the 3' gene block being nearly identical to that of TorCLV, while the P1 (Rap) sequence from the 5' gene block appears to have potentially originated from an unknown virus species that is closely related to, but separate, from TaPV, since these proteins share <90% ID.

With regard to the other polerovirus sequences included the analysis, these viruses all clustered in the same lineages as their respective reference isolates and shared >90% ID with them. While the CRLV, TorCLV, and TaPV lineages clustered together in a super clade, FvPV fell into a clade outside this grouping. In the P1 comparisons, FvPV shared almost as little ID (40%, 38%, and 39%, respectively) with the TaPV, TorCLV, and CRLV lineages as did the BVG outgroup (33%, 34%, and 35%, respectively). In the P3 comparisons, FvPV shares much greater % IDs (68%, 72%, and 65%) than does BVG (51%, 53%, and 51%) with the TaPV, TorCLV, and CRLV groups.

Recombination analysis of the putative hybrid virus sequences

Recombination analysis of two of the hybrid sequences (56020 and 35161) and the TaPV and TorCLV reference genomes was performed using RDP4 software, using the complete suite of testing options available—RDP, GENECONV, BootScan, MaxChi, Chimaera, SiScan, 3Seq, LARD, and Phylpro. A recombination event was detected by all but two of the tests employed (LARD and Phylpro), with predicted probabilities of this event being random ranging from $8.881x10^{-16}$ - $7.702x10^{-132}$; these results are summarized in Table 4. The major parent was predicted to be TaPV and the minor parent was predicted to be TorCLV. The predicted break points in the putative hybrid sequences occurred at nucleotide positions 3276 and 5048 for contig 35161, and at nt positions 3277 and 5151 for contig 56020 (Figure 5). It should be noted that the program did produce a warning stating that it may be possible the putative hybrid sequences may actually be the parental sequences and that TaPV, TorCLV, or both could be the recombinants. As shown previously, the 5' TaPV-portion of the putative hybrid virus genome, while seemingly closely related to TaPV did not meet the demarcation criteria for being the same species as TaPV, which may factor into this uncertainty.

Umbravirus sequence identification

A total of four putative umbravirus sequences—CMoV, CMoMV, wild carrot mottle virus (WCMoV), and tobacco bushy top virus (TBTV)—were identified by RNAseq analysis (Table 2). However, TBTV was excluded from further analysis as it did not meet the criteria outlined in section 3.2.

CMoV contigs were identified in seven of the 12 sequenced carrot samples, with nearly full length (~4.2 kb) recovered from four. Manual BLASTn searches of these contigs determined they shared >98% shared nt identity with CMoV (KF533714.1). According to the returned RNAseq results, CMoV was also identified in 12 of the 18 sequenced parsley samples and in the

2020 cilantro sample, however, manual BLASTn searches of these contigs returned different results; the top hit returned was for a recently described umbravirus, Pastinaca umbravirus 1 (PasUV1), and despite nearly full length (~4.3–4.4) kb sequences being recovered from the cilantro and 11 parsley samples, the queried contigs only had QC scores of 81% - 86% and shared up to 82% nt sequence identity with this virus. The next closest hit was for CMoV, with a max QC score of 69% and 80.4% shared identity, perhaps explaining the output of the RNAseq results. The third identified umbravirus, WCRLV, was found in a single flat leaf parsley sample and in eight carrot samples, with nearly full length (~4.2 kb) contigs being recovered from 5 of these. BLASTn analysis of these contigs concordantly returned WCRLV, with a max QC score of 99% and ~83% shared nt identity.

Phylogenetic and pairwise identity comparisons of identified umbravirus sequences

According to the ICTV, the current species demarcation for umbravirus species is >70% shared nt sequence identity of the entire genome or >75% shared amino acid sequence identity of the RdRp (P2) and cell-to-cell movement proteins (P4). ML phylogenetic and pairwise identity analyses were conducted using the nearly full length genome sequences and the P2 (RdRp) and P4 (MP) and translated amino acid sequences of the putative umbraviruses identified in this study to determine their relationships; groundnut rosette virus (GRV) was used as an outgroup.

In all three comparisons—genomic nt sequence, and P2 (RdRp) and P4 (MP) amino acid sequences—the canonical umbraviruses already known to be associated with CMD disease—CMoV and CMoMV—clustered in distinct clades along with the respective reference isolate sequences used in the analyses (Figure 6a, c, e). The CMoV isolates shared ≥96% nt identity, and ≥98% and ≥99% P2 and P4 amino acid identity, both between themselves and with the reference isolate (LT615232.1). The CMoMV isolates shared ≥95% nt identity, and >97% identity for each

both the P2 and P4 amino acid sequences, between themselves and the reference isolate (NC_001726.1). Conversely, for all comparisons, CMoV and CMoMV shared <70% nt identity and <75% amino acid identity for either of the analyzed proteins (Figure 6b, d, f).

Comparisons of the PasUV1 and WCMoV sequences produced somewhat contradictory results. At the nt level, while all of the WCMoV isolates in this study seemed somewhat divergent from the reference isolate, and the single isolate from parsley seemed to be somewhat divergent from those found in carrot; all shared ≥79% identity amongst each other. These differences were much less apparent in the P2 and P4 comparisons, in which ≥90% and ≥92% shared average identity was observed, respectively. The PasUV1 isolates from this study shared ~80% average nt identity, and 89% (P2) and 92% (P4) amino acid identity with the reference isolate (OL472236.1). Unexpectedly, however, the WCMoV and PasUV1 sequences (references and from this study) shared ≥70% nt identity and ≥75% amino acid identity for both proteins, suggesting these viruses are not distinct species.

Of particular interest is how WCMoV and PasUV1 are related to CMoV and CMoMV. In all pairwise comparisons with CMoMV, ≤72% shared identity was observed in either the nucleotide or amino acid sequences, for both WCMoV and PasUVI, confirming these to be distinct species from CMoMV. Conversely, this was not the case in comparisons with CMoV; WCMoV shared ≥71% average nt identity and ≥81% (P2) and ≥78% (P4) amino acid identity with CMoV, while PasUV1 shared ≥77% average nt identity and ≥84% amino acid identity for both proteins with CMoV, which do not meet the demarcation criteria for classification as distinct species from CMoV.

Phylogenetic comparisons of the nt sequences of PasUV1 and WCMoV placed each of these viruses in their own distinct subclades that were grouped into a larger clade with CMoV,

with CMoV being more closely related to PasUV1 than WCMoV (Figure 6a). Phylogenetic comparisons of the P2 and P4 amino acid sequences yielded somewhat different results; for the P2 protein, while both WCMoV and PasUV1 clustered together in their own distinct subclades, WCMoV was somewhat unexpectedly placed within a larger clade more closely related to CMoMV, while PasUV1 was placed in a larger clade more closely related to CMoV (Figure 6c). For the P4 protein, PasUV1 reference isolates clustered in a larger clade with CMoV, and the PasUV1 reference isolate P4 sequences were more closely related to CMoV than they were to the PasUV1 isolates identified in this study (Figure 6e). All WCMoV isolates grouped together within their own distinct subclade which was adjacent to the larger PasUV1/CMoV clade.

TlaRNA sequence identification

Nine different tlaRNAs were identified by the initial RNAseq analysis (Table 2), and seven of these were associated with contigs that met the criteria outlined in section 3.2. After closer visual inspection and manual BLASTn searches of the retrieved contigs confirmed the presence of the following CRLVaRNAs: CRLVaRNAs a25, alpha, beta, gamma, sigma, and FR373 (which appears to be very closely related to a25). Additionally, another recently discovered tlaRNA, Arracacha latent virus E associated RNA (ALVEaRNA), that has not previously been found in association with the CMD disease complex, was also identified and appeared to be the most abundant tlaRNA in terms of the number of samples in which it was found—four parsley samples and one carrot sample. Of the CRLVaRNAs, a25, alpha, gamma, and FR373 were found exclusively in the carrot samples, and were present in four, two, one, and one samples, respectively, with nearly full length contigs being retrieved for all except for FR373. CRLVaRNA sigma was found exclusively in four separate parsley samples, each yielding nearly full length contigs.

Phylogenetic and pairwise identity comparisons of identified tlaRNA sequences

As tlaRNAs remain formally unclassified, there are no specified species criteria against which to compare them, nonetheless we conducted phylogenetic and pairwise comparisons of the tlaRNAs found in this study using nearly complete P1a+P1b (RdRp) translated amino acid sequences; the turnip yellows virus (TuYV) ST9 TuYVaRNA (NC_004045.2), tobacco bushy top disease (TBTD) aRNA (EF529625.1), and cucurbit aphid borne yellows virus (CABYV) aRNA (NC_026508.1) were used as outgroups. Among the tlaRNAs found in this study, the CRLVaRNAs a25, alpha, beta, gamma appeared to be closely related, clustering within the same clade and sharing ≥94% amino acid identity (Figure 7a and b); the reference isolates used were: a25 AF020617.1, alpha KM486095.1, beta KM486096.1, and gamma KM486092.1. CRLVaRNA sigma isolates clustered within their own clade adjacent to the larger CRLVaRNA clade, with the isolates in this study sharing 100% identity amongst themselves and with the reference isolate (KM486093.1), and 82-84% identity with the other CRLVaRNAs. Interestingly, the ALVEaRNA isolates obtained in this study were farther removed from the CRLVaRNAs than the outgroup tlaRNAs used in this study, sharing only up to 39% - 43% identity with either the CRLV or outgroup aRNAs.

RT-PCR and whole plasmid Nanopore sequencing validation of RNAseq results

Using primers designed for the specific detection of each of the poleroviruses, umbraviruses, tlaRNA Sigma and ALVEaRNA, and primers designed for the general detection of the other CRLVaRNAs identified in this study we were able to recover nearly full length amplicons of each of these viruses, and after cloning these into the pCR-XL2-TOPO vector backbone, were able to confirm the sequences for most of these by whole plasmid Nanopore sequencing. For polerovirus detection, we recovered ~3.1 – ~4.6 kb long amplicons of TorCLV, a

~5.4 kb amplicon of CRLV, ~4.3 kb amplicons of FvPV, and ~4.6 – ~4.7 kb sequences of the putative hybrid virus for which we are proposing the tentative name Parsley mottle hybrid polerovirus (PMoHPV). Hybrid specific primers were used to test all of the samples that had truncated TaPV-like sequences, and a few samples that had neither hybrid nor TaPV-like sequences; all samples with TaPV-like sequences yielded PCR products of the same size as those in hybrid virus positive samples, whereas the other samples tested negative, indicating the truncated TaPV-like samples were likely incomplete hybrid sequences. For the umbraviruses, we obtained ~3.9 kb amplicons of CMoMV from both parsley and carrot samples, a ~4.1kb amplicon of CMoV, ~4 kb long amplicons of PasUV1 from parsley, and ~4 kb long amplicons of WCMoV. For the tlaRNAs, we retrieved ~ 2.3 kb long amplicons of ALVEaRNA from both parsley and carrot samples, an ~2.8 kb amplicon of CRLVaRNA sigma, and ~2.8 kb long amplicons of both CRLVaRNAs a25 and alpha from carrot and cilantro samples.

Discussion

In this work we used RT-PCR and RNA sequencing based approaches to characterize poleroviruses, umbraviruses, and tombusvirus-like associated RNAs (tlaRNAs) in carrot, cilantro, and parsley samples exhibiting typical symptoms of carrot motley dwarf (CMD). In addition to finding viruses previously known to contribute to this multi-virus disease complex and which occur in the United States, namely the polerovirus carrot red leaf virus (CRLV), the umbraviruses carrot mottle virus (CMoV) and carrot mottle mimic virus (CMoMV), and a range of CRLV associated RNAs (CRLVaRNAS), we also identified two recently discovered poleroviruses—Torilis crimson leaf virus (TorCLV) and Foeniculum vulgare polerovirus (FvPV). Additionally, we found two recently discovered potentially divergent strains of CMoV, which we refer to by the names given them in public reports—Pastinaca umbravirus 1 (PasUV1) and Wild

carrot mottle virus (WCMoV). We also found a recently described tlaRNA (Arracacha latent virus E associated RNA (ALVEaRNA), that has not been previously known to contribute to CMD or to occur in the United States. Lastly, we discovered a putative new polerovirus that appears to be a recombinant of TorCLV and an unknown polerovirus that shares the greatest homology with another recently described polerovirus not known to occur in the U.S. or be associated with CMD, Trachyspermum ammi polerovirus (TaPV), which we are tentatively calling Parsley mottle hybrid virus (PMoHV).

Of the poleroviruses identified in this study, CRLV was exclusively found in carrot samples, FvPV was identified from a single cilantro sample, TorCLV was identified in both parsley and cilantro samples, and PMoHV was found exclusively in parsley samples. While a full length genome of TorCLV has been deposited in Genbank, there currently exist no published reports of this virus, and as such there is very little known about its biology, distribution, its effects on symptoms, or what sort of risk, if any, it may pose to the production of economically important crop plants. According to the details included in the GenBank accession, this virus was first isolated in Greece, as part of a BioProject (PRJEB14424) referred to as "Insights into the etiology of apiaceae red leaf disease", in which cultivated and weedy apiaceous plant samples were surveyed using next generation sequencing (NGS) to characterize their associated viromes. While the plants that were sampled were not specified in the GenBank accession, the name Torilis crimson leaf virus implies that this virus was isolated from a plant in the genus *Torilis*, which are non-cultivated apiaceous plants broadly referred to as hedge parsleys, which are native to Northern Africa and Eurasia but have been spread to other countries, including the U.S. (www.itis.gov). This report therefore adds to the limited information we have about this virus, expanding its host range to both parsley (*Petroselinum crispum*) and cilantro (*Coriandrum*

sativum), and implicating it as a potential causative agent of CMD-like symptom development in these hosts.

FvPV was identified in an exploratory study in which transcriptome datasets from a variety of plant species that had been made publicly available in the NCBI Transcriptome Shotgun Assembly (TSA) Sequence Database were bioinformatically mined for the presence of putative novel polerovirus sequences (Kavi et al., 2022). Partial (~4.3 kb and ~1.4 kb long) FvPV sequences were recovered from the transcriptomes of *Foeniculum vulgare* (fennel) leaf samples that had been collected in Italy. The authors of this study note that FvPV shared 88.5% - 89.1% nt sequence identity with partial RdRp coding sequences designated as belonging to Fennel motley virus (FMV), which would explain our initial detection of FMV in our preliminary RT-PCR diagnostic assessment of the cilantro sample in which we identified FvPV. Our finding of FvPV therefore represents the first report of this virus in cilantro as well as in the U.S.

TaPV was reported in the same study by Kavi et al. (2022), found in the transcriptomes of *Trachyspermum ammi* inflorescence tissue collected in Iran. *T. ammi,* also known as Ajwain, is an apiaceous herb that is distributed widely throughout India and cultivated for both culinary and medicinal purposes (www.itis.gov). While we did not identify this virus in our samplings, the first 5' two thirds of the genome of the putative hybrid virus, PMoHV, shared, respectively, 83% and 96%, amino acid identity with the translated P1 (Figure 4a) and P2 (RdRp) sequences (Figure S1) of TaPV. The last third of the PMoHV genome shared very high amino acid identity (99%) with the translated P3 (CP) sequence of TorCLV (Figure 4c), suggesting that PMoHV is either a recombinant of TorCLV and an unknown polerovirus that is closely related to TaPV, or alternatively, that TorCLV and TaPV may be recombinant viruses descended from PMoHV.

Of the umbraviruses identified in this study, CMoV was found exclusively in carrot samples, while CMoMV was found in both carrot and parsley samples. Sequences of two recently reported, reportedly novel, umbraviruses were also identified in this study. WCMoV was found exclusively in carrot samples; like TorCLV, no published reports of this virus currently exist, excluding the accession of the full length WCMoV genomic sequence in the GenBank database, which was tied to same BioProject (PRJEB14424) from which TorCLV was identified. As such, the host in which this virus was first identified was not specified, however given its designated name, it was likely identified in carrots. In our own analyses of this virus sequence, we found that it shared >70% nt identity (Figure 6b) and >75% amino acid identity with both the P2 (RdRp) and P4 (cell-to-cell movement protein) sequences (Figures 6d and e) of CMoV, suggesting that it is not a newly described species but rather a divergent strain of CMoV.

We also identified the putative novel umbravirus PasUV1 in this study, finding it in both parsley and cilantro samples. PasUV1 was recently described in a study in which the viromes of field and greenhouse grown tomato plants from Slovenia, along with weeds found in the surrounding area, were sequenced and characterized (Rivarez et al., 2023). Among the plant species tested, PasUV1 was found in *Pastinaca sativa* (parsnip) plants. After conducting phylogenetic and pairwise identity analyses using the RdRp sequence of this virus, the authors proposed it to be a new umbravirus, however, this conclusion was made using a species demarcation of <80% shared amino acid identity of the RdRp. This however does not align with the >70% nt identity and >75% amino acid identity of the RdRp and/or cell-to-cell movement sequences, as established by the ICTV (Adams et al. 2015; Walker et al. 2022). In this study we report up to 77% shared nt identity between PasUV1 and CMoV isolates, well above the 70% threshold (Figure 6b). Rivarez et al. report 76% amino acid identity of the RdRp shared between

PasUV1 and CMoV. However, in our own analyses, we found that not only did our PasUV1-like sequences share >84% amino acid identity with the P2 (RdRp) protein of CMoV, but the PasUV1 sequences isolated by Rivarez et al. (2023) likewise shared 85% amino acid identity with the CMoV RdRp (Figure 6d). The discrepancy in our respective analyses may occur if the authors of this study used the P1 (Rap) or combined P1+P2 amino acid sequences in their analysis, as we found in our own analysis that the P1 protein shares much less amino acid identity (58%; Figure S2) with CMoV than does the more highly conserved P2 RdRp sequence. To further examine the relationship between the PasUV1 reference isolate and our PasUV1-like isolates with CMoV, we subjected the P4 amino acid sequences to phylogenetic and pairwise analyses (Figure 6e), and found that our PasUV1 isolates and the reference PasUV1 isolates from Rivarez et al. shared, respectively, 85% and 84% amino acid identity with the P4 of CMoV, lending further support to these viruses being divergent strains of CMoV rather than a novel umbravirus species.

Among the tlaRNAs found, a multitude of CRLVaRNAS—a25, alpha, beta, gamma, and FR373—were found exclusively in carrot samples, whereas another CRLVaRNA, sigma, was found exclusively in parsley. Lastly, a recently described tlaRNA, ALVEaRNA, was found both in parsley and carrot samples. ALVEaRNA was first identified in arracacha (*Arracacia xanthorrhiza*) plants—a type of starchy root vegetable that is widely cultivated and eaten throughout South America—from Peru, in association with an enamovirus (family *Solemoviridae*) designated Arracacha latent virus E (De Souza et al. 2021). This tlaRNA has subsequently been identified in cultivated carrots in France and Spain, in association with CRLV, indicating that it's associations with a helper virus may not be strictly specific (Schönegger et al., 2022) and in composite weed samples from Slovenia, in which the polerovirus Barley virus G was also found, although it can't be said if they were isolated from the same plant (Rivarez et al.,

2023). This is the first report of ALVEaRNA being found in parsley plants and in association with yet another potential helper virus (TorCLV), and it's first finding in the U.S.. Table 5 summarizes the viruses identified by RNAseq and confirmed by RT-PCR and Nanopore sequencing in this study.

The findings of this study add to the growing body of literature on the deployment of high throughput sequencing techniques, such as RNAseq, for the detection and identification of emergent viruses from symptomatic cultivated and weedy plant species. Our results also highlight the variability in the species and combinations of viruses associated with CMD and in the hosts each of them can infect, underscoring the plasticity of these polerovirus, umbravirus polerovirus interactions. As such, given the nature of these disease complexes, chance introductions of a polerovirus into a plant with unfamiliar umbraviruses and/or tlaRNAs could not only result in vector and/or host range expansions of such umbraviruses and/or tlaRNAs, but could also potentially result in novel virus combinations that could lead to enhanced development and unexpected disease complex epidemics, which could have significant epidemiological implications for crop production.

Acknowledgements

We thank Steve Koike and Lindsey duToit for us the plant materials for diagnosis and thereby providing us with the plant materials that made this work possible. This work was supported in part by the University of California, Davis.

References

Adams, M. J., E. J. Lefkowitz, A. M.Q. King, D. H. Bamford, M. Breitbart, A. J. Davison, S. A. Ghabrial, et al. 2015. "Ratification Vote on Taxonomic Proposals to the International Committee on Taxonomy of Viruses (2015)." *Archives of Virology*. Vol. 160.

https://doi.org/10.1007/s00705-015-2425-z.

Campbell, A. J., Anna Erickson, Evan Pellerin, Nidá Salem, Xiaohan Mo, Bryce W. Falk, and Inmaculada Ferriol. 2020. “Phylogenetic Classification of a Group of Self-Replicating RNAs That Are Common in Co-Infections with Poleroviruses.” *Virus Research* 276 (January). https://doi.org/10.1016/J.VIRUSRES.2019.197831.

Cilia, Michelle, Stewart Gray, and Murad Ghanim. 2014. “Circulative, ‘Nonpropagative’ Virus Transmission: An Orchestra of Virus-, Insect-, and Plant-Derived Instruments.” *Advances in Virus Research* 89 (0065–3527). https://doi.org/10.1016/B978-0-12-800172-1.00004-5.

De Souza, Joao, Segundo Fuentes, Giovanna Müller, Heidy Gamarra, Mónica Guzmán, Wilmer Cuellar, and Jan Kreuze. 2021. “High Throughput Sequencing for the Detection and Characterization of New Virus Found in Arracacha (Arracacia Xanthorrhiza).” *Scientia Agropecuaria* 12 (4): 471–80. https://doi.org/10.17268/sci.agropecu.2021.051.

Delfosse, Verónica C., Maria P. Barrios Barón, and Ana J. Distéfano. 2021. “What We Know about Poleroviruses: Advances in Understanding the Functions of Polerovirus Proteins.” *Plant Pathology* 70 (5): 1047–61. https://doi.org/10.1111/PPA.13368.

Elnagar, S., and A. F. Murant. 1978. “Relations of Carrot Red Leaf and Carrot Mottle Viruses with Their Aphid Vector, Cavariella Aegopodii.” *Annals of Applied Biology* 89 (2): 237–44. https://doi.org/10.1111/j.1744-7348.1978.tb07695.x.

Elnagar, S., and A. F. Murant. 1978. “Aphid-Injection Experiments with Carrot Mottle Virus and Its Helper Virus, Carrot Red Leaf.” *Annals of Applied Biology* 89 (2): 245–50. https://doi.org/10.1111/j.1744-7348.1978.tb07696.x.

Gibbs, M. J., J. I. Cooper, and P. M. Waterhouse. 1996. “The Genome Organization and Affinities of an Australian Isolate of Carrot Mottle Umbravirus.” *Virology* 224 (1): 310–13. https://doi.org/10.1006/VIRO.1996.0533.

Gibbs, M. J., A. Ziegler, D. J. Robinson, P. M. Waterhouse, and J. I. Cooper. 1996. “Carrot Mottle Mimic Virus (CMoMV): A Second Umbravirus Associated with Carrot Motley Dwarf Disease Recognised by Nucleic Acid Hybridisation.” *Molecular Plant Pathology On-Line*.

Halk, E. L., D. J. Robinson, and A. F. Murant. 1979. “Molecular Weight of the Infective RNA from Leaves Infected with Carrot Mottle Virus.” *Journal of General Virology* 45 (2): 383–88. https://doi.org/10.1099/0022-1317-45-2-383.

Huang, L. F., M. Naylor, D. W. Pallett, J Reeves, J. I. Cooper, and H. Wang. 2005. “The Complete Genome Sequence, Organization and Affinities of Carrot Red Leaf Virus.” *Arch Virol* 150: 1845–55. https://doi.org/10.1007/s00705-005-0537-6.

LaTourrette, Katherine, Natalie M. Holste, and Hernan Garcia-Ruiz. 2021. “Polerovirus Genomic Variation.” *Virus Evolution* 7 (2): 1–18. https://doi.org/10.1093/VE/VEAB102.

Lotos, Leonidas, Konstantinos Efthimiou, Varvara I. Maliogka, and Nikolaos I. Katis. 2014. “Generic Detection of Poleroviruses Using an RT-PCR Assay Targeting the RdRp Coding Sequence.” *Journal of Virological Methods* 198 (March): 1–11. https://doi.org/10.1016/J.JVIROMET.2013.12.007.

Mark, Selda Rivarez, Anja Pecman, Katarina Bačnik, Olivera Maksimović, and Ana Vučurović. 2023. “In - Depth Study of Tomato and Weed Viromes Reveals Undiscovered Plant Virus Diversity in an Agroecosystem.” *Microbiome* 11 (60): 1–24. https://doi.org/10.1186/s40168-

023-01500-6.

Muhire, Brejnev Muhizi, Arvind Varsani, and Darren Patrick Martin. 2014. “SDT: A Virus Classification Tool Based on Pairwise Sequence Alignment and Identity Calculation.” *PLoS ONE* 9 (9). https://doi.org/10.1371/journal.pone.0108277.

Murant, A. F., and I. M. Roberts. 1979. “Virus-like Particles in Phloem Tissue of Chervil (Anthriscus Cerefolium) Infected with Carrot Red Leaf Virus.” *Annals of Applied Biology* 92 (3): 343–46. https://doi.org/10.1111/J.1744-7348.1979.TB03883.X.

Murant, A. F., R. A. Goold, I. M. Roberts, and J. Cathro. 1969. “Carrot Mottle-a Persistent Aphid-Borne Virus with Unusual Properties and Particles.” *J. Gen. Virol.* 4: 329–41. https://doi.org/10.1099/0022-1317-4-3-329.

Murant, A. F., P. M. Waterhouse, J. H. Raschki, and D. J. Robinson. 1985. “Carrot Red Leaf and Carrot Mottle Viruses: Observations on the Composition of the Particles in Single and Mixed Infections.” *J. Gen. Virol*. Vol. 66. https://doi.org/10.1099/0022-1317-66-7-1575.

Rochow, W. F. 1972. “The Role of Mixed Infections in the Transmission of Plant Viruses by Aphids.” *Annual Review of Phytopathology* 10 (1): 101–24. https://doi.org/10.1146/annurev.py.10.090172.000533.

Schönegger, Deborah, Bisola Mercy Babalola, Armelle Marais, Chantal Faure, and Thierry Candresse. 2022. “Diversity of Polerovirus-Associated RNAs in the Virome of Wild and Cultivated Carrots.” *Plant Pathology* 71 (9): 1892–1900. https://doi.org/10.1111/PPA.13623.

Sidharthan, Kavi V., Krishnan Nagendran, and V. K. Baranwal. 2022. “Exploration of Plant

Transcriptomes Reveals Five Putative Novel Poleroviruses and an Enamovirus." *Virus Genes* 58 (3): 244–53. https://doi.org/10.1007/S11262-022-01896-7/FIGURES/2.

Syller, Jerzy. 2003. "Molecular and Biological Features of Umbraviruses, the Unusual Plant Viruses Lacking Genetic Information for a Capsid Protein." *Physiological and Molecular Plant Pathology* 63 (1): 35–46. https://doi.org/10.1016/J.PMPP.2003.08.004.

Taliansky, Michael E., and David J. Robinson. 2003. "Molecular Biology of Umbraviruses: Phantom Warriors." *Journal of General Virology*. Microbiology Society. https://doi.org/10.1099/vir.0.19219-0.

Tamura, Koichiro, Glen Stecher, and Sudhir Kumar. 2021. "MEGA11: Molecular Evolutionary Genetics Analysis Version 11." *Molecular Biology and Evolution* 38 (7): 3022–27. https://doi.org/10.1093/molbev/msab120.

Tang, J., B. D. Quinn, and G. R. G. Clover. 2009. "First Report of Carrot Red Leaf Virus - Associated RNA Co-Infecting Carrot with Carrot Red Leaf Virus and Carrot Mottle Mimic Virus to Cause Carrot Motley Dwarf Disease in New Zealand." *Australian Plant Disease Notes* 4: 15–16. https://doi.org/10.1071/DN09006.

Vercruysse, P., M. Gibbs, L. Tirry, and M. Höfte. 2000. "RT-PCR Using Redundant Primers to Detect the Three Viruses Associated with Carrot Motley Dwarf Disease." *Journal of Virological Methods* 88 (2): 153–61. https://doi.org/10.1016/S0166-0934(00)00196-8.

Walker, Peter J., Stuart G. Siddell, Elliot J. Lefkowitz, Arcady R. Mushegian, Evelien M. Adriaenssens, Poliane Alfenas-Zerbini, Donald M. Dempsey, et al. 2022. "Recent Changes to Virus Taxonomy Ratified by the International Committee on Taxonomy of Viruses (2022)." *Archives of Virology* 167 (11): 2429–40. https://doi.org/10.1007/S00705-022-

05516-5.

Waterhouse, P. M., and A. F. Murant. 1983. “Further Evidence on the Nature of the Dependence of Carrot Mottle Virus on Carrot Red Leaf Virus for Transmission by Aphids.” *Annals of Applied Biology* 103 (3): 455–64. https://doi.org/10.1111/j.1744-7348.1983.tb02783.x.

Waterhouse, P. M., and A. F. Murant. 1981. “Purification of Carrot Red Leaf Virus and Evidence from Four Serological Tests for Its Relationship to Luteoviruses.” *Annals of Applied Biology* 97 (2): 191–204. https://doi.org/10.1111/j.1744-7348.1981.tb03012.x.

Watson, M.; Serjeant, E.P. 1964. “The Effect of Motley Dwarf Virus on Yield of Carrots and Its Transmission in the Field by Cavariella Aegopdiae Scop.” *Annals of Applied Biology* 53 (1): 77–93. https://doi.org/10.1111/j.1744-7348.1964.tb03782.x.

Watson, M. T., and B. W. Falk. 1994. “Ecological and Epidemiological Factors Affecting Carrot Motley Dwarf Development in Carrots Grown in the Salinas Valley of California.” *Plant Disease*. https://doi.org/10.1094/PD-78-0477.

Watson, Marion, E. P. Serjeant, and E. A. Lennon. 1964. “Carrot Motley Dwarf and Parsnip Mottle Viruses.” *Annals of Applied Biology* 54 (2): 153–66. https://doi.org/10.1111/j.1744-7348.1964.tb01179.x.

Watson, Michael T., Tongyan Tian, Elizabeth Estabrook, and Bryce W. Falk. 1998. “A Small RNA Resembling the Beet Western Yellows Luteovirus ST9-Associated RNA Is a Component of the California Carrot Motley Dwarf Complex.” *Phytopathology*. Vol. 88. https://doi.org/10.1094/PHYTO.1998.88.2.164.

Yoshida, Naoto. 2020. “Biological and Genetic Characterization of Carrot Red Leaf Virus and Its

Associated Virus/RNA Isolated from Carrots in Hokkaido Japan." *Plant Pathology* 69 (7): 1379–89. https://doi.org/10.1111/ppa.13202.

Zhou, Cui-Ji; Xiao-Yan Zhang, Song-Yu Liu, Ying Wang, Da-Wei Li, Jia-Lin Yu & Cheng-Gui Han. 2017. "Synergistic Infection of BrYV and PEMV 2 Increases the Accumulations of Both BrYV and BrYV-Derived SiRNAs in Nicotiana Benthamiana." *Scientific Reports* 7 (45132): 1–13. https://doi.org/10.1038/srep45132.

Table 1: Library IDs, number of clean reads per library, and descriptive information for the plant samples used in this study						
Library ID	**No. clean reads**	**Host**	**Sample group**	**Location**	**Collection year**	**Notes**
AECMD_01	16,400,000	Cilantro	H1	Davis, CA	2021	Grown from seed in growth chamber
AECMD_02	14,600,000	Carrot	H2			
AECMD_03	14,900,000	Curly	H3			
AECMD_04	13,800,000	Flat	H4			
AECMD_05	15,600,000	Flat parsley	1	Ventura Co., CA	2020	Same field/planting, different blocks
AECMD_06	15,800,000					
AECMD_07	13,400,000					
AECMD_08	13,200,000	Curly parsley	2	Ventura Co., CA	2020	
AECMD_09	19,600,000					
AECMD_10	12,700,000					
AECMD_11	12,200,000	Flat parsley	3	Ventura Co., CA	2021	No additional information provided
AECMD_12	10,800,000					
AECMD_13	13,800,000					
AECMD_14	12,500,000	Curly parsley	4	Ventura Co., CA	2021	Overwintered samples from same field as groups 1 and 2
AECMD_15	15,000,000					
AECMD_16	11,200,000	Flat				
AECMD_17	14,400,000	Curly parsley	5	Ventura Co., CA	2021	
AECMD_18	15,900,000					
AECMD_19	11,200,000					
AECMD_20	12,400,000	Curly parsley	6	Monterey Co., CA	2021	No additional information provided
AECMD_21	14,900,000					
AECMD_22	15,900,000					
AECMD_23	10,700,000	Cilantro	7	Yolo, Co., CA	2020	From resident yard; *Dysaphis apifolia* aphids present
AECMD_24	12,200,000	Cilantro	8	Yolo, Co., CA	2021	From UC Davis student
AECMD_25	15,200,000	Carrot	9	Jefferson Co., WA	2020	Cage grown; red variety
AECMD_26	15,200,000					
AECMD_27	14,900,000					
AECMD_28	12,900,000	Carrot	10	Jefferson Co., WA	2020	Cage grown; variety unspecified
AECMD_29	14,600,000					
AECMD_30	11,700,000					
AECMD_31	15,800,000	Carrot	11	Jefferson Co., WA	2020	Field grown; red variety
AECMD_32	13,500,000					
AECMD_33	8,900,000					
AECMD_34	9,700,000	Carrot	12	Grant Co., WA	2020	Field grown; variety
AECMD_35	10,900,000					
AECMD_36	11,500,000					

Listed are details of the samples used for RNAseq analysis in this study, including the plant hosts, library IDs, number of clean reads obtained for each sample, the sample group, locations

of origin, year when the samples were collected, and descriptive details that had been provided for the samples. Healthy (H) plants were included as negative controls for contaminating sequences; results from these are not discussed in the paper as dew viral sequences were recovered, none of which were a polerovirus, umbravirus or tombusvirus-like RNA.

Table 2: Contig counts, lengths, and sample group of plant viruses identified by RNAseq analysis					
Family	**Genus**	**Species**	**No. contigs**	**Contig lengths**	**Sample group(s)**
Solemoviridae	*Polerovirus*	Torilis crimson leaf virus	43	240 - 8329	1-7; 9*-12*
		carrot red leaf virus	13	281 - 6630	1*-6*; 9-12
		wild carrot red leaf virus	12	548 - 6313	2-5; 6*; 8*-12*
		parsley mottle virus	1	719	H2*; H4*; 1*-7*
		parsley mottle mimic virus	3	253 - 360	2*-4*
	Luteovirus	red clover associated virus	6	3242 - 5831	3*; 4*
Tombusviridae	*Umbravirus*	carrot mottle virus	48	282 - 5466	1-5; 6*; 7-11; 12*
		carrot mottle mimic virus	21	1260 - 5117	2-4; 5*-6*; 9-11
		wild carrot mottle virus	16	398 - 6263	1,2; 3-5*; 9-12
		tobacco bushy top virus	1	574	2-7*
Unclassified	tombusvirus-like associated RNA (tlaRNA)	arracacha latent virus E aRNA	8	507 - 4023	H3*;2*;6*; 9*-10*; 11; 12*
		CRLVaRNA a8	1	1284	9; 10*; 12*
		CRLVaRNA a25	8	458 - 5910	9*; 10-12
		CRLVaRNA alpha	4	310 - 919	9; 10*-11*; 12
		CRLVaRNA gamma	3	2009 - 2493	9-12
		CRLVaRNA sigma	8	281 - 3411	2; 5*-6*
		CRLVaRNA SH	5	496 - 3333	9-12
		CRLVaRNA HK2	3	314 - 870	2*; 6*; 8*-10*; 11-12
		tlaRNA POR19SW	1	859	6
Rhabdoviridae	*Cytorhabdovirus*	alfalfa dwarf virus	1	566	4*; 5
		raspberry vein chlorosis virus	1	859	4-5; 7
		Suaeda salsa virus 1	4	376 - 8330	H1*; 8*-9*
Closteroviridae	*Crinivirus*	beet pseudoyellows virus	3	7088 - 7924	7-8
Potyviridae	*Potyvirus*	carrot thin leaf virus	1	9711	12
		watermelon mosaic virus	1	12645	8
Secoviridae	*Waikavirus*	bellflower vein chlorosis virus	3	310 - 12119	7*; 12
	Torradovirus	carrot torradovirus 1	3	4581 - 8941	12
Partitiviridae	*Alphapartitivirus*	carrot cryptic virus	1	2170	11
	Betapartitivirus	dill cryptic virus 2	4	2344 - 2520	9*-10*; 11
	Unclassified	persimmon cryptic virus	4	655 - 1744	H3*; 11
Bromoviridae	*Alfamovirus*	alfalfa mosaic virus	1	6432	10
	Cucumovirus	cucumber mosaic virus	1	327	11*
	Ilarvirus	Raphanus latent virus	1	468	3*
Totiviridae	*Totivirus*	black raspberry virus F	3	5122 - 7012	11*; 12
Unclassified	Unclassified	red clover RNA virus 1	4	6124 - 8209	11*-12*

Listed are all of the plant viruses identified in this study, along with the families and genera (when known) they belong to, the number and lengths of contigs retrieved for each virus, and the sample groups the virus contigs were found in. Contigs that were longer than the known genome size of the respective viruses were found to have contaminating host sequences at the 5' and 3' ends, which were manually trimmed prior to further analysis. Sample groups with asterisks indicate the virus contigs in these samples were >1000 nt long, represented by >1% of the total sequencing reads, and/or had >100x average genome coverage, and were therefore excluded from downstream analysis.

Table 3: The average genome coverage, number, and percentage of sequencing reads that mapped back to potential CMD associated virus contigs identified by BLASTn and BLASTx analysis of RNAseq results

Viruses		Host	Sample group	No. Virus reads	% Virus reads	Average genome coverage
Poleroviruses	TorCLV	Parsley	1	6226019	13.9%	1025
			2	5709876	12.5%	1005
			3	6009999	16.3%	1508
			4	15449038	39.9%	3831
			5	14503124	34.9%	2670
			6	2610644	6.0%	471
	CRLV	Carrot	9	1093563	2.4%	682
			10	1701116	4.3%	1163
			11	713196	1.9%	492
			12	3651518	11.4%	3293
	WCRLV	Cilantro	8	2800544	3.0%	6207
Umbraviruses	CMoV	Parsley	2	3121520	6.9%	823
			3	1565616	4.3%	508
			4	1502702	3.9%	405
			5	1427207	3.4%	341
		Carrot	9	2189317	4.8%	613
			10	2257445	5.8%	636
			11	1019243	2.7%	334
	CMoMV	Parsley	3	591679	1.6%	395
			4	593670	1.5%	313
		Carrot	9	1066909	2.4%	539
			10	1520888	3.9%	948
			11	1801653	4.7%	1307
	WCMoV	Parsley	1	2218037	5.0%	984
			2	2796696	6.1%	1529
		Carrot	9	2039937	4.5%	1123
			10	2272673	5.8%	1473
			11	3871682	10.1%	2640
			12	1388004	4.3%	1419
tlaRNAs	ALVEaRNA	Carrot	11	3417453	8.9%	8808
	a25	Carrot	9	3057812	6.8%	3393
			10	1584673	4.0%	2780
			11	2104029	5.5%	4491
			12	1951914	6.1%	7335
	gamma	Carrot	11	2104029	5.5%	3985
	alpha	Carrot	9	557056	1.2%	8014
	a8	Carrot	9	933920	2.1%	34168
	SH	Carrot	10	605490	1.5%	2525
			12	2020040	6.3%	16258
	sigma	Parsley	2	5486414	12.1%	14800

Listed are the potential carrot motley dwarf associated polerovirus, umbravirus, and tombusvirus-like associated RNA (tlaRNA) sequences obtained from the RNAseq analysis. The sample groups in which virus sequences were found, the total number virus reads and associated percentage of the total sequencing reads, and the average genome coverage of each virus are detailed. Polerovirus, umbravirus, and tlaRNA hits >1000 nt long, represented by >1% of the total sequencing reads, and with >100x average genome coverage are excluded.

Table 4: Summary of RDP4 recombination analysis of putative hybrid virus sequences

Virus contig	Recombination break points	Major parent	Minor Parent	No. of supporting methods	Probabilities
35161	3276 - 5048	TaPV	TorCLV	7/9	8.881×10^{-16} - 7.702×10^{-132}
56020	3277 – 5151				

Shown are the results from the preliminary recombination analysis of the putative hybrid polerovirus sequences using RDP4 software. One hybrid contig was excluded from the analysis due to very large alignment gaps that seemed to disrupt the analysis. The major and minor viral parents, nucleotide positions of predicted recombination break points, number of recombination analysis methods that supported the results, and the probabilities of the results are shown.

Table 5. Virus sequences identified by RNAseq and verified by Nanopore sequencing analysis

Genus	Species	Hosts
Polerovirus	carrot red leaf virus (CRLV)	carrot
	Torilis crimson leaf virus (TorCLV)	parsley; cilantro
	Foeniculum vulgare polerovirus (FvPV)	cilantro
	parsley mottle hybrid polerovirus (PMoHPV)	parsley
Umbravirus	carrot mottle virus (CMoV)	carrot
	carrot mottle mimic virus (CMoMV)	carrot; parsley
	Pastinaca umbravirus 1 (PasUV1)	parsley, cilantro
	wild carrot mottle virus (WCMoV)	carrot; parsley
tlaRNAs	CRLVaRNA a25	carrot
	CRLVaRNA alpha	carrot
	CRLVaRNA sigma	parsley
	arracacha latent virus E associated RNA (ALVEaRNA)	carrot; parsley

Listed are the polerovirus, umbravirus, and tlaRNA sequences identified by RNAseq analysis that were confirmed to be real by RT-PCR, cloning, and whole plasmid Nanopore sequencing, along with the plant hosts in which they were present.

Table S1: Primers used in RT-PCR for the initial diagnostic assays and for validating the RNAseq results					
Purpose	**Primer name**	**Sequence**	**Annealing**	**Product**	**References**
Diagnostics	AR3F	CAGATGAATTTCTGGCGTGCTA	56	650 bp	Campbell et al., 2020
	AR5R	TCCACCATCAACACYTGRTCRTCTCCRTCRTT			
	Umbra-NNS	TGGWGTICACAACAACTC	48	408 bp	Vercruysse et al., 2000
	Umbra-IBS	AAGGCTTTGTACAACATTGG			
	CRLV-1	GAGGTGAGAAATCGCYTGAC	59	211 bp	
	CRLV-2	MGGCGCCACARTGATAGG			
	PolGen RT3	ACCTCGACTTTDA	*For RT: 45	593 bp	Lotos et al., 2014
	PolGenUp2	GATGARGGTCGYTACCG	58, 54, 52 (ramp down)		
	PolGenDown2	ACCTCGACTTTRAARCC			
RNAseq validation	CRLV_F	ATACACCACGTGCTTGCT	50	~5.4 kb	Designed for this study
	CRLV_R2	GGAACTAGTTGTGCTGCCGCTTAGC			
	TorCLV_F	CGAGGAAGATATATGCAGCTTGAG	52	~4.6 kb	
	TorCLV_R2	CTGCCCACTGGCTTAATGAGG			
	FvPV_F2	CGGGCATAAAGATCATATTTCAGCTTGC	55	~4.3 kb	
	FvPV_R2	GCTCCCCATTCTATCTTTTTATCAGTATAACCTCC			
	Hybrid_F	AGGCACTTCTCTGTGGGAGC	55	~4.6 kb	
	Hybrid_R	TGTTGGAACCGGCGTTTTCC			
	CMoV_F	AGCACTTAGATTCCCAGTTTAGC	51	~4.1 kb	
	CMoV_R	TTGAGGCGGGCTTTTACTGT			
	CMoMV_F	ATGTGTGCATGGTACGAGGG	53	~3.9 kb	
	CMoMV_R	CTTGGGCTGTTACTCCTCAACC			
	PasUV1_F	TGTCCACCGCTCTCTCCAC	53	~3.9 kb	
	PasUV1_R	CCTGCAGCTCAGGTTGGAT			
	WCMoV_F	TTGGTACTCCTGTAACGCGG	53	~3.9 kb	
	WCMoV_R	AGACCTTGTTTTAAGGACAAGGATCC			
	Sigma_F	TTAGCAACCGCGGGAAAAATTTCC	55	~2.8 kb	
	Sigma_R	TCCGAAAGGATATGTTGGCTAGTCAG			
	ALVEaRNA_F	ACCATCATAGCCAGCATTCGTGG	55	~2.3 kb	
	ALVEaRNA_R	GCGCATTATGGACACGTTGC			
	GenaRNA_F	CCGAAAGGATAAGTTGCCACACGA	55	~2.8 kb	
	GenaRNA_R	GTCGCTAGTGGAAACCCAGC			

The names, sequences, and annealing temperatures of the primers used for the initial diagnostic assays and for amplifying nearly full length virus sequences for cloning and Nanopore sequencing validation are listed. The references for the primers used for the diagnostic assays are also included.

Table S2: Parameters and substitution models used for phylogenetic tree construction					
Virus genus	**Nucleotide or amino acid sequence used in the analysis**	**No. of sequences in final dataset**	**No. of positions in final alignment**	**Substitution model used**	**Figure in paper**
Polerovirus	P1; Rap	28	573	JTT+G+I	4a
	P3; CP	16	196	WAG + I	4c
Umbravirus	Genome	33	3729	GTR+G	6a
	P2; RdRp	27	434	LG+G	6c
	P4; MP	22	248	JTT+G	6d
tlaRNAs	P1a+P1b; RdRp	21	578	JTT+G	7a

Summary of the nucleotide or amino acid sequences used for phylogenetic analyses of the poleroviruses, umbraviruses, and tombusvirus-like associated RNAs found in this study. The number of sequences used in the analysis, number of positions in the final alignments of the respective nucleotide or amino acid sequences, and the substation models used when constructing the tree as determined MEGA11 model selection software are detailed, and the figures where each of the resulting phylogenetic trees is depicted in the paper are listed.

Table S3: Putative mycovirus sequences identified by BLASTx and BLASTn analysis of RNAseq data

Family	Genus	Species	Contigs
Amalgaviridae	Unclassified	Plasmopara viticola lesion assoc. amalga like virus	2
Botourmiaviridae	*Botourmiavirus*	Pestalotiopsis botourmiavirus	1
	Magoulivirus	Botrytis cinerea ourmia-like virus	3
		Acremonium sclerotigenum ourmia-like virus	1
		Cladosporium cladosporioides ourmia-like virus	1
	Penoulivirus	Plasmopara viticola lesion assoc. ourmia-like virus	40
	Scleroulivirus	Soybean leaf-assoc. ourmiavirus	4
	Unclassified	Erysiphe necator assoc. ourmia-like virus	56
Discoviridae	*Orthodiscovirus*	Plasmopara viticola lesion assoc. mycobunyavirales-	1
Fusariviridae	*Fusarivirus*	Erysiphe necator assoc. fusarivirus	4
		Fusarium poae fusarivirus	1
	Unclassified	Pleospora typhicola fusarivirus	1
Hypoviridae	*Alphahypovirus*	Bipolaris oryzae hypovirus	1
	Betahypovirus	Fusarium oxysporum dianthi hypovirus	1
Mitoviridae	*Duamitovirus*	Beta vulgaris mitovirus	1
	Mitovirus	Erysiphe necator assoc. mitovirus	41
		Plasmopara viticola lesion assoc. mitovirus	28
		Erysiphe necator mitovirus	21
		pea assoc. mitovirus	19
		Mitovirus sp.	4
		Erysiphales assoc. mitovirus	3
		soybean leaf-assoc. mitovirus	3
		Fusarium andiyazi mitovirus	2
		Colletotrichum higginsianum mitovirus	1
		Leptosphaeria biglobosa mitovirus	1
		Sclerotinia sclerotiorum mitovirus	1
	Unuamitovirus	Alternaria arborescens mitovirus	6
		Ophiostoma mitovirus	1
Mymonaviridae	*Sclerotimonavirus*	Sclerotinia sclerotiorum negative-stranded RNA virus	1
Narnaviridae	*Narnavirus*	Erysiphe necator assoc. narnavirus	9
		Plasmopara viticola lesion assoc. narnavirus	6
		Monilinia narnavirus	3
		Cladosporium tenuissimum narnavirus	1
		Sclerotinia sclerotiorum narnavirus	1
	Unclassified	Erysiphales narna-like virus	11
Partitiviridae	*Partitivirus*	Fusarium solani partitivirus	2
		Picoa juniperi partitivirus	1
Potyviridae	Unclassified	Plasmopara viticola lesion assoc. poty-like virus	1
Tombusviridae	*Tombusvirus*	Erysiphales assoc. tombus-like virus	1
		Erysiphe necator assoc. tombus-like virus	1
		Leveillula taurica assoc. tombus-like virus	1
Totiviridae	*Totivirus*	red clover powdery mildew-assoc. totivirus	8

		Erysiphe necator assoc. totivirus	2
		Xanthophyllomyces dendrorhous virus	2
		Puccinia striiformis totivirus	1
	Unclassified	Plasmopara viticola lesion assoc. toti	4
		Erysiphales assoc. toti-like virus	3
		Rhodosporidiobolus odoratus RNA virus	2
Unclassified	Unclassified	Riboviria sp.	5
		Uromyces virus A	3
		Erysiphe necator assoc. virus	2
		Erysiphe necator assoc. abispo virus	1
		Erysiphe necator assoc. negative-stranded RNA virus	1
		Fusarium graminearum dsRNA mycovirus	1
		Macrophomina phaseolina fusagravirus	1
		Plasmopara viticola lesion assoc. ambiguivirus	1
		Sclerotinia sclerotiorum bunyavirus	1
Virgaviridae	*Tobamovirus*	Plasmopara viticola lesion assoc. tobamo-like virus	3
		Erysiphe necator assoc. tobamo-like virus	2
	unclassified	Erysiphe necator assoc. virga-like virus	6

Summary of the species, genera, and families—when known—of putative mycovirus sequences recovered from the RNAseq dataset and the number of contigs each virus is represented by.

Table S4: Putative insect sequences identified by BLASTx and BLASTn analysis of RNAseq data

Family	Genus	Species	No. of Contigs
Chuviridae	Unclassified	lishi spider virus	2
Lispiviridae	*Nematovirus*	Wuchang romanomermis nematode virus	2
Mitoviridae	*Mitovirus*	Thrips tabaci associated mitovirus	3
Orthomyxoviridae	Unclassified	Hemipteran orthomyxo-related virus	1
Phasmaviridae		Wuhan insect virus	5
Phenuiviridae		hymenopteran phenui-related virus	1
Solemoviridae		nelson sobemo-like virus	1
		Frankliniella occidentalis associated sobemo-like virus	1
Tombusviridae		crane fly tombus-like virus	1
Unclassified		brandeis virus	4
		Hubei levi-like virus	1
		Hubei Wuhan insect virus	1
		muthill virus	1
		shahe levi-like virus	1
		barley aphid RNA virus	4
		gorebridge virus	2
		Hubei partiti-like virus	1
		Beihai narna-like virus	1

Summary of the species, genera, and families—when known—of putative arthropod associated viral sequences recovered from the RNAseq dataset and the number of contigs each virus is represented by.

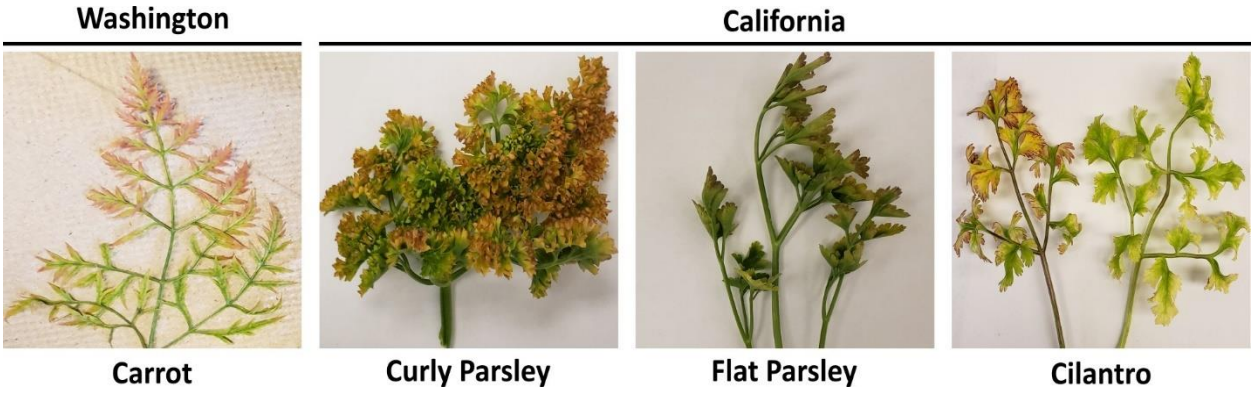

Figure 1. Carrot, parsley, and cilantro samples exhibiting typical symptoms of carrot motley dwarf disease.

Depicted are representative carrot, flat and curly leaf parsley, and cilantro samples exhibiting typical symptoms of carrot motley dwarf disease. Labels below the images indicate what the plant sample is and labels above the images indicate the state from which the samples originated.

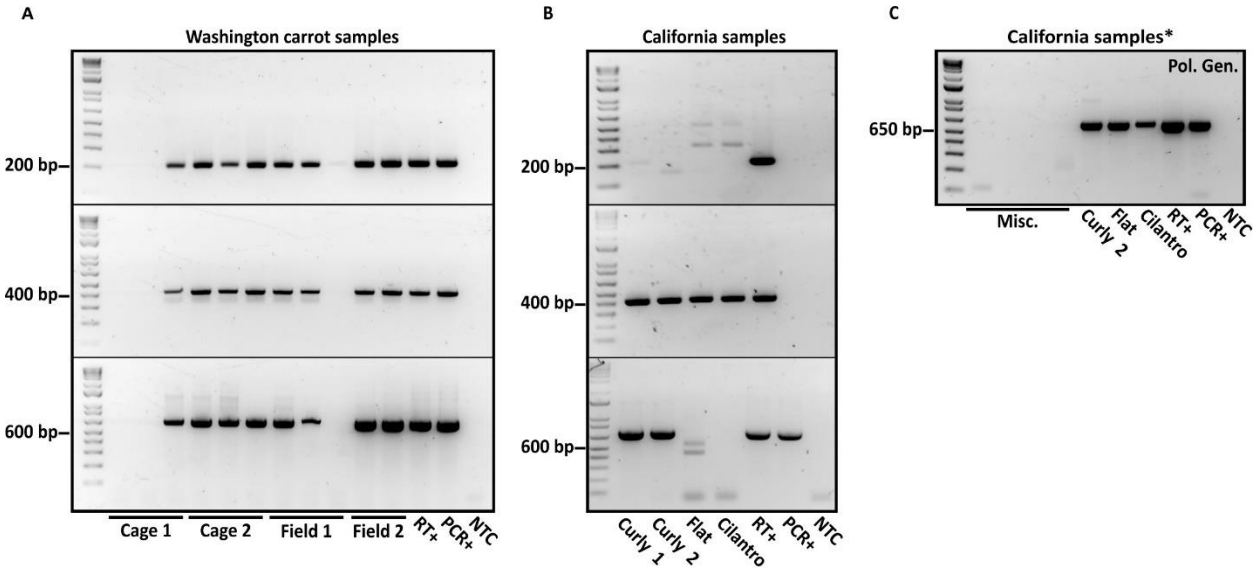

Figure 2. Diagnostic RT-PCR assays for the detection of carrot motley dwarf associated viruses.

Depicted are gel images of PCR products obtained from diagnostic RT-PCR assays for the detection of the typical polerovirus (CRLV; product size: 211 bp), umbraviruses (CMoV/CMoMV; product size: 408 bp), and tlaRNAs (product size: 650 bp) associated with carrot motley dwarf disease in **a)** pooled carrot samples and **b)** pooled parsley samples and an individual cilantro sample. PCR products from a separate RT-PCR diagnostic assay for the generic detection of poleroviruses (product size: 593 bp) is depicted in panel **c.** Labels in the upper right corner of the gels indicate the PCR target(s), labels above the gels indicate the state from which the samples originated, and labels below indicate the sample or sample group. CRLV: carrot red leaf virus; CMoV/CMoMV: carrot mottle virus / carrot mottle mimic virus; tlaRNAs: tombusvirus-like associated RNAs; RT+: reverse transcription positive control; PCR+: positive control for PCR; NTC: no template control; Misc.: miscellaneous barley samples that had also been submitted to us for diagnosis.

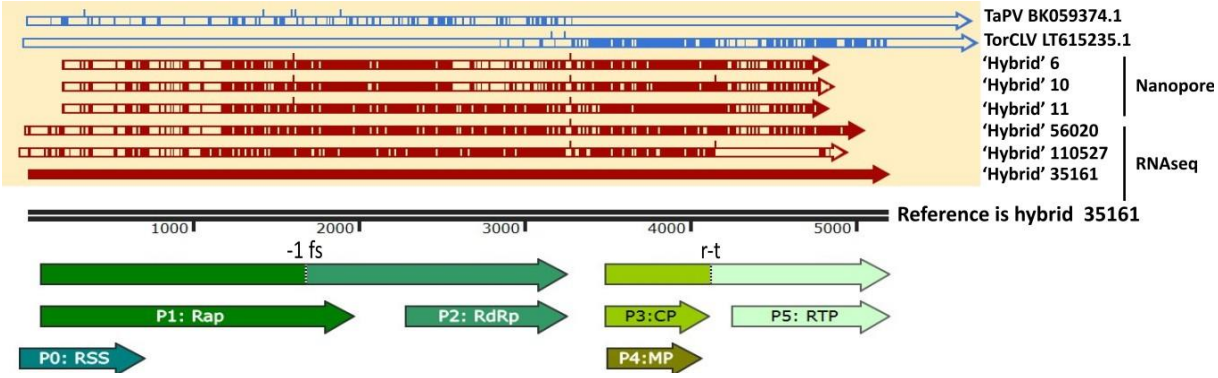

Figure 3. Alignments of putative hybrid polerovirus sequences found in this study with TorCLV and TaPV reference sequences.

Alignments of the putative hybrid polerovirus sequences (colored red; beneath reference sequences) with the putative parental TorCLV and TaPV reference sequences (colored blue; above hybrid sequences), obtained in this study both by the initial RNAseq assay and by Nanopore sequencing. Labels to the right indicate aligned hybrid contigs and the reference sequence names; the perpendicular black lines to the right of these labels indicate whether the aligned sequence came from the RNAseq or Nanopore analyses. The base reference sequence used was that of hybrid contig 35161, as this was the longest contig obtained by RNAseq. The double black line is a size marker for the aligned sequences, and the arrows beneath this line indicate the predicted open reading frame (ORF) translations of these putative polerovirus sequences. TaPV: Trachyspermmum ammi polerovirus; TorCLV: Torilis crimson leaf virus; RSS: RNA interference silencing suppressor; Rap: replication associated protein; -1fs: depicts a -1 frameshifting site that enables P1 and P2 to be translated as a fusion protein; RdRp: RNA dependent RNA polymerase; CP: capsid protein; MP: movement protein; RTP: readthrough protein; r-t: indicates a readthrough site that allows P3 and P5 to be translated as a fusion protein.

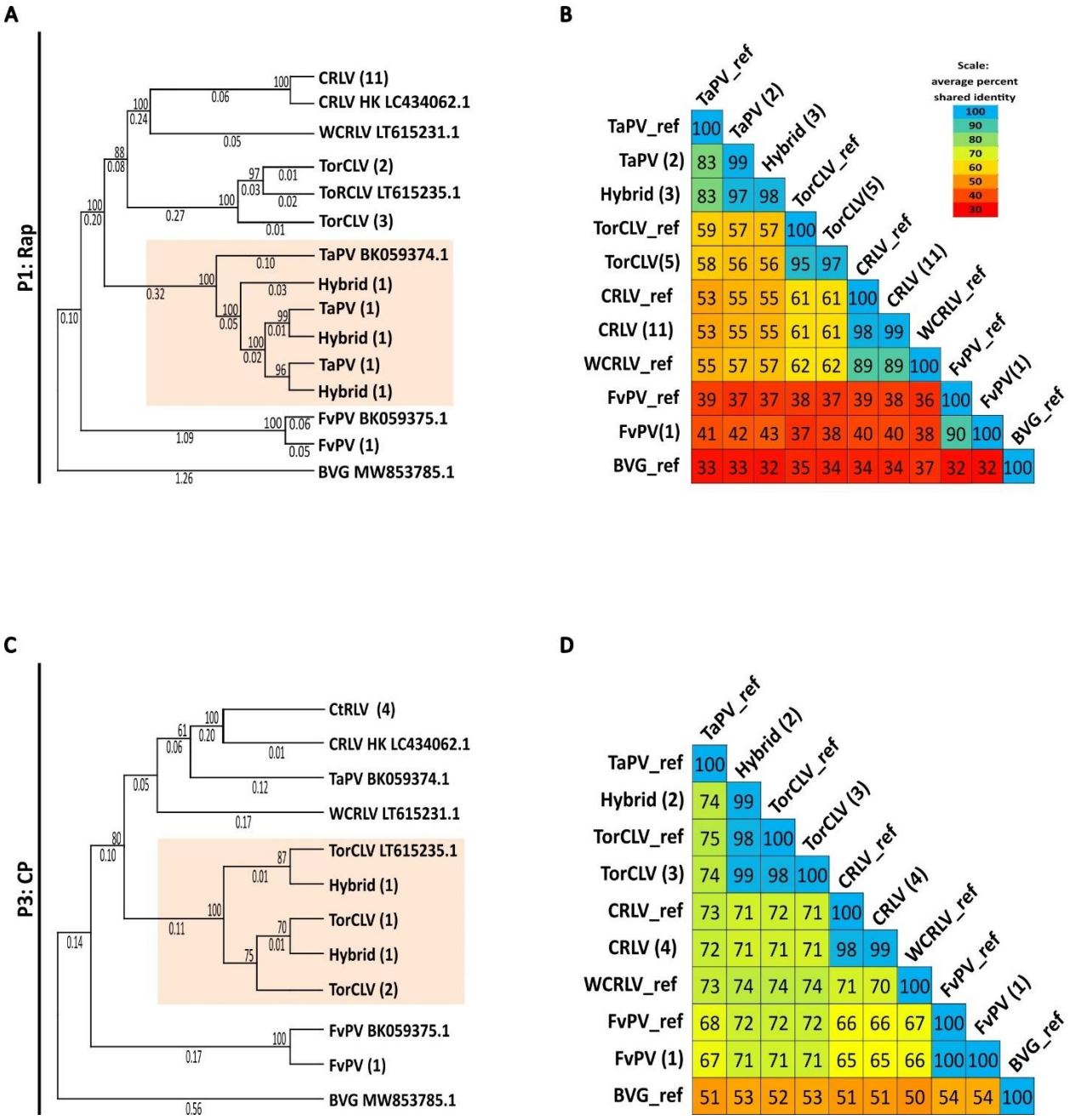

Figure 4. Phylogenetic trees and average percent pairwise matrices depicting relationships of the polerovirus sequences found in this study.

Depicted are maximum likelihood phylogenetic trees (**a** and **c**) and averaged percent pairwise identity matrices (**b** and **d**) constructed using the translated amino acid sequences of the (**a** and **b**) P1 replication associated protein (Rap) and the (**c** and **d**) P3 capsid protein (CP) genes of the

poleroviruses identified in this study. Black perpendicular lines to the left of the figures indicate the amino acid sequences used for the comparison. For the phylogenetic trees, numbers below the line indicate the amino acid substitutions per site, and numbers above the lines indicate the bootstrap support values; bootstrap values below 50% are not shown. Numbers in parentheses after the virus labels indicates the number of viral sequences used in the analysis. Reference sequences are indicated by their GenBank accession numbers to the right of the virus label. Tan boxes are used to highlight the positions of the putative hybrid polerovirus sequences in the phylogenetic trees. The percent identity shared between the amino acid sequences of different viruses are listed in the boxes of the matrices as well as in the scale bar in the upper right corner of the figure. TaPV: Trachyspermum ammi polerovirus; TorCLV: Torilis crimson leaf virus; CRLV: carrot red leaf virus; Hybrid: hybrid polerovirus sequences; FvPV: Foeniculum vulgare polerovirus; WCRLV: wild carrot red leaf virus; BVG: barley virus G (outgroup).

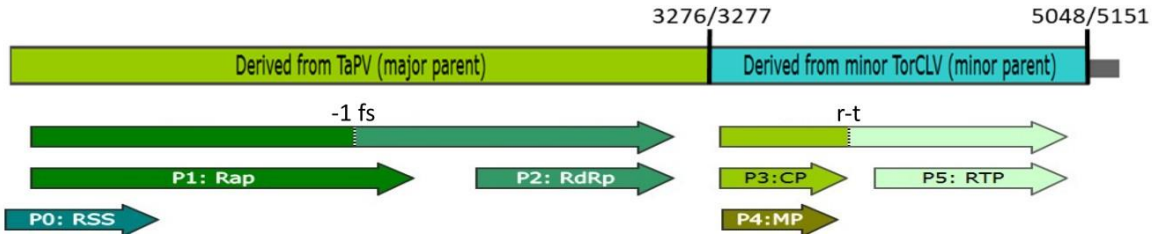

Figure 5. Parental origins of the 5' and 3' ends of putative hybrid polerovirus sequences. Depicted is schematic representation of the putative hybrid polerovirus genome. The green box covering the 5' two thirds of the genome indicates the portion of the genome that likely originated from TaPV (or an unknown virus closely related to TaPV). The teal box covering the 3' last third of the genome indicates the portion of the genome that likely originated form TorCLV. The nucleotide positions of the predicted recombination break points are indicated above the diagram. The arrows below the diagram depict predicted open reading frame translations. RSS: RNA interference silencing suppressor; Rap: replication associated protein; -1fs: depicts a -1 frameshifting site that enables P1 and P2 to be translated as a fusion protein; RdRp: RNA dependent RNA polymerase; CP: capsid protein; MP: movement protein; RTP: readthrough protein; r-t: indicates a readthrough site that allows P3 and P5 to be translated as a fusion protein.

A

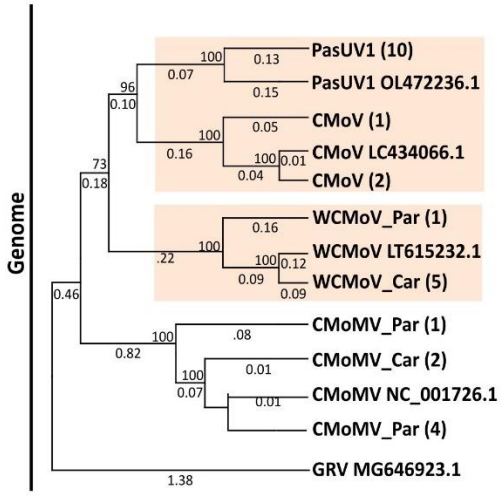
Genome
PasUV1 (10)
PasUV1 OL472236.1
CMoV (1)
CMoV LC434066.1
CMoV (2)
WCMoV_Par (1)
WCMoV LT615232.1
WCMoV_Car (5)
CMoMV_Par (1)
CMoMV_Car (2)
CMoMV NC_001726.1
CMoMV_Par (4)
GRV MG646923.1

B

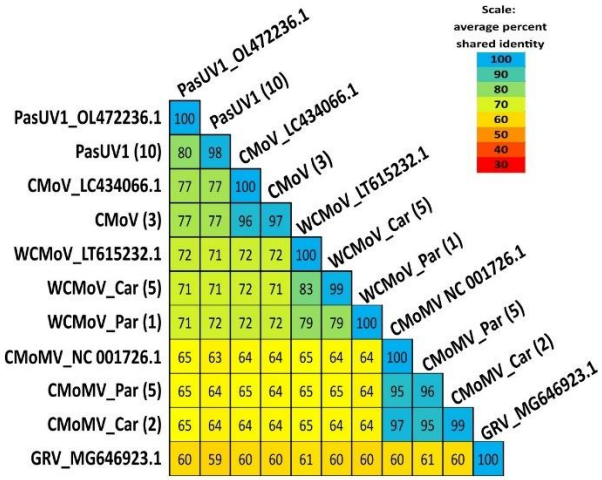
Scale:
average percent
shared identity
100
90
80
70
60
50
40
30
PasUV1_OL472236.1
PasUV1 (10)
CMoV_LC434066.1
CMoV (3)
WCMoV_LT615232.1
WCMoV_Car (5)
WCMoV_Par (1)
CMoMV NC 001726.1
CMoMV_Par (5)
CMoMV_Car (2)
GRV_MG646923.1

C

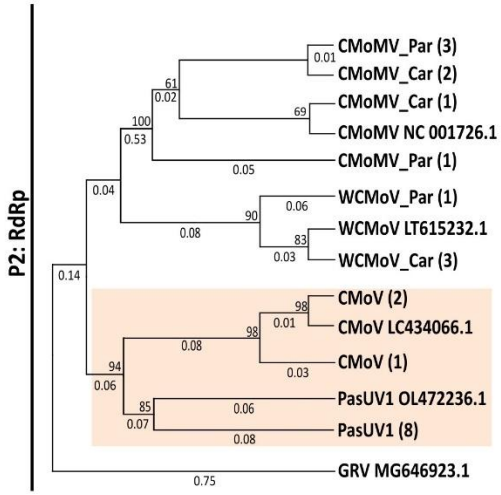
P2: RdRp
CMoMV_Par (3)
CMoMV_Car (2)
CMoMV_Car (1)
CMoMV NC 001726.1
CMoMV_Par (1)
WCMoV_Par (1)
WCMoV LT615232.1
WCMoV_Car (3)
CMoV (2)
CMoV LC434066.1
CMoV (1)
PasUV1 OL472236.1
PasUV1 (8)
GRV MG646923.1

D

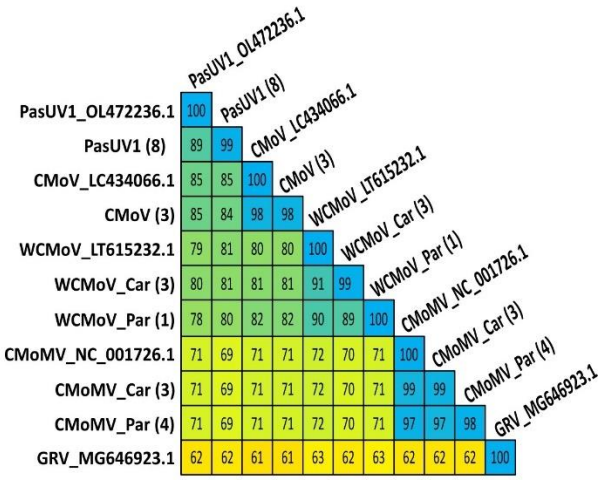
PasUV1_OL472236.1
PasUV1 (8)
CMoV_LC434066.1
CMoV (3)
WCMoV_LT615232.1
WCMoV_Car (3)
WCMoV_Par (1)
CMoMV_NC_001726.1
CMoMV_Car (3)
CMoMV_Par (4)
GRV_MG646923.1

E

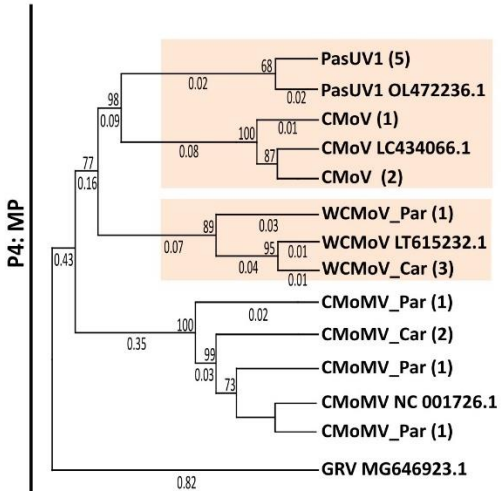
P4: MP
PasUV1 (5)
PasUV1 OL472236.1
CMoV (1)
CMoV LC434066.1
CMoV (2)
WCMoV_Par (1)
WCMoV LT615232.1
WCMoV_Car (3)
CMoMV_Par (1)
CMoMV_Car (2)
CMoMV_Par (1)
CMoMV NC 001726.1
CMoMV_Par (1)
GRV MG646923.1

F

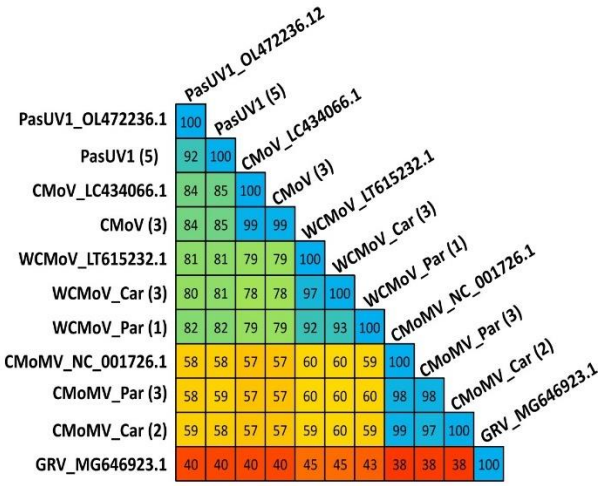
PasUV1_OL472236.12
PasUV1 (5)
CMoV_LC434066.1
CMoV (3)
WCMoV_LT615232.1
WCMoV_Car (3)
WCMoV_Par (1)
CMoMV_NC_001726.1
CMoMV_Par (3)
CMoMV_Car (2)
GRV_MG646923.1

Figure 6. Phylogenetic trees and average percent pairwise matrices depicting relationships of the umbravirus sequences found in this study.

Depicted are maximum likelihood phylogenetic trees (**A, C,** and **D**) and averaged percent pairwise identity matrices (**B, D,** and **F**) constructed using the nucleotide sequences of the near complete genomes (**A** and **B**), and the translated amino acid sequences of the (**C** and **D**) P2 RNA dependent RNA polymerase (RdRp) and the (**E** and **F**) P4 cell-to-cell movement protein (MP) genes of the umbraviruses identified in this study. Black perpendicular lines to the left of the figures indicate the genome or amino acid sequences used for the comparison. For the phylogenetic trees, numbers below the line indicate the nucleotide or amino acid substitutions per site, and numbers above the lines indicate the bootstrap support values; bootstrap values below 50% are not shown. Numbers in parentheses after the virus labels indicates the number of viral sequences used in the analysis. References sequences are indicated by their GenBank accession numbers to the right of the virus label. Tan boxes are used to highlight the positions of the WCMoV and PasUV1 sequences suspected of being divergent strains of CMoV. The percent identity shared between the amino acid sequences of different viruses are listed in the boxes of the matrices as well as in the scale bar in the upper right corner of the figure. CMoV: carrot mottle virus; CMoMV: carrot mottle mimic virus; WCMoV: wild carrot mild virus; PasUV1: Pastinaca umbravirus 1 (PasUV1); GRV: groundnut rosette virus (outgroup).

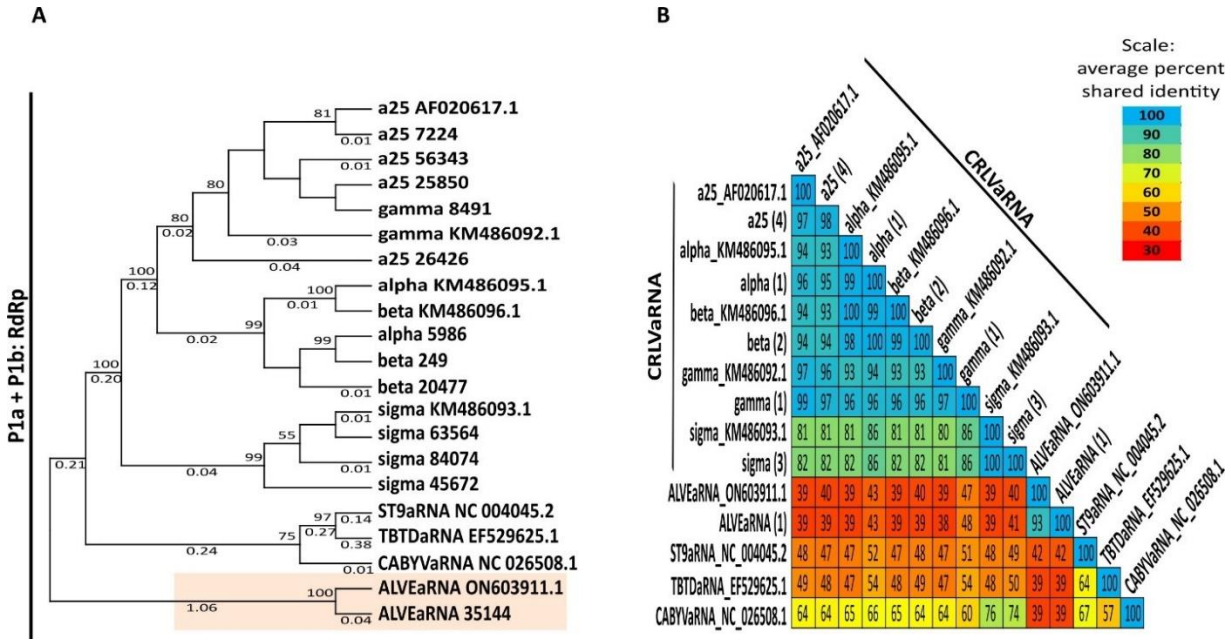

Figure 7. Phylogenetic trees and average percent pairwise matrices depicting relationships of the tombusvirus-like associated RNA sequences found in this study.

Depicted are a maximum likelihood phylogenetic tree (**A**) and averaged percent pairwise identity matrix (**B**) constructed using the translated amino acid sequence of the fused P1a+P1b RdRp gene sequences the tombusvirus-like associated RNA (tlaRNA) sequences identified in this study. For the phylogenetic trees, numbers below the line indicate the amino acid substitutions per site, and numbers above the lines indicate the bootstrap support values; bootstrap values below 50% are not shown. Numbers after the tlaRNA names indicate the contig label or GenBank accession for reference sequences, and parentheses after tlaRNA names indicate the number of tlaRNA sequences that were averaged. The tan box highlights the position of the most recently described tlaRNA, ALVEaRNA. The percent identity shared between the amino acid sequences of different viruses are listed in the boxes of the matrices as well as in the scale bar in the upper right corner of the figure. CRLVaRNA: carrot red leaf virus associated RNA. ALVEaRNA: arracacha latent virus E associated RNA. Outgroup sequences: TBTDaRNA:

tobacco busy top disease associated RNA; CABYVaRNA: cucurbit aphid borne yellows virus associated RNA.

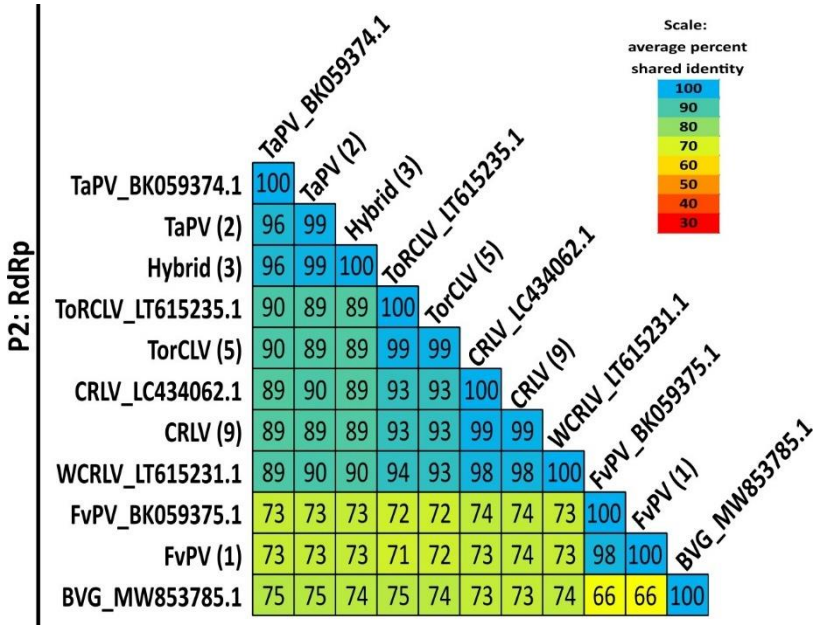

Figure S1. Average percent pairwise identity matrix of polerovirus P2 (RdRp) translated amino acid sequences.

Depicted is an averaged percent pairwise identity matrix showing shared amino acid identities of the P2 RNA dependent RNA polymerase (RdRp) sequences of the poleroviruses identified in this study. It can be seen that viruses known to be different species share high identity of this sequence, likely because the RdRp sequence is highly conserved amongst polerovirus species. The percent identity shared between the amino acid sequences of different viruses are listed in the boxes of the matrices as well as in the scale bar in the upper right corner of the figure. CRLVaRNA: carrot red leaf virus associated RNA. ALVEaRNA: arracacha latent virus E associated RNA; TBTDaRNA. Outgroup sequences: tobacco busy top disease associated RNA; CABYVaRNA: cucurbit aphid borne yellows virus associated RNA. TaPV: Trachyspermum ammi polerovirus; TorCLV: Torilis crimson leaf virus; CRLV: carrot red leaf virus; Hybrid: hybrid polerovirus sequences; FvPV: Foeniculum vulgare polerovirus; WCRLV: wild carrot red leaf virus; BVG: barley virus G (outgroup).

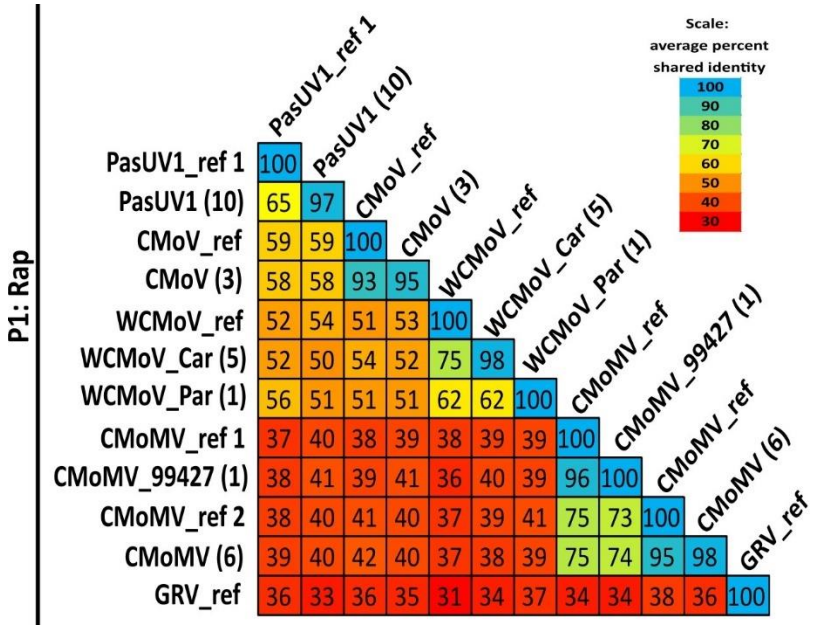

Figure S2. Average percent pairwise identity matrix of umbravirus P1 (Rap) translated amino acid sequences.

Depicted is an averaged percent pairwise identity matrix showing shared amino acid identities of the P1 replication associated protein (Rap) sequences of the umbraviruses identified in this study. It can be seen that these sequences appear to be highly divergent, even between the different umbravirus sequences. The percent identity shared between the amino acid sequences of different viruses are listed in the boxes of the matrices as well as in the scale bar in the upper right corner of the figure. CMoV: carrot mottle virus; CMoMV: carrot mottle mimic virus; WCMoV: wild carrot mild virus; PasUV1: Pastinaca umbravirus 1 (PasUV1); GRV: groundnut rosette virus (outgroup).

Chapter 4

Construction and use of an infectious cDNA clone to identify aphid vectors and susceptible monocot hosts of the *Polerovirus* Barley virus G

Anna Erickson[1], Jun Jiang [1], Yen-Wen Kuo[1], Bryce W. Falk[1]

[1] Department of Plant Pathology, University of California, Davis, CA 95616, USA

Abstract

Since its discovery in 2016, the *Polerovirus* Barley virus G has been reported in at least nine countries and multiple species of monocot plants. All of these reports have used PCR and/or sequencing based assays to identify BVG, however none have investigated the biology of BVG. In this study we detail the generation of the first infectious cDNA clone of BVG from archived RNA, thereby producing a valuable experimental tool and system for studying BVG biology. Using this system we identified two compatible aphid vectors and confirmed the susceptibility of several monocot plants, and the dicotyledonous plant host *Nicotiana benthamiana*, to BVG.

Introduction

Yellow dwarf disease of small grain crops—considered the 'yellow plague' of small grains—is caused by viruses broadly referred to as barley and cereal yellow dwarf viruses (BYDVs and CYDVs), and has long been considered one of the most severe and widely spread viral diseases of small grain crops worldwide (Burgess et al., 1999; Griesbach et al., 1989; Miller and Rasochová, 1997; Walls et al., 2019; Wegulo, 2013). Yellow dwarf viruses (YDVs) can infect over 100 species of plants in the family *Poaceae*, including economically important crop species such as barley (*Hordeum vulgare*), oats (*Avena sativa*), wheat (*Triticum aestivum*), rye (*Secale cereale*), maize (*Zea maize*), and rice (*Oryza sativa*), as well as many non-cultivated grass and weedy species that can serve as reservoirs of viral infection (Burgess et al., 1999). Symptom presentation, severity, and effects on yield vary greatly depending on a variety of factors including virus and host plant species/cultivar, host age at the time of inoculation, and environmental conditions (Burgess et al., 1999; Griesbach et al., 1989). Symptoms typically include yellowing or reddening of leaf tips and margins, stunted growth, reduced root mass,

increased tillering, and reduced grain yields. Identification of YDV infection based on symptoms alone is difficult, as many abiotic factors such as drought or nutrient deficiencies can cause similar symptoms, therefore it is necessary to confirm YDV infection by additional means such as serological or PCR-based assays (Griesbach et al., 1989; Malmstrom and Shu, 2004).

YDVs belong to the genera *Luteovirus* (family *Tombusviridae*) and *Polerovirus* (family *Solemoviridae*), according to the International Committee on Taxonomy of Viruses (Walker P.J., et al., 2022). They are positive sense, single stranded RNA (ssRNA) viruses with T=3 icosahedral virion morphology, that are restricted to the phloem tissues of their host plants (Burgess et al., 1999; Miller and Rasochová, 1997). These viruses are obligately transmitted between hosts exclusively by aphid vectors in a persistent-non-propagative manner, and often times this virus-vector relationship occurs in a fairly species-specific manner (Miller and Rasochová, 1997; Rochow, 1969). Cereal infecting *Luteovirus* species are broadly referred to as BYDVs, while those belonging to the genus *Polerovirus* are referred to as CYDVs (Malmstrom and Shu, 2004; Walls et al., 2019; Wegulo et al., 2013). Individual virus species are differentiated based on the percent of shared identity in amino acid sequence of any encoded proteins (>10% difference in identity demarcates different species), serological properties, and the species of aphids that vector them; among these the most commonly found and most damaging virus species are BYDV-PAV and CYDV-RPV (Miller et al., 2002). While over 25 species of aphids can vector YDVs, four are regarded as the most economically relevant: the corn-leaf aphid (*Rhopalosiphum maidis*), the bird cherry-oat aphid (*R. padi*), the English grain aphid (*Sitobion avenae*), and the greenbug (*Schizaphis graminum*) (Walls et al., 2019).

In 2016, Zhao at al. first determined the complete genome sequence and identified—based on genome sequence and organization (Figure 1)—a novel *Polerovirus* in barley samples

exhibiting typical symptoms of YDV infection (stunting and yellow leaf discoloration), collected in the Gimje province of South Korea, which they designated Barley virus G (BVG) (Zhao et al., 2016). Since its initial discovery BVG has been, and continues to be, detected in other *Poaceous* plant species and locations throughout the world. In South Korea, BVG has now been reported in six additional locations and two additional hosts, foxtail (*Setaria italica*) and proso (*Panicum milaceum*) millets (Jo et al 2018; Oh, J. et al 2017; Park et al., 2016 and 2017). In 2018 BVG was detected in a switch grass (*Panicum virgatum*) sample from the Netherlands, in maize from Greece, and in barley samples from multiple other countries in Europe including Hungary, Germany, and France (Dumas et al., 2022; Gavrili et al., 2021; Kumar et al., 2018; Pasztor et al., 2020; Svanella-Dumas, L., et al., 2022). In Kenya, BVG was identified in a metagenomic study surveying viruses associated with maize lethal necrosis disease (Waimatha et al., 2018). In Australia BVG was identified in freshly collected barley and wheat samples and also, intriguingly, in a 34-year-old oat herbarium sample (Nancarrow, N., et al., 2019 a and b). Our lab recently reported the first detection of BVG in barley in the United States in California (Erickson and Falk, 2021). Until now, all work on BVG has been limited to PCR and sequencing-based assays of field collected samples, but no work has been done to isolate and investigate the biology of this recently discovered virus.

In this study we describe the generation of an infectious cDNA clone of BVG from archived RNA from the barley sample in which we first found BVG, to use as a tool to study the biology of this virus. Using agroinoculation, we established a productive BVG infection in the model plant *Nicotiana benthamiana*, from which we partially purified infectious BVG virions, which were used as inoculum in transmission experiments using three different common aphid vector species (*R. maidis*, *R. padi*, and the green peach aphid *Myzus persicae*) to identify vectors

of BVG; of these *R. maidis* was found to be the most effective vector. The efficiency of BVG transmission to barley plants by *R. maidis,* was subsequently determined. Additionally, a small host range study of several monocot plant species was conducted. This is the first study to generate an infectious BVG clone and to employ it as a tool to determine important biological traits—such as aphid vectors and susceptible hosts—relevant to the epidemiology of this virus. This provides a valuable research tool and information on the biology of this recently identified *Polerovirus*, which should help inform future studies on the potential impacts of BVG on the productivity of economically important small grain crops.

Materials and methods

BVG detection

As described in our previous report (Erickson and Falk, 2021) BVG was initially detected in a barley sample exhibiting symptoms of yellow dwarf disease submitted to the lab for diagnosis. In brief, total RNA was extracted using Trizol™ Reagent (www.thermofisher.com) according to the manufacturer's protocol and used as template in a multiplexed reverse transcriptase–polymerase chain reaction (RT-PCR) assay designed for the simultaneous detection of cereal infecting poleroviruses and luteoviruses, as described by Malmstrom and Shu (2004). Sequences of the resulting PCR products were confirmed by Sanger sequencing (www.genewiz.com). We aimed to investigate aspects of BVG biology, therefore we conducted a limited field survey to try and re-isolate BVG in a second year. We used RT-PCR to screen 96 symptomatic samples collected from three different wheat, oat, and barley fields for BVG, however none of the samples tested positive for BVG.

BVG plasmid construction

Lacking live BVG-infected tissue that could be used as inoculum for biological studies, we attempted to clone a full length cDNA copy of the BVG genome using the original archived RNA. Primers targeting the extreme 5' and 3' ends of the BVG genome were designed with SnapGene software using the BVG reference genome (KT962089) available in the NCBI data base (National Center for Biotechnology Information, 1988). The archived RNA extracted from the original BVG-positive barley sample in which we detected BVG was used for cDNA synthesis using PrimeScript reverse transcriptase (www.takarabio.com). The cDNA was used as template for PCR using the PrimeSTAR GXL DNA polymerase kit (www.takarabio.com) in a 50 µl reaction containing 10 µl of 5x buffer, 4 µl of dNTPS (10 mM), 1.5 µl each of forward and reverse primers (10 µM), 5 µl of cDNA, and 2 µl of enzyme. PCR products were gel purified using the Nucleospin Gel and PCR Cleanup Kit (www.takarabio.com), ligated into the pJL89 vector backbone using the In-Fusion HD Cloning kit according to the manufacturer's protocol (www.takarabio.com), and transformed into *Escherichia coli* strain DH5α. Plasmids extracted from three PCR positive colonies (14, 15, and 18) were selected for further testing. The full-length sequence of the cloned BVG genome was confirmed by Sanger sequencing (https://www.genewiz.com) and deposited in the GenBank database under accession number MW853785. All primers used in this study are listed in Supplementary Table S1.

Confirming infectivity of the BVG construct

Cultures of *A. tumefaciens* strain GV3101 were transformed with each of the three selected BVG-pJL89 recombinant plasmids described above. Two colonies from each culture (isolates designated BVG- 14.1, 14.2, 15.1, 15.2, 18.1, and 18.2) were picked for screening, inoculated into five mL of LB broth amended with kanamycin (MacWilliams and Liao, 2006), and cultured at 28 ℃ with shaking at 250 RPM for two days in darkness. One mL of culture was

inoculated into 25 mL of L-MESA media (25 mL of LB + kanamycin broth, one ml of 0.5 M MES (pH 5.7), five µl of 0.1 M acetosyringone) and cultured as described above. The cells were pelleted by centrifugation at ~4,100 x g for 10 minutes and resuspended in infiltration buffer (0.01 M $MgCl_2$, 0.01 M MES (pH 5.7), 10^{-4} M acetosyringone). The suspension was adjusted to an optical density at 600 nm ($O.D._{600}$) of ~0.6, then incubated at room temperature in darkness for three hours. A needleless syringe was used to infiltrate the suspensions into leaves of transgenic *Nicotiana benthamiana* plants expressing the potyviral silencing suppressor HC-Pro (Wang et al., 2009), which were kept in an air conditioned room (22 ℃, 12:12 h light/dark cycle). Three plants were infiltrated with each construct and a non-infiltrated plant was used as a healthy control.

Total RNA extracted from tissue sampled from the upper non-inoculated leaves one week post inoculation (wpi) was used as template for cDNA synthesis using the SuperScript II (www.thermofisher.com) reverse transcription kit; control reactions excluding RT enzyme were used to verify absence of contaminating plasmid DNA. PCR was done with the GoTaq Flexi DNA polymerase kit (www.promega.com) in a 25 µl reaction containing five µl of 5x buffer, 1.5 µl of $MgCl_2$ (25 mM), 1.25 µl each of forward and reverse primers (Table S1), 0.5 µl of dNTPs (10 mM), 0.125 µl of enzyme, and one µl of cDNA. Thermocycling conditions were as follows: 94 ℃ for two min, followed by 35 cycles of 94 ℃ for 30 s, 50 ℃ for 30 s, and 72 ℃ for one min, with a final extension at 72 ℃ for five min. PCR products were visualized by gel electrophoresis in a 2% agarose gel, and the sequences confirmed by Sanger sequencing (www.genewiz.com). One construct—BVG 18—was found to initiate a strong BVG infection and selected for use in downstream experiments. The experiment was repeated a second time using only the BVG-18 construct. Infectivity in wild type *N. benthamiana* was also confirmed. A

northern blot assay was conducted to verify that BVG was present and replicating, using the protocol described (Jiang et al., 2021). .

Virion partial purification

Approximately 20 g of BVG-infected *N. benthamiana* leaf tissue was ground in liquid nitrogen with a mortar and pestle, transferred to a beaker containing 70 mL of pre-chilled buffer (0.1 M KPO_4 + 0.01% glycine (pH 7.0) with 0.1% 2-beta mercaptoethanol (2-ME)), and stirred for ~five min. The solution was strained through two layers of cheese cloth, mixed with an equal volume of chloroform:butanol (1:1), stirred for one min, transferred to a polypropylene centrifuge tube, then centrifuged at 8000 rpm for 15 min in a prechilled (4 ℃) GSA rotor (Sorvall). The aqueous phase was transferred into a Ti70 polycarbonate ultracentrifuge tube, then underlaid with five ml of 20% sucrose in buffer (no 2-ME). The tubes were centrifuged at 50,000 rpm for two hours in a pre-chilled (4 ℃) Ti70 rotor (Beckman Coulter). The pellet was resuspended in 200 µl of 0.01 M $KP0_4$ + 0.01 M glycine (pH 7.0); the suspension was transferred into a 1.5 mL microfuge tube, and centrifuged at 10,000 rpm for one min to pellet residual debris. The supernatant was transferred into a clean microfuge tube and stored at 4 ℃ until use.

Aphid vector identification experiments

Three species of aphids—*Myzus persicae, Rhopalosiphum maidis,* and *Rhopalosiphum padi*—were tested for their ability to vector BVG. Nonviruliferous *M. persicae* aphids were reared on radish (*Raphanus raphanistrum* subsp. *sativus*) plants, *R. maidis* aphids on barley (*Hordeum vulgare*) plants, and *R. padi* aphids on oat (*Avena sativa*) plants in an air conditioned room (~25 ℃; 16:8 h light/dark cycle). *M. persicae* aphids, which are polyphagous, were given an 18-24 h acquisition access period (AAP) on BVG-infected *N. benthamiana* leaves, after which about 25 aphids/plant were transferred to healthy Butta 12 barley plants and given a four-

day inoculation access period (IAP). *R. maidis* and *R. padi* aphids are selective feeders and will not feed on *N. benthamiana*, so these aphids were fed a 20% sucrose solution mixed 1:1 (v/v) with the partially purified virion preparation. After the IAP, aphids were killed with insecticide (Bioadvanced, 3 in 1 Insect, Disease, and Mite Control), and the inoculated plants were moved to a greenhouse; plants mock inoculated with non-viruliferous aphids were used as negative controls. Inoculations with each aphid were done on separate days to prevent cross contamination. At ~four wpi, tissue was collected for RNA extraction and tested for BVG by RT-PCR. The experiments were repeated a second time using BVG-infected barley tissue as the inoculum for all aphids. Regular inoculations with *R. maidis* were done to maintain BVG-infected barley plants to use as inoculum in further experiments, and it was determined that BVG could be detected in barley as early as two wpi.

Testing the BVG vectoring efficiency of *R. maidis*

To test the vectoring efficiency of *R. maidis* aphids one, five, 10, and 20 aphids/plant were used to inoculate healthy barley plants as described above. Tissue was sampled and tested by RT-PCR at ~two wpi. Data displayed represents pooled data from two experimental repetitions.

Host range study

Plants of the following crop and weedy monocot species were inoculated as described above: maize (*Zea maize* cv Golden Bantam), oats (*Avena sativa* cv California Red), wheat (*Triticum aestivum*), two YDV tolerant barley cultivars (*H. vulgare* cv. UC-Capay and cv. UC-Tahoe), sorghum (*Sorghum bicolor*), cereal rye (*Secale cereale*), switchgrass (*Panicum virgatum*), proso millet (*Panicum miliaceum*) and annual ryegrass (*Lolium multiflorum*). Tissue

was collected after ~three wpi, tested for BVG by RT-PCR, and infected plants were photographed at one to two months post inoculation (mpi). The experiments were repeated twice.

Results

Screening BVG-pJL89 constructs by agroinoculation into *N. benthamiana* plants

Screening of three BVG-pJL89 constructs by agroinoculation into transgenic HC-Pro expressing *N. benthamiana* plants revealed one construct, BVG-18, to be capable of initiating a stable BVG infection. At one wpi, non-infiltrated leaves were tested for BVG infection by RT-PCR, and DNA products of the expected size (~400 bp) were detected in all infiltrated plants; no products were detected in control reactions lacking RT enzyme (Figure 2a), confirming positive PCR amplifications were from viral RNA and not infiltrated DNA plasmids. BVG replication was confirmed by northern blot analysis using the same RNA used for RT-PCR. In the BVG infiltrated sample two distinct signal bands corresponding to the expected sizes of the genomic (~6 kb) and subgenomic (~3 kb) RNAs typical of poleroviruses were detected, while no such signal was detected in the non-infiltrated sample (Figure 2b). No discernable symptoms were observed in this host (Figure 3).

Aphid vector identification and transmission

Three common species of aphids known to vector poleroviruses—*M. persicae*, *R. padi*, and *R. maidis*—were tested for their capacity to vector BVG. Aphids of each species were allowed to acquire BVG virions by feeding, then transferred to healthy Butta 12 barley plants which were tested for BVG infection by RT-PCR at ~four wpi; plants mock inoculated with non-viruliferous aphids served as negative controls. Both *R. maidis* and *R. padi* aphids were capable of acquiring and transmitting BVG; based on the infection rate (number of inoculated plants that were infected), *R. maidis* (14/15 plants) appeared to be a more effective vector of BVG than *R.*

padi (1/20 plants). *M. persicae* aphids did not transmit BVG to any of the inoculated plants. Results are summarized in Table 1. After about two mpi, BVG-infected plants began to exhibit mild symptoms of YDV infection—yellow discoloration of leaf tips and margins (Figure 4). Since a better transmission rate was achieved with *R. maidis*, these aphids were used to transmit BVG in subsequent experiments.

BVG vectoring efficiency of *R. maidis*

To determine how efficiently *R. maidis* aphids could vector BVG, sets of one, five, 10, or 20 aphids fed on BVG-infected barley tissue were used to inoculate healthy Butta 12 barley plants, which were tested for the presence of BVG by RT-PCR at 2 wpi. When only one aphid was used, two out of 27 (7.4%) inoculated plants became infected with BVG. When five aphids were used almost half (47.6%) of the inoculated plants became infected. The infection rate rapidly approached 100% when the number of aphids/plant was increased to 10 (90.9%) and 20 (93.3%) (Table 2). These results demonstrate that *R. maidis* could efficiently transmit BVG to barley plants, since a nearly 50% transmission rate was achieved with as few as five aphids, and a nearly 100% transmission rate was achieved as the number of aphids per plant was increased to 20.

Host range study

Previous reports on BVG were done using naturally infected field-collected plants followed by combined RT-PCR and sequencing analyses. Therefore, we conducted a small host range study using most of the plant species in which BVG was previously detected: switchgrass (*Panicum virgatum*), wheat (*Triticum aestivum*), oats (*Avena sativa* cv California red), maize (*Zea mays* cv Golden Bantam) and proso millet (*Panicum miliaceum*). In addition, sorghum (*Sorghum bicolor*), cereal rye (*Secale cereale*), annual ryegrass (*Lolium multiflorum*), and two

additional barley cultivars (*Hordeum vulgare* cv.s UC-Capay and UC-Tahoe) bred to have high tolerance to BYDV (del Blanco et al., 2022) were also included in this study. In total, plants of nine different monocot species were tested for BVG susceptibility.

Plants from seven of these monocot species were confirmed as hosts for BVG, however the infection rates for each host varied greatly. The infection rate was highest in UC-Capay and UC-Tahoe barley plants (7/9 and 12/14 positive plants, respectively), and in California red oat plants (6/9). Annual ryegrass (3/17), switchgrass (1/10), maize (2/15), proso millet (2/14), and wheat (7/17) also experienced much lower infection rates, the cause of which was not determined. Cereal rye and sorghum plants did not become infected in this study. Results are summarized in Table 3.

At one mpi, BVG-positive UC-Capay and UC-Tahoe barley plants developed mild yellowing symptoms in a few leaves, however some mild leaf yellowing was also observed in the healthy controls (Figures 5a and 5b, respectively). Slightly more prominent leaf yellowing symptoms were observed in BVG-infected wheat plants (Figure 5c). BVG positive annual ryegrass plants did not develop obvious symptoms (Figure 5d).

At one mpi, pronounced symptoms were observed in BVG-infected CA red oat, proso millet, switch grass, and maize plants. In BVG infected CA red oat plants, some leaves developed a bright reddish leaf discoloration, similar to symptoms induced by other YDV viruses in this host (Figure 6a). Similar reddish leaf discoloration was also observed in BVG-infected proso millet plants (Figure 6b). At two mpi, the leaves of BVG-infected switchgrass turned a deep red color (Figure 6c). BVG-infected maize plants did not develop notable leaf symptoms however reddish discoloration of the tassel and corn silk was observed (Figure 7).

Discussion

At the time of this writing, the *Polerovirus* BVG has been described in at least nine countries and seven additional monocot hosts, since its initial discovery in South Korea in 2016 (Erickson and Falk, 2021; Gavrili et al., 2021; Jo et al. 2018; Kumar et al., 2018; Nancarrow et al. 2019 a and b; Oh et al., 2016; Park et al. 2016 and 2017; Pasztor et al. 2020; Svanella-Dumas, L., et al., 2022; Wamaitha et al., 2018; Zhao et al., 2016). Intriguingly, one plant sample from Australia was a 34-year-old oat herbarium sample (Nancarrow et al., 2019 b), indicating BVG has been circulating, undetected, for at least three decades. BVG going undetected for so long is likely due to limitations of traditional methods used for *Polerovirus* detection. Traditional detection methods, such as serological and PCR-based assays, are diagnostically useful for known pathogens but limited in their utility for viral discovery (Sõmera et al., 2021).

While serological assays are rapid and inexpensive diagnostic tools, they can lack specificity as polyclonal antibodies raised against the capsid protein (CP) of one *Polerovirus* species can cross react with the CPs of other closely related species, creating the potential for misdiagnosis of an unknown virus if its CP is similar enough to that of a known virus to be recognized by the same antibodies. PCR assays are specific and can be paired with Sanger sequencing to determine the exact nucleotide sequence of a target virus, but prior knowledge of the target sequence is needed for primer design; PCR assays using degenerate primers targeting conserved sequences flanking a variable sequence region can, to a limited extent, be used to identify new virus isolates when paired with amplicon sequencing (Campbell et al., 2020). However, when not paired with sequencing, as with serological assays, an unknown virus could potentially be detected, but misdiagnosed, as a closely related known virus. This was observed for the 34-year-old BVG-positive oat sample, which tested positive for MYDV by RT-PCR, but

sequencing revealed the amplicon shared less than 80% sequence identity with MYDV (Nancarrow et al., 2019 b).

High throughput sequencing (HTS) technology—which generates sequence information for the total population of RNA sequences in a sample, known and unknown—has greatly expanded our capacity for novel virus detection. One key example of this is the discovery of the Grapevine red blotch virus (GRBV; family *Geminiviridae*) by HTS in grapevines exhibiting symptoms similar to grapevine leafroll disease that were PCR negative for any known grapevine leafroll associated virus (Sudarshana et al., 2015). BVG serves as another example of the utility of HTS in viral discovery.

While proven invaluable for viral discovery, HTS cannot be used to confirm the infectivity or pathogenicity of a detected virus. In this study we constructed the first infectious cDNA clone of BVG (Figure 1) to use as a tool to study the biology of BVG. With this clone, we initiated a productive BVG infection in *Nictotiana benthamiana* plants, thereby producing a useful experimental system that can be used for further biological characterization and biotechnological manipulation of this virus. No notable symptoms were observed in BVG-infected *N. benthamiana* plants (Figure 3).

Results from aphid vector identification experiments revealed *R. padi* and *R. maidis* aphids to be competent BVG vectors, the results of which are summarized in Table 1. These results are unsurprising, since in one report of BVG in Australia, large populations of *R. maidis* aphids were present on symptomatic barley, wheat, and oat samples in which BVG was detected (Nancarrow, et al., 2019 b). In this study, *R. maidis* was a more efficient vector under the conditions used in this study, and subsequent transmission efficiency experiments determined that a single viruliferous *R. maidis* aphid could initiate an infection, with the infection rate

increasing dramatically when more viruliferous aphids were used for inoculation (Table 2). BVG-infected Butta 12 barley plants developed mild foliar symptoms (yellow leaf discoloration) typical of YDV infection after 2 mpi. Many other cereal feeding aphid species are known to vector various YDV species (Walls et al., 2019), so it would be interesting to screen additional aphid species for their capacity to vector BVG.

BVG was previously reported in seven different monocot hosts, suggesting it may have a broad host range among monocot plants. Therefore we conducted a limited, greenhouse-based host range study to confirm its infectivity in previously reported monocot plants (excluding foxtail millet, which did not germinate), in three additional monocot species—sorghum (*S. bicolor*), cereal rye (*S. cereale*), and annual ryegrass (*L. multiflora*)—and in two barley cultivars (UC-Capay and UC-Tahoe) known to exhibit YDV tolerance (del Blanco et al., 2022). Interestingly, all but two monocot plants (cereal rye and sorghum) became infected with BVG, thereby verifying the susceptibility of the reported plants, along with annual ryegrass and the two YDV tolerant barley cultivars (Table 3). In several BVG susceptible hosts (annual ryegrass, wheat, and UC-Capay and -Tahoe barley), symptoms were mild or even absent (Figure 5). More prominent symptoms—primarily yellow or red leaf (or tassel and corn silk in maize) discoloration—were observed in proso millet, oat, switchgrass (Figure 6) and maize plants (Figure 7).

This is the first report to detail the generation of an infectious cDNA clone of BVG from archived RNA, which was used as a tool to determine important aspects of BVG biology, including two competent aphid vectors and several susceptible monocot hosts. This report lays the groundwork for understanding BVG biology and epidemiology, and provides valuable information and a robust experimental system for further study of this emergent virus.

Acknowledgements

This research was supported in part by the University of California, a Jastro-Shields research fellowship to A. Erickson, and as part of a team research effort supporting DARPA's Insect Allies Program. The views and conclusions contained in this document are those of the authors and should not be interpreted as representing the official policies, either expressed or implied, of DARPA or the US Government. The US Government is authorized to reproduce and distribute reprints for government purposes notwithstanding any copyright notation hereon.

We thank Dr. Georg Jander for supplying the *R. maidis* aphids used here. We thank Professor C. O. Qualset for supplying the first BVG sample used by us. We thank Dr. Isabel A. del Blanco for supplying some of the seeds used here.

References

Burgess, A.J., Harrington, R. RTP. Barley and Cereal Yellow Dwarf Virus Epidemiology and Control Strategies. In: In Smith, HG, & Barker, H (Eds), The Luteoviridae. CABI publishing; 1999. p. 248–61.

Campbell AJ, Erickson A, Pellerin E, Salem N, Mo X, Falk BW, et al. Phylogenetic classification of a group of self-replicating RNAs that are common in co-infections with poleroviruses. Virus Res. 2020 Jan 15;276:197831.

del Blanco IA, Hegarty JM, Dubcovsky J. Registration of 'UC-Capay', a low-grain-protein, non–glycoside nitrile producing, California-adapted, two-rowed spring malting barley. J Plant Regist. 2022 Sep 1;16(3):487–94. Available from: https://onlinelibrary.wiley.com/doi/full/10.1002/plr2.20240

Erickson A, Falk BW. First Report of Barley virus G in the United States and California. https://doi.org/101094/PDIS-03-21-0478-PDN. 2021 Oct 26;105(10). Available from: https://apsjournals.apsnet.org/doi/full/10.1094/PDIS-03-21-0478-PDN

Gavrili V, Lotos L, Mollov D, Grinstead S, Tsialtas IT, Katis NI, et al. First report of barley virus G infecting corn in Greece. J Plant Pathol. 2021;

Griesbach JA, Creamer R, Lorens G, Falk BW, Qualset C, Jackson LF. Barley yellow dwarf of California cereals. Hilgardia. 1989;43(1):23–4.

Kumar LM, Foster JA, McFarland C, Malapi-Wight M. First report of barley virus G in switchgrass (Panicum virgatum). Vol. 102, Plant Disease. American Phytopathological Society; 2018. p. 466. Available from: https://apsjournals.apsnet.org/doi/abs/10.1094/PDIS-09-17-1390-PDN

Macwilliams MP, Liao M-K. Luria Broth (LB) and Luria Agar (LA) Media and Their Uses Protocol. 2016; Available from: www.asmscience.org

Malmstrom CM, Shu R. Multiplexed RT-PCR for streamlined detection and separation of barley and cereal yellow dwarf viruses. J Virol Methods. 2004 Sep 1;120(1):69–78.

Miller WA, Rasochová L. BARLEY YELLOW DWARF VIRUSES. Annu Rev Phytopathol . 1997;35:167–90. Available from: http://www.public.iastate.edu/~wamiller/

Miller WA, Liu S, Beckett R. Barley yellow dwarf virus: Luteoviridae or Tombusviridae? Mol Plant Pathol. 2002;3(4):177–83. Available from: https://pubmed.ncbi.nlm.nih.gov/20569325/

Nancarrow N, Aftab M, Zheng L, Maina S, Freeman A, Rodoni B, et al. First report of barley virus G in Australia. Plant Dis. 2019 Jul 1;103(7):1799. Available from: https://apsjournals.apsnet.org/doi/abs/10.1094/PDIS-01-19-0166-PDN

Nancarrow N, Maina S, Zheng L, Aftab M, Freeman A, Kinoti WM, et al. Coding-Complete Sequences of Barley Virus G Isolates from Australia, Obtained from a 34-Year-Old and a 1-Year-Old Sample. Microbiol Resour Announc. 2019 Nov 21;8(47):1292–311. Available from: /pmc/articles/PMC6872893/

National Center for Biotechnology Information (NCBI). Bethesda (MD): National Library of Medicine (US), National Center for Biotechnology Information; 1988. Available from: https://www.ncbi.nlm.nih.gov/

Oh J, Park CY, Min HG, Lee HK, Yeom YA, Yoon Y, et al. First report of barley virus G in foxtail millet (Setaria italica) in Korea. Plant Dis. 2017 Jun 1;101(6):1061. Available from: https://apsjournals.apsnet.org/doi/abs/10.1094/PDIS-01-17-0036-PDN

Park CY, Oh JH, Min HG, Lee HK, Lee SH. First Report of Barley virus G in Proso Millet (Panicum miliaceum) in Korea. https://doi.org/101094/PDIS-07-16-0952-PDN. 2016 Nov 17;101(2):393. Available from: https://apsjournals.apsnet.org/doi/full/10.1094/PDIS-07-16-0952-PDN

Park CY, Min HG, Oh J, Kim BS, Lim S, Yoon Y, et al. First complete genome sequence of barley virus G identified from proso millet (Panicum miliaceum) in South Korea. Genome Announc. 2017 Jul 1;5(29):523–40. Available from: /pmc/articles/PMC5522924/

Pasztor G, Zsuzsanna GN, Kossuth T, Demian E, Nadasy E, Takacs AP, et al. Millet Could Be both a Weed and Serve as a Virus Reservoir in Crop Fields. Plants 2020, Vol 9, Page 954. 2020 Jul 28;9(8):954. Available from: https://www.mdpi.com/2223-7747/9/8/954/htm

Rochow WF. Biological properties of four isolates of barley yellow dwarf virus. Phytopathology. 1969;59(11):1580–9.

Sõmera M, Massart S, Tamisier L, Sooväli P, Sathees K, Kvarnheden A. A Survey Using High-Throughput Sequencing Suggests That the Diversity of Cereal and Barley Yellow Dwarf Viruses Is Underestimated. Front Microbiol. 2021 May 11;12:992.

Sudarshana MR, Perry KL, Fuchs MF. Grapevine red blotch-associated virus, an emerging threat to the grapevine industry. Phytopathology. 2015 Jul 1;105(7):1026–32. Available from: https://apsjournals.apsnet.org/doi/10.1094/PHYTO-12-14-0369-FI

Svanella-Dumas L, Vitry C, Valade R, Robin N, Thibord JB, Marais A, et al. First report of barley virus G infecting winter barley (Hordeum vulgare L.) in France. Plant Dis. 2022 Jun 30; Available from: https://pubmed.ncbi.nlm.nih.gov/35771104/

Walker PJ, Siddell SG, Lefkowitz EJ, Mushegian AR, Adriaenssens EM, Alfenas-Zerbini P, et al. Recent changes to virus taxonomy ratified by the International Committee on Taxonomy of Viruses (2022). Arch Virol. 2022 Nov 1;167(11):2429–40. Available from: https://pubmed.ncbi.nlm.nih.gov/35999326/

Walls J, Rajotte E, Rosa C. The Past, Present, and Future of Barley Yellow Dwarf Management. Agric 2019, Vol 9, Page 23. 2019 Jan 18;9(1):23. Available from: https://www.mdpi.com/2077-0472/9/1/23/htm

Wamaitha MJ, Nigam D, Maina S, Stomeo F, Wangai A, Njuguna JN, et al. Metagenomic analysis of viruses associated with maize lethal necrosis in Kenya. Virol J. 2018;15(1).

Wegulo SN. Yellow Dwarf of Wheat, Barley, and Oats.; Available from: http://citnews.unl.edu/winter_wheat_tool/

Zhao F, Lim S, Yoo RH, Igori D, Kim SM, Kwak DY, et al. The complete genomic sequence of a tentative new polerovirus identified in barley in South Korea. Arch Virol. 2016 Jul 1;161(7):2047–50. Available from: https://pubmed.ncbi.nlm.nih.gov/27146139/

Table 1: Results of aphid vector identification experiments					
	Rep	**mock**	**M. persicae**	**R. padi**	**R. maidis**
# plants infected	1	0/9	0/10	0/10	4/5
	2	0/9	0/10	1/10	10/10
	Total	0/18	0/20	1/20	14/15

Listed are the results from experiments to identify the aphid vector(s) of BVG, testing three aphid species: *Myzus persicae, Rhopalosiphum padi*, and *R. maidis*. The top row indicates the experimental replicate, species of aphid being tested, along with a column for mock inoculations done with non-viruliferous, data in this column is pooled for all aphid species. Data in the table represents the number of inoculated plants that tested positive for BVG by RT-PCR. The bottom row gives the total number of plants infected from two experimental repetitions.

Table 2: Results of *R. maidis* BVG vectoring efficiency experiments				
Number of aphids/plant	**1**	**5**	**10**	**20**
Number Plants Infected/treatment	2/27	10/21	20/22	14/15
Infection rate (%)	7.4	47.6	90.9	93.3

Listed are the results from vector efficiency experiments using *R. maidis* aphids. The top row indicates the number of viruliferous aphids used for inoculation, the second row indicates the exact number of inoculated plants that became infected, and the bottom row indicates the infection rate (number of plants infected divided by the number of plants inoculated. Data is pooled from two experimental repetitions.

Table 3: Summary of monocot host susceptibility experiments		
Common name	**Latin name**	**Susceptible?**
Annual ryegrass	*Lolium multiflorum*	Yes
Cereal rye	*Secale cereale*	No
Switchgrass	*Panicum virgatum*	Yes
Maize	*Zea mays*	Yes
Proso millet	*Panicum miliaceum*	Yes
Oats	*Avena sativa c.v. California red*	Yes
Sorghum	*Sorghum bicolor*	No
Wheat	*Triticum aestivum*	Yes
Barley (Capay)	*Hordeum vulgare* c.v. UC Capay	Yes
Barley (Tahoe)	*Hordeum vulgare c.v. UC Tahoe*	Yes

Listed are the results from experiments determining the susceptibility of various monocot species of plants to BVG. The first column lists the common names of the plants tested, the second column lists the Latin names of tested plants, and the third column indicates whether or not (yes or no) that species of plant was susceptible to BVG infection.

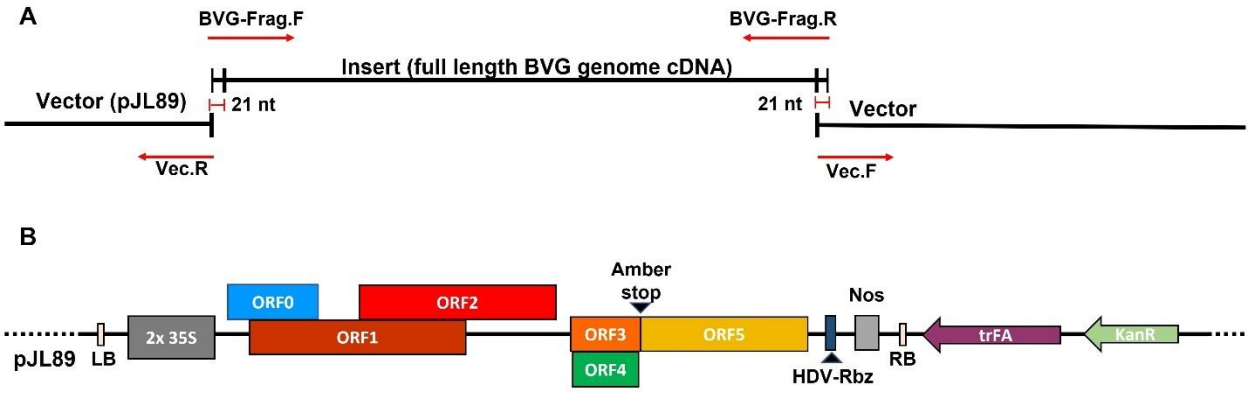

Figure 1. Construction and genome organization of the BVG-pJL89 construct

Full length cDNA copy of the Barley virus G genome inserted into the pJL89 plasmid backbone. **A.** Schematic representation of the cloning strategy. A full length cDNA copy of the BVG genome was RT-PCR-amplified using primers BVG-Frag.F and BVG-Frag.R targeting the 5' and 3' ends respectively, of the BVG genome and containing 21 nt of overlap with the pJL89 vector. The pJL89 binary vector backbone was PCR linearized using Vec.F and Vec.R primers, and the BVG cDNA was inserted into the pJL89 backbone by Gibson assembly. **B.** Schematic representation of the BVG genome in the pJL89 vector. LB and RB: left and right borders of the binary vector transfer DNA (T-DNA); 2x 35S: enhanced Cauliflower mosaic virus 35 S promoter; HDV-Rbz: hepatitis delta virus ribozyme. Colored boxes above and below the solid black line depict viral encoded open reading frames (ORFs) and are numbered as convention per other poleroviruses. NOS: nopaline synthase terminator sequence; KanR: kanamycin resistance gene; trFA: plasmid replication initiator protein sequence.

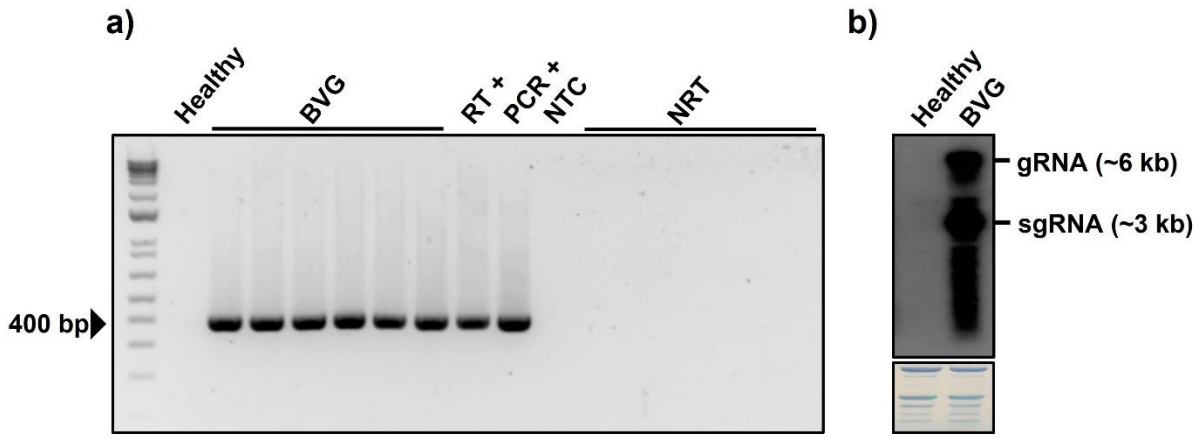

Figure 2. RT-PCR and northern blot analyses confirming BVG infection in HC-Pro *N. benthamiana* plants agroinoculated with BVG-pJL89

Transgenic HC-Pro *Nicotiana benthamiana* plants were agroinoculated with the BVG-pJL89 construct, RNA was extracted from non-infiltrated leaves at one wpi and tested for BVG by RT-PCR and northern blot analysis. **A.** Gel image of RT-PCR-amplified products detecting BVG. RT+: archived, BVG-positive RNA was used as a positive control for reverse transcription; PCR+: BVG18.2 plasmid was used as the positive control for PCR; NTC: no template control; NRT: no RT enzyme control. The arrowhead to the left of the gel indicates the position of the 400 bp PCR product. **B.** Northern blot hybridization to confirm BVG replication. The panel on the bottom is the methylene blue stained blot showing equal rRNAs. The upper signal in the BVG sample corresponds with the ~6 kb BVG genomic (gRNA) fragment, the lower signal corresponds with the ~3 kb subgenomic RNA (sgRNA).

Figure 3. Symptoms of BVG infection in HC-Pro *N. benthamiana* plants.

The plant on the left was agroinoculated with BVG, the plant on the right is the non-inoculated healthy control. No obvious symptoms were apparent in the BVG-infected plant. The picture was taken at ~two mpi.

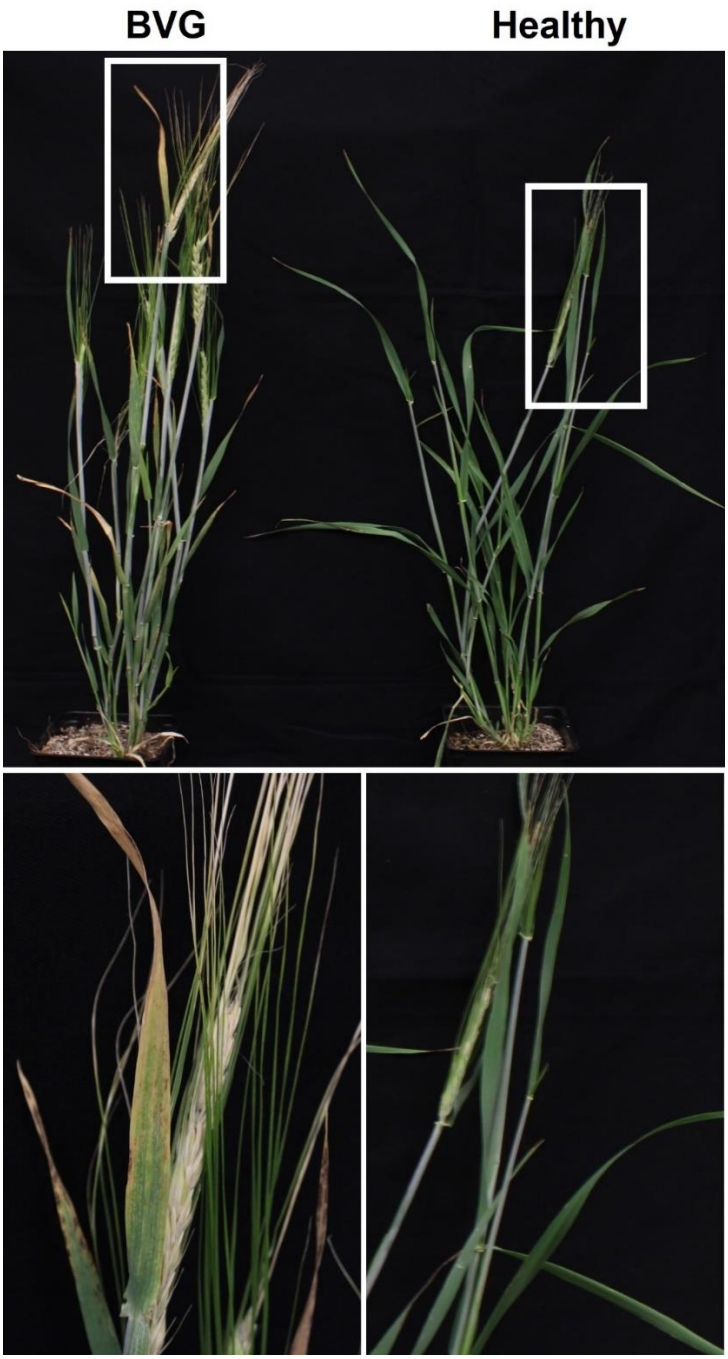

Figure 4. Symptoms of BVG infection in barley cultivar Butta 12.

The plant on the left was inoculated with BVG using viruliferous *R. maidis* aphids, the plant on the right was mock inoculated with non-viruliferous aphids. White boxes indicate the locations of the zoomed in photo panels beneath the top image. The picture was taken at ~two mpi.

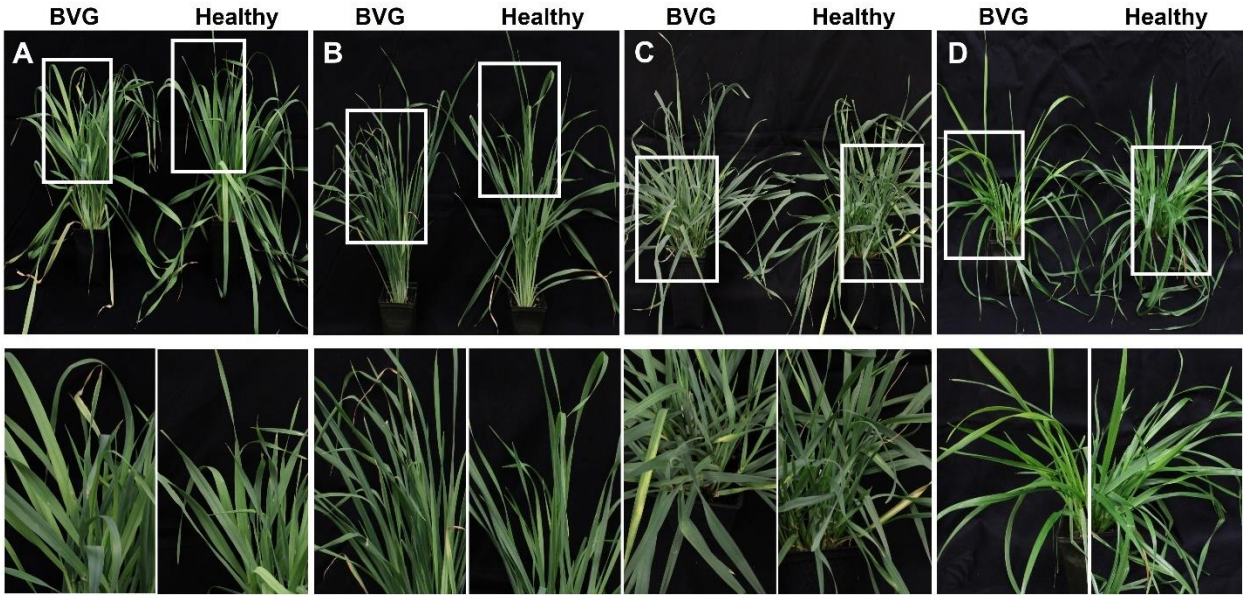

Figure 5. Symptoms of BVG infection in UC-Capay and -Tahoe barley cultivars, wheat, and annual ryegrass plants.

For all images, the plants depicted on the left were aphid inoculated with and tested positive for BVG by RT-PCR, the plants on the right are mock inoculated healthy controls. **A:** Barley cultivar UC-Capay. **B:** Barley cultivar UC-Tahoe. **C:** Wheat. **D:** Annual rye grass. White boxes indicate the locations of the zoomed in photo panels beneath the top image. Pictures were taken at ~one mpi.

Figure 6. Symptoms of BVG infection in CA red oat, proso millet, and switchgrass plants. For all images, the plants depicted on the left were aphid inoculated with and tested positive for BVG by RT-PCR, the plants on the right are mock inoculated healthy controls. **A:** CA red oat. **B:** Proso millet. **C:** Switchgrass. White boxes indicate the locations of the zoomed in photo panels beneath the top image. Oat and millet pictures were taken at ~one mpi, the switchgrass picture was taken at ~two mpi.

Figure 7. Symptoms of BVG infection in Golden Bantam maize plants.

Images to the left are of a BVG inoculated maize plant, images on the right are of the mock inoculated healthy control plant. White boxes indicate the locations of the zoomed in photo panels beneath the top image. For the zoomed in photo panels, the left most pictures are of the maize tassel, and the right most images of are the corn silk. The picture was taken at ~two mpi.

Chapter 5

Concluding statements and future directions

In this thesis I've detailed several interesting findings regarding coinfection interactions of poleroviruses, umbraviruses, and tlaRNAs, and discovered new viruses composing these multi-virus disease complexes. In Chapter 2, using the polerovirus turnip yellows virus (TuYV) and its naturally co-occurrent tombusvirus-like associated RNA (tlaRNA) ST9, and the carrot motely dwarf disease associated umbravirus carrot mottle virus (CMoV) and tlaRNAs Gamma and Sigma I show how these interact to produce symptoms in infected plants, and how these interactions affect virus movement within the plant host and transmission to new hosts. In Chapter 3, I detailed the identification of several recently discovered poleroviruses, umbraviruses, and tlaRNAs found in apiaceous plants expressing typical symptoms of CMD disease, and in Chapter 4 I described the biological characterization of yet another emergent polerovirus, barley virus G (BVG). While the results of these studies are quite interesting on their own, they also open up vast avenues for further research into these fascinating and unique viruses and their interactions, some of which I will discuss here.

Chapter 2: Molecular mechanisms underpinning polerovirus, umbravirus, and tlaRNA coinfection interactions

In Chapter 2 of this thesis, some of the most interesting results observed were those demonstrating that the umbravirus carrot mottle virus (CMoV) could support systemic movement of all of the tombusvirus-like associated RNAs (tlaRNAs) as well as mechanical co-transmission of tlaRNAs Sigma and ST9. These results raise the question of what underlying molecular mechanisms are responsible for these interactions. Given the known long distance function of the umbravirus ORF3 encoded protein and the cell-to-cell movement function of the ORF4 encoded protein, it is likely that interactions between these proteins and the genomic RNAs of the tlaRNAs would explain these observations.

Using heterologous tobacco mosaic virus (TMV) and potato virus x (PVX) vectors—which harbored loss of function mutations in their own movement proteins—were used to express the ORF3 encoded protein of the umbravirus groundnut rosette virus (GRV), researchers were able to determine that this protein can form loose ribonucleoprotein (RNP) complexes both with homologous umbravirus RNAs and heterologous viral vector RNAs (Ryabov et al. 1999; Ryabov et al. 2001b; Taliansky et al. 2003). These RNPs act to protect these RNAs from degradation and, through incompletely defined interactions with fibrillarin proteins in the host cell nucleolus, enable long distance movement of these RNAs within the host phloem tissues (Kim et al. 2007a and 2007b; Ryabov et al. 1998). Other work has also determined that this protein can function to protect both viral and host RNAs from degradation by the host nonsense mediated decay (NMD) pathway (May et al. 2020). In similar work, GRV ORF4 (either fused to or co-expressed with GFP) was expressed from movement defective TMV and PVX vectors, and it was found that this protein localized to plasmodesmata and induced tubule formation in the infected cells—two functions commonly associated with cell-to-cell movement proteins; it was also found that this protein alone supported cell-to-cell movement of the heterologous viral vectors (Nurkiyanova et al. 2001; Ryabov et al. 1998; Ryabov et al. 2001a). Additional work done using transient expression of a GFP labeled ORF4 encoded protein from CMoV not only corroborated these functions, but also demonstrated that plasmodesmata targeting required interaction of the ORF4 protein with the host cell SUMOylation system (Jiang et al. 2021).

Given this information, I attempted similar preliminary experiments to determine if heterologous expression of one or both of the CMoV encoded movement proteins was sufficient to impart systemic movement to the tlaRNAs Sigma and ST9. After confirming that co-infection with wild type (WT) TMV and PVX vectors did not support systemic movement of either of

these tlaRNAs—which also suggests this interaction with tlaRNAs may be somewhat unique to umbraviruses and compatible poleroviruses—I engineered TMV and PVX vectors to individually express the CMoV ORF3 or ORF4 proteins (we did not mutate any of the proteins these viruses need for their own movement). I then coinoculated the tlaRNAs individually with TMV-ORF3 (TMV3), PVX-ORF3 (PVX3), TMV-ORF4 (TMV4), or PVX-ORF4 (PVX4) constructs, or in combination with different viral vectors expressing different proteins—so tlaRNA+PVX3+TMV4, or tlaRNA+PVX4+TMV3—then used RT-PCR to determine if any of these co-inoculation treatments could support systemic movement of either of the tlaRNAs Sigma or ST9, as well as check the stability of the ORF3 and ORF4 inserts; the co-inoculation treatments are summarized below.

Single inoculation	Double inoculations		Triple inoculations
tlaRNA (Sigma or ST9)	WT TMV + tlaRNA	WT PVX + tlaRNA	TMV3 + PVX4 + tlaRNA
	TMV3 + tlaRNA	PVX3 + tlaRNA	PVX3 + TMV4 + tlaRNA
	TMV4 + tlaRNA	PVX-4 + tlaRNA	

While neither of the ORF3 or ORF4 inserts appeared to be completely stable in either of the TMV or PVX constructs I was able to detect full length inserts from either vector for up to 22 days post inoculation (dpi), although it should be noted the ORF4 insert seemed to be more unstable in the TMV vector. Interestingly, I found both tlaRNAs Sigma and ST9 were able to move systemically—although not as efficiently as when either of these tlaRNAs were co-inoculated with WT CMoV—when co-inoculated with TMV3 or PVX3 vectors alone, and the presence of the ORF4 protein did not appear to be necessary. It should be noted, however, in a few samples co-inoculated with ST9 and WT TMV, TMV4, or WT PVX alone, faint bands for ST9 were detected, and in one sample co-inoculated with PVX4 alone a strong PCR band for

ST9 was observed; I suspect this may have resulted from cross contamination but did not confirm this. It is interesting that the CMoV ORF3 long distance movement protein alone appeared to support systemic movement of the tlaRNAs, as the tlaRNAs hypothetically would also require help to travel from the initially agroinoculated cells. One may naively interpret this data to mean the ORF3 protein may also harbor some degree of cell-to-cell movement functionality, this was determined to not be the case in the aforementioned experiments conducted with the GRV ORF3 and ORF4 movement proteins, therefore it could be that either the agroinoculation itself introduced the tlaRNAs and heterologous ORF3 constructs into the phloem tissues or that the cell-to-cell movement functions of the TMV and PVX vectors aided in the translocation of tlaRNAs from agroinoculated mesophyll cells to the phloem tissues. It could be interesting to generate stably transformed plants capable of expressing the ORF3 protein to determine if it alone could support systemic movement of these tlaRNAs. As described in Chapter 2, I also observed that while CMoV could support systemic movement of all three tlaRNAs tested, this interaction was much less efficient for tlaRNA Gamma, which only moved systemically about 40% of the time. It would be interesting to see if there are perhaps some nucleotide sequence motifs or RNA structural features that tlaRNAs Sigma and ST9 have that Gamma does not that could account for these differences.

Another key finding from Chapter 2 was that the polerovirus TuYV was more efficiently mechanically co-transmitted from plants co-inoculated with both CMoV and either tlaRNA Sigma or ST9 than when TuYV was co-inoculated with CMoV alone. Multiple studies have shown that some—but not all—co-inoculations of a polerovirus with an umbravirus can allow the polerovirus to escape its phloem limitation and become mechanically transmissible, though often with low efficiency (Hoffman et al. 2001; Ryabov et al. 2001a; Zhou et al. 2017). In

experiments in which the ORF4 protein of GRV was expressed from a cucumber mosaic virus (CMV) heterologous viral vector, it was found that co-inoculation of the CMV(ORF4) vector with the polerovirus potato leafroll virus (PLRV) enabled PLRV to invade mesophyll cells and become mechanically transmissible (Ryabov et al. 2001a). However, when these experiments were repeated with a CMV(ORF4) vector with a loss of function mutation in its 2b gene—which is known to function as a suppressor of the host RNA silencing (RNAi) system—PLRV was no longer able to escape it's phloem limitation and gain mechanical transmissibility. Due to these findings, along with the observation that the RNAi silencing suppressors of multiple distantly related plant viruses appear to play critical roles in the movement functions of these viruses, it has been widely hypothesized that virus within host movement involves an interplay of movement protein functions along with suppression of host defense responses (Cooper et al. 1996; Ryabov et al. 1999; Ryabov et al. 2001a;).

Regarding my findings that the tlaRNAs Sigma and ST9 seemingly boosting the efficiency with which TuYV could be mechanically co-transmitted with CMoV, a recent study has found that tlaRNA ST9 harbors in its 3' untranslated region (UTR) of its genome a structural feature that acts to stall the host XRN1 system that functions to degrade aberrant RNAs—including viral RNAs (Campbell et al. 2022). As described in Chapter 2—and has been observed in other published works (Passmore et al. 1993)—when I looked at differences in virus accumulation as a function of different virus coinfections, I found that co-infection with ST9 significantly increased TuYV accumulation, as well as CMoV accumulation. Therefore it may be possible that the XRN1 stalling function of ST9 may not only account for this dramatic increase in the accumulation of TuYV and CMoV, but may also partially contribute to the increased rate of TuYV mechanical co-transmission from plants co-infected with CMoV. However, it should be

noted that it has not been determined if tlaRNA Sigma likewise possesses similar XRN1 stalling capabilities, and according to my results co-infection of this tlaRNA did not have a similarly dramatic impact on TuYV or CMoV accumulation, however co-infection with this tlaRNA also increased the efficiency with which TuYV could be mechanically co-transmitted, implying that the tlaRNA elicited host defense suppression may not actually contribute to this interaction or that it is at the very least not the sole contributor. The exact molecular mechanism by which umbravirus co-infection alone imparts mechanical transmission to a co-infecting polerovirus—whether it be through direct interaction with movement proteins, benefits of host defense suppression, or both—also remains unknown, therefore further research into these interactions could lead not only to a better understanding of these specific virus coinfection interactions but of plant virus within and between host movement overall.

Chapter 3: Biological characterization of emergent viruses associated with carrot motley dwarf disease

In Chapter 3 of this thesis I detailed the identification of two recently identified poleroviruses, Torilis crimson leaf virus (TorCLV) and Foeniculum vulgare polerovirus (FvPV) (Sidharthan et al. 2022), two recently identified umbraviruses, wild carrot mottle virus (WCMoV) and Pastinaca umbravirus 1 (PasUV1) (Rivarez et al. 2022), which were named as novel viruses but I believe to potentially be divergent strains of the well-known carrot mottle virus (CMoV), and a recently described tombusvirus-like associated RNA (tlaRNA)—arracacha latent virus E associated RNA (ALVEaRNA) (De Souza et al. 2021; Fox et al. 2022)—from carrot, parsley and cilantro samples exhibiting typical symptoms of carrot motley dwarf (CMD) disease. Additionally, I identified a novel, potentially recombinant polerovirus that I have tentatively designated parsley mottle hybrid polerovirus (PMoHPV). None of these viruses had

formerly been attributed to CMD nor had they been found to occur in the United States. While finding these viruses for the first time in the U.S. and in association with CMD, especially after decades of only a few viruses—the polerovirus carrot red leaf virus (CRLV), the umbraviruses CMoV and carrot mottle mimic virus, and a multitude of CRLVaRNAs—the real intrigue lies with the potential for exploring the biology of these viruses and the variety of interactors that could contribute to CMD.

Having all been found by RT-PCR and high throughput sequencing (HTS) based methods, essentially nothing is known about these viruses beyond their genome sequences and the host plants in which they have been identified (De Souza et al. 2021; Rivarez et al. 2023; Schönegger et al. 2022; Sidharthan et al. 2022). Much like the work I presented in Chapter 4, where I made an infectious clone of the emergent polerovirus barley virus G (BVG), which enabled me to not only identify two competent aphid vectors and conduct experiments to expand information on the known host range of this polerovirus, similar experiments should be conducted with the viruses identified in Chapter 3 of this work. It would be particularly interesting to determine the aphid vectors of the emergent viruses—TorCLV and FvPV—and the novel virus PMoHPV, as this could provide valuable insights into the potential host range overlap and epidemiological implications of the appearance of these poleroviruses. The polerovirus historically associated with CMD, CRLV, is vectored by the carrot-willow aphid *Cavariella aegopodii*, which is known to feed on plants in at least 10 different families, though they are most often found colonizing plants in the family *Apiaceae* such as carrot, cilantro, and parsley which serve as secondary hosts, but its primary host plants belong to those in the willow family, *Salicaceae* (Favret and Miller 2012). It would be interesting to know if *C. aegopodii* could likewise vector the emergent viruses described in this work, or if these viruses have

alternative primary aphid vectors, and if they do it would be interesting to see if those vectors could also vector CRLV. It should be noted that I found *Dysaphis apifolia* (Hawthorne-parsley) aphids on the cilantro sample that was collected in 2020, making this one candidate aphid vector of TorCLV. Given that, depending on the location, many aphids are known to alternate between secondary plant hosts that support the asexual stage of their life cycles, and primary plant hosts that support the reproductive stage of their life cycles, it would be interesting to see if the viruses that make up these unique disease complexes can infect both the secondary and primary plant hosts of their aphid vectors (Moran 1992). Many of the polerovirus, umbravirus, and tlaRNA disease complexes described to date have been found in annual crop plant species, which generally serve as secondary plant hosts to aphids (Abraham et al. 2014; Falk et al. 1979; Falk and Duffus 1984; Mo et al. 2007; Okusanya and Watson 1966; Watson and Falk 1994); if it were to be the case that these viruses could also infect the primary plant host of their aphid vectors, this may reveal a previously underappreciated reservoir for these viral disease complexes.

In addition to identifying aphid vectors of the poleroviruses identified in this study, it would be intriguing to scope out the host ranges of each of the poleroviruses, umbraviruses, and tlaRNAs identified in this study, and in particular, determine how those host ranges overlap for both the viruses as well as aphid vectors. Furthermore, it would be intriguing to investigate the capacity of each of these viruses to interact with one another. As highlighted in Chapter 2 of this work, interactions between poleroviruses, umbraviruses and tlaRNAs can be somewhat promiscuous, which has long been speculated to have significant epidemiological implications of disease complexes composed of these viruses. Given that tlaRNAs and umbraviruses have the potential to non-specifically be encapsidated by the capsid proteins of different polerovirus species, such instances in which novel combinations of these viruses occur in a host plant could

result in both vector and host range expansions of the tlaRNAs and umbraviruses involved. Additionally, given the potential host defense functions of umbraviruses and tlaRNAs, conducive combinations of these with a compatible but novel polerovirus partner could hypothetically result in a host range expansion of the polerovirus as well, should the host defense functions be sufficient to overcome the resistance or tolerance a previously non-host plant may have had against certain poleroviruses. Overall, the findings of Chapters 2 and 3 of this thesis not only highlight the unique, variable, and dynamic interactions that occur in polerovirus, umbravirus, and tlaRNA disease complexes, but also highlight an entire body of research that lays in waiting to be done to broaden our still somewhat limited understanding of these remarkable mixed virus infections.

Chapter 4: functional utilization of the barley virus G (BVG) infectious clone

While I have already described the construction of an infectious clone of the polerovirus barley virus G (BVG) and its proven utility to characterize basic features of this viruses biology, potentially much broader uses could come from this infectious clone (Erickson et al. 2023). As described in Chapter 4, I found that BVG—which was initially identified in a variety of monocot plant species—could also infect at least one dicot plant species, *Nicotiana benthamiana.* Currently there are few infectious clones of monocot infecting viruses that can be easily manipulated and also infect *N. benthamiana* . Therefore it would be interesting to see what potential this infectious clone holds as a delivery system for transgenes and/or virus induced gene silencing (VIGS) for monocot plants. Protocols for engineering the polerovirus Turnip yellows virus (TuYV) to semi-stably express GFP or be used as a VIGS vector (Boissinot et al. 2017; Bortolamiol-Bécet et al. 2018), it would be intriguing to see of these protocols would work similarly for the BVG infectious clone. Additionally, as I demonstrated in preliminary

experiments in which I co-infiltrated BVG with the tlaRNAs studies in Chapter 2 of this thesis, BVG is capable of transcapsidating heterologous RNAs, and as such could potentially be used for the packaging and delivery of other heterologous molecules. Not only could this clone be used to continue important fundamental research into the molecular biology of polerovirus infections in monocot plants, it has the potential to be developed into a useful biotech tool that could be used to improve the production of economically important monocot crop species. Overall, the work in presented in this thesis expands our knowledge of the fundamental biology of poleroviruses, umbraviruses, and tlaRNAs, and paves the way for even more interesting fundamental, as well as applied, research concerning these viruses.

References

Abraham, Adane D., Wulf Menzel, Berhanu Bekele, and Stephan Winter. 2014. "A Novel Combination of a New Umbravirus, a New Satellite RNA and Potato Leafroll Virus Causes Tobacco Bushy Top Disease in Ethiopia." *Archives of Virology* 159 (12): 3395–99. https://doi.org/10.1007/s00705-014-2202-4.

Boissinot, Sylvaine, Elodie Pichon, Céline Sorin, Céline Piccini, Danièle Scheidecker, Véronique Ziegler-Graff, and Véronique Brault. 2017. "Systemic Propagation of a Fluorescent Infectious Clone of a Polerovirus Following Inoculation by Agrobacteria and Aphids." *Viruses* 9 (7). https://doi.org/10.3390/v9070166.

Bortolamiol-Bécet, Diane, Baptiste Monsion, Sophie Chapuis, Kamal Hleibieh, Danièle Scheidecker, Abdelmalek Alioua, Florent Bogaert, Frédéric Revers, Véronique Brault, and Véronique Ziegler-Graff. 2018. "Phloem-Triggered Virus-Induced Gene Silencing Using a Recombinant Polerovirus." *Frontiers in Microbiology* 9 (2449). https://doi.org/10.3389/fmicb.2018.02449.

Campbell, A. J., John R. Anderson, and Jeffrey Wilusz. 2022. “A Plant-Infecting Subviral RNA Associated with Poleroviruses Produces a Subgenomic RNA Which Resists Exonuclease XRN1 in Vitro.” *Virology* 566: 1–8. https://doi.org/10.1016/j.virol.2021.11.002.

Cooper, Bret, Isabelle Schmitz, A. L.N. Rao, Roger N. Beachy, and J. Allan Dodds. 1996. “Cell-to-Cell Transport of Movement-Defective Cucumber Mosaic and Tobacco Mosaic Viruses in Transgenic Plants Expressing Heterologous Movement Protein Genes.” *Virology* 216 (1): 208–13. https://doi.org/10.1006/viro.1996.0048.

Erickson, Anna, Jun Jiang, Yen-wen Kuo, and Bryce W. Falk. 2023. “Construction and Use of an Infectious CDNA Clone to Identify Aphid Vectors and Susceptible Monocot Hosts of the Polerovirus Barley Virus G.” *Virology* 579: 178–85. https://doi.org/10.1016/j.virol.2023.01.011.

Falk, B. W. and Duffus, J. E. 1984. “Identification of Small Single- and Double-Stranded RNAs Associated with Severe Symptoms in Beet Western Yellows Virus-Infected Capsella Bursa-Pastoris.” *Phytopathology* 74 (10): 1224–29. https://doi.org/10.1094/phyto-74-1224.

Falk, B.W., J.E. Duffus, and T.J. Morris. 1979. “Transmission, Host Range, and Serological Properties of the Viruses That Cause Lettuce Speckles Disease.” *Phytopathology* 69: 612–17.

Fox, Adrian, Adrian J. Gibbs, Aimee R. Fowkes, Hollie Pufal, Sam McGreig, Roger A.C. Jones, Neil Boonham, and Ian P. Adams. 2022. “Enhanced Apiaceous Potyvirus Phylogeny, Novel Viruses, and New Country and Host Records from Sequencing Apiaceae Samples.” *Plants* 11 (15). https://doi.org/10.3390/plants11151951.

Hoffmann, K., M. Verbeek, A. Romano, A. M. Dullemans, J. F.J.M. Van Den Heuvel, and F. Van

Der Wilk. 2001. “Mechanical Transmission of Poleroviruses.” *Journal of Virological Methods* 91 (2): 197–201. https://doi.org/10.1016/S0166-0934(00)00256-1.

Jiang, Jun, Yen Wen Kuo, Nidà Salem, Anna Erickson, and Bryce W. Falk. 2021. “Carrot Mottle Virus ORF4 Movement Protein Targets Plasmodesmata by Interacting with the Host Cell SUMOylation System.” *New Phytologist* 231 (1): 382–98. https://doi.org/10.1111/nph.17370.

Kim, Sang Hyon, Stuart Macfarlane, Natalia O. Kalinina, Daria V. Rakitina, Eugene V. Ryabov, Trudi Gillespie, Sophie Haupt, John W. S. Brown, and Michael Taliansky. 2007a. “Interaction of a Plant Virus-Encoded Protein with the Major Nucleolar Protein Fibrillarin Is Required for Systemic Virus Infection.” *PNAS* 104 (26): 11115–20. https://doi.org/10.1073/pnas.0704632104.

Kim, Sang Hyon, Eugene V. Ryabov, Natalia O. Kalinina, Daria V. Rakitina, Trudi Gillespie, Stuart MacFarlane, Sophie Haupt, John W.S. Brown, and Michael Taliansky. 2007b. “Cajal Bodies and the Nucleolus Are Required for a Plant Virus Systemic Infection.” *EMBO Journal* 26 (8): 2169–79. https://doi.org/10.1038/sj.emboj.7601674.

May, Jared P., Philip Z. Johnson, Muhammad Ilyas, Feng Gao, and E. Simon. 2020. “The Multifunctional Long-Distance Movement Protein of Pea Enation Mosaic Virus 2 Protects Viral and Host Transcripts from Nonsense-Mediated Decay.” *MBio* 11 (2): 1–16.

Mo, X.-H., X.-Y. Qin, Z.-X. Tan, T.-F. Li, J.-Y. Wu, and H.-R. Chen. 2007. “First Report of Tobacco Bushy Top Disease in China.” *Https://Doi.Org/10.1094/PDIS.2002.86.1.74B* 86 (1): 74–74. https://doi.org/10.1094/PDIS.2002.86.1.74B.

Moran, N. A. 1992. “The Evolution of Aphid Life Cycles.” *Annual Review of Entomology. Vol.*

37, no. 129: 321–48. https://doi.org/10.1146/annurev.ento.37.1.321.

Nurkiyanova, Kulpash M., Eugene V. Ryabov, Natalia O. Kalinina, Yongchang Fan, Igor Andreev, Alexander G. Fitzgerald, Peter Palukaitis, and Michael Taliansky. 2001. "Umbravirus-Encoded Movement Protein Induces Tubule Formation on the Surface of Protoplasts and Binds RNA Incompletely and Non-Cooperatively." *Journal of General Virology* 82 (10): 2579–88. https://doi.org/10.1099/0022-1317-82-10-2579.

Okusanya, Bolajoko A.M., and Marion A. Watson. 1966. "Host Range and Some Properties of Groundnut Rosette Virus." *Annals of Applied Biology* 58 (3): 377–87. https://doi.org/10.1111/j.1744-7348.1966.tb04398.x.

Passmore, Boni K., Margaret Sanger, Lih Shen Chin, Bryce W. Falk, and George Bruening. 1993. "Beet Western Yellows Virus-Associated RNA: An Independently Replicating RNA That Stimulates Virus Accumulation." *Proceedings of the National Academy of Sciences of the United States of America* 90 (21): 10168–72. https://doi.org/10.1073/pnas.90.21.10168.

Rivarez, Mark Paul Selda, Anja Pecman, Katarina Bačnik, Olivera Maksimović Carvalho Ferreira, Ana Vučurović, Gabrijel Seljak, Nataša Mehle, Ion Gutiérrez-Aguirre, Maja Ravnikar, and Denis Kutnjak. 2022. "In-Depth Study of Tomato and Weed Viromes Reveals Undiscovered Plant Virus Diversity in an Agroecosystem." *BioRxiv* 11 (60): 2022.06.30.498278. https://doi.org/10.1186/s40168-023-01500-6.

Ryabov, E. V., K. J. Oparka, S. Santa Cruz, D. J. Robinson, and M. E. Taliansky. 1998. "Intracellular Location of Two Groundnut Rosette Umbravirus Proteins Delivered by PVX and TMV Vectors." *Virology* 242 (2): 303–13. https://doi.org/10.1006/viro.1997.9025.

Ryabov, Eugene V., Gillian Fraser, Mike A. Mayo, Hugh Barker, and Michael Taliansky. 2001a.

"Umbravirus Gene Expression Helps Potato Leafroll Virus to Invade Mesophyll Tissues and to Be Transmitted Mechanically Between Plants." *Virology* 286 (2): 363–72. https://doi.org/10.1006/viro.2001.0982.

Ryabov, Eugene V., David J. Robinson, and Michael Taliansky. 2001b. "Umbravirus-Encoded Proteins Both Stabilize Heterologous Viral Rna and Mediate Its Systemic Movement in Some Plant Species." *Virology* 288 (2): 391–400. https://doi.org/10.1006/viro.2001.1078.

Ryabov, Eugene V., David J. Robinson, and Michael E. Taliansky. 1999. "A Plant Virus-Encoded Protein Facilitates Long-Distance Movement of Heterologous Viral RNA." *Proceedings of the National Academy of Sciences of the United States of America* 96 (4): 1212–17. https://doi.org/10.1073/pnas.96.4.1212.

Schönegger, Deborah, Bisola Mercy Babalola, Armelle Marais, Chantal Faure, and Thierry Candresse. 2022. "Diversity of Polerovirus-Associated RNAs in the Virome of Wild and Cultivated Carrots." *Plant Pathology* 71 (9): 1892–1900. https://doi.org/10.1111/ppa.13623.

Sidharthan, V. Kavi, Krishnan Nagendran, and V. K. Baranwal. 2022. "Exploration of Plant Transcriptomes Reveals Five Putative Novel Poleroviruses and an Enamovirus." *Virus Genes* 58 (3): 244–53. https://doi.org/10.1007/s11262-022-01896-7.

Souza, Joao De, Segundo Fuentes, Giovanna Müller, Heidy Gamarra, Mónica Guzmán, Wilmer Cuellar, and Jan Kreuze. 2021. "High Throughput Sequencing for the Detection and Characterization of New Virus Found in Arracacha (Arracacia Xanthorrhiza)." *Scientia Agropecuaria* 12 (4): 471–80. https://doi.org/10.17268/sci.agropecu.2021.051.

Taliansky, Michael, Ian M. Roberts, Natalia Kalinina, Eugene V. Ryabov, Shri Krishna Raj, David J. Robinson, and Karl J. Oparka. 2003. "An Umbraviral Protein, Involved in Long-

Distance RNA Movement, Binds Viral RNA and Forms Unique, Protective Ribonucleoprotein Complexes." *Journal of Virology* 77 (5): 3031–40. https://doi.org/10.1128/jvi.77.5.3031-3040.2003.

Watson, M. T., and B. W. Falk. 1994. "Ecological and Epidemiological Factors Affecting Carrot Motley Dwarf Development in Carrots Grown in the Salinas Valley of California." *Plant Disease*. https://doi.org/10.1094/PD-78-0477.

Zhou, Cui-Ji, Xiao-Yan Zhang, Song-Yu Liu, Ying Wang, Da-Wei Li, Jia-Lin Yu, and Cheng-Gui Han. 2017. "Synergistic Infection of BrYV and PEMV 2 Increases the Accumulations of Both BrYV and BrYV-Derived SiRNAs in Nicotiana Benthamiana." *Scientific Reports* 7 (45132): 1–13. https://doi.org/10.1038/srep45132.